Integrated Study of Soil Compaction in the Agricultural Field: Numerical Modelling, Experimental Analysis, and the Influence of Soil Physico-Chemical Properties

Yared Seifu Woldeyohannis

A Dissertation Submitted to
The Department of Mechanical Engineering
School of Mechanical, Chemical and Materials Engineering

Presented in Fulfillment of the Requirement for the Degree of Doctor of Philosophy in Agricultural Machinery Engineering

Office of Graduate Studies
Adama Science and Technology University

September, 2024
Adama, Ethiopia

Integrated Study of Soil Compaction in the Agricultural Field: Numerical Modelling, Experimental Analysis, and the Influence of Soil Physico-Chemical Properties

Yared Seifu Woldeyohannis

Supervisor: Somashekhar S. Hiremath (Professor)
Co Supervisor: Simie Tola (Associate Professor)
Co Supervisor: Amana Wako (Associate Professor)

A Dissertation Submitted to
The Department of Mechanical Engineering
School of Mechanical, Chemical and Materials Engineering

Presented in Fulfillment of the Requirement for the Degree of Doctor of Philosophy in Agricultural Machinery Engineering

Office of Graduate Studies
Adama Science and Technology University

September, 2024
Adama, Ethiopia

DECLARATION

I hereby declare that this dissertation entitled "Integrated study of soil compaction in the agricultural field: numerical modelling, experimental analysis, and the influence of soil physico-chemical properties" is my original work. That is, it has not been submitted for the award of any academic degree, diploma or certificate in any other university. All sources of materials used for this thesis have been duly acknowledged through appropriate citations.

Yared Seifu Woldeyohannis		
Name of student	Signature	Date

RECOMMENDATION

we, the supervisors of this dissertation, hereby certify that we have read and revised the dissertation entitled "Integrated study of soil compaction in the agricultural field: numerical modelling, experimental analysis, and the influence of soil physico-chemical properties" prepared under our guidance by Yared Seifu Woldeyohannis submitted in fulfilment of the requirements for the degree of Doctor of Philosophy in Agricultural Machinery Engineering. Therefore, we recommend the submission of the dissertation to the department for further review and defence.

Prof. Somashekhar S. Hiremath		
Main Supervisor	Signature	Date
Dr. Simie Tola		
Co-supervisor	Signature	Date
Dr. Amana Wako		
Co-supervisor	Signature	Date

APPROVAL PAGE

we hereby certify that the recommendations and suggestions made by the Board of Examiners are appropriately incorporated into the final version of the dissertation entitled "Integrated study of soil compaction in the agricultural field: numerical modeling, experimental analysis, and the influence of soil physico-chemical properties" by Yared Seifu.

Prof. Somashekhar S. Hiremath Main supervisor	Signature	Date
Dr. Simie Tola Co-supervisor	Signature	Date
Dr. Amana Wako Co-supervisor	Signature	Date

We, the undersigned, members of the board of examiners of the dissertation open defense by Yared Seifu Woldeyohannis have read and evaluated the dissertation entitled "Integrated study of soil compaction in the agricultural field: numerical modelling, experimental analysis, and the influence of soil physico-chemical properties" and examined the candidate during open defense. This is, therefore, to certify that the dissertation is accepted for fulfillment of the requirement of the degree of Doctor of Philosophy in Agricultural Machinery Engineering

Chairperson	Signature	Date
Dr Brook Abate Internal Examiner	Signature	25/07/2024 Date
Dr. S.Karunanidhi External Examiner 1	Signature	07/08/2024 Date
Dr.-Ing. Zewdu A. Debele External Examiner 2	Signature	08/03/2024 Date
Dr. Alemayehu Regassa External Examiner 3	Signature	07/08/2024 Date
Dr. T. Thyagaraj External Examiner 4	Signature	07.08.2024 Date

Finally, approval and acceptance of the dissertation is contingent upon submission of its final copy to the office of Postgraduate Studies through the candidate's Department Graduate Council and School Graduate Committee.

Department Head	Signature	Date
School Dean	Signature	Date
Office of Postgraduate Studies, Dean	Signature	Date

ACKNOWLEDGEMENTS

Foremost, I would like to express my deepest gratitude to Prof. Somashekhar S Hiremath, Dr. Simie Tola, and Dr. Amana Wako who introduced me to scientific research and shaped me during the entire duration of my Ph.D. dissertation work. I thank them for their immense help, valuable guidance, constant encouragement, and technical support, which helped me to complete the work. Working under them was a pleasant and great learning experience for me.

I am thankful to Mr. Sintayehu department head of mechanical engineering, at Adama science and technology university (ASTU) for their support during my days as a student.

I am thankful to Dr. Alemayehu Wakjira school head of mechanical, chemical, and materials engineering for his support during my days as a student. I am also grateful to the post graduate dean of ASTU Dr. Legesse for facilitating everything related to my research work by discussing it with the school dean.

I am thankful to Mr. Dereje Alemu department head of engineering unit at Melkasa Agricultural Research Center for his permission to use measuring instruments. I would like to express warm gratitude to all the laboratory staff members of the Melkasa Agricultural Research Center for their support.

My special gratitude goes to my dear friends Mr. Megnote Zegeye, Mr. Adis Alemayehu, Dr. Amanuel Gabissa, Dr. Habtamu Deresso, Dr. Samuel Tamirat and Dr. Tatek Mamo for being there for me in all my ups and downs. Thank you for being there for me in proposal writing, experimental studies, data analysis, editing and journal and final document preparation.

I am grateful to have the blessings of my wife Mrs. Hirut Demeke, my children Finot Yared and Holly Yared and my brothers Mr. Amare Seifu, Mr. Ayele Seifu and Mr. Zeyed seifu who gave their hearts and soul to bring me up to this level. I also feel blessed to have wonderful family members and friends. My warmest and most enduring gratitude is to my brothers, sisters, and all my best friends for giving me constant support during all these years.

TABLE OF CONTENT

LIST OF TABLES

LIST OF FIGURES

LIST OF ACRONYMS

ASABE	America Society of Agricultural and Biological Engineering
CBD	Complete Block Design
CG	Center of Gravity
CI	Cone Index
DAC	Double Acting Cylinder
DAS	Data Acquisition System
DCV	Directional Control Valve
ENAMS	Ethiopian National Agricultural Mechanization Strategy
FAO	Food and Agriculture Organization of the United Nations
FO	Food Organization
GDP	Gross Domestic Product
GPS	Global Positioning System
IBC	Institute of Biodiversity Conservation
MC	Moisture Content
PTO	Power Take-Off
RCBD	Randomized Complete Block Design
SAS	Statistical Analysis Software
SQL	Structured Query Language
WES	Waterways Experiment Station
RMSE	Route Mean Square Error
ARC	Aeronautical Reconnaissance Coverage
GIS	Geographic Information System

LIST OF NOTATIONS

D	Diameter of Cylinder Rod (m)
E	Young's Modulus of Elasticity (N/m^2)
F	Force (N)
I	Moment of Inertia ($kg.m^2$)
L	Length of Cylinder Rod (m)
Q	Flow Rate (m^3/s)
WD	Working Depth (m)
b	Section Width Tractor Front Wheel (in.)
d	Tyre Diameter (m)
D_i	Implement Draft (N)
D_m	Modified Draft (N)
e	Longitudinal Shift of Wheel Reaction (m)
h	Section Teight (m)
r	Rolling Radius (m)
R	Dynamic Wheel Reaction (N)
S	Wheel Slips (decimal or %)
V_a	Tractor Rorward Velocity (m/s)
Vt	Drive Wheel Theoretical Velocity (m/s)
W_t	Tractor Static Weight (kg)
Bn	Brixius Number (Unit less)
CI	Cone Index (kPa)
Pdb	Drawbar Power (kW)
GTR	Gross Traction Ratio (decimal)
MRR	Motion Resistance Ratio (decimal)
NTR	Net Traction Ratio (decimal)
PDE	Power Delivery Efficiency (%)
Ppto	Rated PTO Power (kW)
FC	Fuel Consumption (L/ha)
TE	Tractive Efficiency (decimal or %)

ABSTRACT

In many parts of the world, farm land has been heavily compacted as a result of large farm equipment. The use of farm equipment and other energy in agricultural processes results in a reduction in the air spaces between soil particles. Soil compaction have been conventionally measured by using a manually operated cone penetrometer which has certain ergonomic restrictions tackled by the operator, it takes more time and it is difficult to obtain data required for agriculture operation. The objective of the research is numerical modelling of a hydraulic system, integrate the system with a tractor to control the cone penetrometer, making a field test to measure soil compaction and evaluating the performances with drawbar performance with the help of visual basics software. The materials used in this research work were a tractor, tillage implement, cone penetrometer, and hydraulic system, soil physical test apparatus and soil chemical property test instruments. The average soil compaction of the field soil for Kulumsa farm field ranges from 3,511.8 kPa to 3,730.3 kPa and 1,195.5 kPa to 1,227.4 kPa for harvesting and seeding season respectively. For the Melkasa farm field, the average soil compaction value ranges from 3,180.3 kPa to 3,947.3 kPa and 978.3 kPa to 1,383.5 kPa for harvesting and seeding season respectively. Bishoftu farm fields have an average soil compaction value ranging from 1,011.2 kPa to 1,838.3 kPa and 548.2 kPa to 630.1 kPa for harvesting and seeding season respectively. From all experimental farm sites, cone index value had a general tendency to increase with soil depth except for the Bishoftu farm field for the seeding season. When depth increases, percent of soil moisture content also increases for both experimental seasons for all experimental fields. In addition, it was observed that total organic carbon, organic matter, and total nitrogen levels tend to rise with increased soil compaction, and conversely, decrease as soil compaction decreases. The numerical study of tractor implements performance result showed the maximum performance parameters were found at 300 mm depth with a drawbar power of 35.7 kW, pull of 7.9 kN, fuel consumption of 3.64 kg/h, slip12.5%, power delivery efficiency of 60%, and dynamic weight of 31.19 kN. This study's insights are invaluable for agricultural mechanization. Given the substantial weight of farm machinery, comprehending soil properties and their correlation with compaction rates is critical in farming practices.

Keywords: Cone penetrometer, Drawbar performance, Hydraulics, Soil compaction, Soil depth, visual basics

CHAPTER 1

INTRODUCTION

1.1. Background of the Study

Farm mechanization is a sign of agricultural modernization because it involves the use of farm equipment. Soil is compacted when farm equipment is driven across it, from the preparation of the ground to the harvesting process (Ungureanu et al., 2015). Soil compaction is caused by farm equipment and livestock trampling (Chyba J. et al., 2014). Crop rotation, soil moisture, and working depth are additional factors that affect the risk of compaction.

In Ethiopia, agriculture plays a crucial role in overall development. It contributes about 42% of the GDP and the lion's share of its foreign currency, also 80–85% of the jobs come primarily from this sector (ENAMS, 2010). The (IBC, 2012) agricultural survey estimated that the total private farmer holding was about 13 million hectares and most of the agricultural land (more than 76%) was under annual crops. The average land holding per household was 1.18 hectares. Increased food demand as a result of population growth, combined with limited land, has put a lot of pressure on land to increase output per unit area through mechanization. Soil compaction is a problem for the environment(Keller et al., 2012). It contributes to increased soil erosion and flooding (Serem et al., 2016). It also has an impact on nutrient availability and pesticide leaching into groundwater (Lipiec et al., 2012).

Soil physical properties are important in determining soil suitability for agricultural, environmental, and engineering uses. The physical characteristics of the soil have a direct impact on its capacity for supporting life, movement, retention, and availability of water and nutrients to plants, as well as the ease with which roots can penetrate the soil and the flow of heat and air. Soil texture and soil structure are the most important physical properties of soil for its use as a medium for plant growth. Soil texture refers to the size range of mineral particles and is defined both qualitatively and quantitatively. It describes the way soil feels when it is rubbed between the thumb and forefinger, whether it is fine and smooth or coarse and gritty. Soil texture is the weighted proportion of sand, silt, and clay content (Phogat et al., 2015).

The oxen draft is one of the main sources of farm power for primary and secondary tillage in cereal-based farming systems. Additionally, the agricultural sector relies on a hand-hoe-based farming system (Dembner, 1988). Ethiopian agriculture is gradually shifting from traditional farming practices to more contemporary ones. Due to its impact on the intended use of the soil, the study of soil compaction in tillage is extremely important (Wong, 2001).

A manually operated soil cone penetrometer is a common tool for measuring soil compaction (Guimaraes Junnyor et al., 2019). To measure soil compaction, the soil cone index is frequently used. Soil compaction is measured in Ethiopian research centers and agricultural ministries using a hand-held soil penetrometer, which has some ergonomic limitations that the operator must overcome. It is used to establish or maintain the soil in a suitable state of compactness for a particular use during tillage operations. A good root environment is hampered by excessive compactness, which also reduces water penetration and worsens runoff and erosion (Mudarisov et al., 2020). The forces generated by agricultural equipment cause soil particles to compact closer together and organize themselves into a smaller volume. Soil compaction is one of the most significant negative factors associated with heavy agricultural machinery in the agricultural field, limiting plant growth capacity and crop yield (Benevenute et al., 2020). Compaction reduces soil aeration, impairing root metabolic activities (GILL, 1968).

In agricultural machinery, three methods exist general for transmitting power from one point to other components of a tractor. Hydraulic systems have several fundamental advantages over other power sources, including being straightforward, simple to run, accurate to control, and great at force multiplication up to several hundred tons (Roeber et al., 2016). Due to the different advantages of fluid power in many types of research work hydraulic power is used for hydraulic-operated soil resistance and compaction measurement using a cone penetrometer on the indigenously developed system as a driving unit. The cone penetrometer test provides valuable information in farm mechanization and geotechnical investigations when used in conjunction with other equipment and procedures. The output of tillage implements and cone penetrometer tests can be used to make reliable estimates of basic information about the soil engineering property. In almost, all past research work for measuring soil compaction cone shape is selected due to simplicity for finding the area immersed in the soil and the power used for measuring the soil compaction.

1.2. Justification

Recent studies show cone penetrometers measure soil compaction, while multiple cone penetrometers assess horizontal soil resistance (Perumpral, 1987). However, their cone geometry makes precise data collection difficult. In Ethiopia, outdated soil compaction practices and poor methods hinder sustainable farming.

The study has the following justifications;

1) To increase output and profitability, the findings will be utilized to educate the farming community about the main effects of compacted soil and the precautions they should take to prevent or alleviate the problem.
2) The output findings will guide the main impacts of soil physical and chemical characteristics on soil compaction to the farming community and on the steps they should take to balance the relationship between soil physiochemical properties and soil compaction.
3) It compiles data on how heavy farm machinery and equipment affect soil's physical and chemical properties, as well as how compaction and yields are affected.

1.3. Statement of the Problem

The primary sign that agriculture is being modernized is increased farm mechanization. During field operations, the weight of farm machinery compacts agricultural soil, increasing soil bulk density and decreasing soil porosity, particularly when tractors' tires or tracks come into contact with it (Ungureanu et al., 2015). The year of soil tillage, crop rotation, soil moisture, and working depth all affect the compaction (Chyba J. et al., 2014). Due to its increased strength and draft resistance during compaction, compacted earth is challenging to plow (Guimaraes Junnyor et al., 2019).

Soil compaction on tillage implements are interconnected parameters that have been measured conventionally by using a manual-operated cone penetrometer which has certain ergonomic restrictions tackled by the operator, it takes more time and due to the nature of cone geometry, it is difficult to get the soil resistance data perfectly for agriculture operation (Margolin, 1991). Soil resistance on tillage implements and soil compaction measuring in fieldwork to study the nature of soil compaction at a different depth, soil resistance on tillage implements during tillage operation mounted on a tractor specifically in our county Ethiopian level is necessary to overcome the above-mentioned problems.

A multifunctioning system operated by hydraulic power used to measure soil resistance and compaction mounted on a tractor in a tillage field has not been studied by past researchers. This research therefore addressed the design and development of hydraulically actuated tractor-mounted soil compaction measuring at tillage field. Then it goes to the field experiment to measure soil compaction and resistance at different tillage parameters like; depth of operation, working speed, and soil physical properties. After the measurement of soil cone index value and soil physiochemical property at the laboratory level the effect of those parameters on tractor performance was studied.

1.4. Objectives

1.4.1. General objective

The general objective of the study is numerical modeling and experimental investigation of soil compaction and the effect of soil physico-chemical properties on agricultural fields.

1.4.2. Specific objectives

1) To design, construct, and test the performance of a hydraulic-driven cone penetrometer system
2) To investigate the effect of soil physicochemical properties on soil compaction
3) To develop software for calculating drawbar using visual basic programming language

1.5. Significance

This research uses a digital cone penetrometer on three farms to measure soil compaction. It studies the performance of tillage implements by varying depth and analyzing soil cone index values with Visual Basic simulation. The project involves designing a tractor-mounted, hydraulically operated compaction measurement system. The research on the application of tillage operation and factors related to soil property and tillage implement draft resistance has many relevancies with relation to soil compaction.

Some of them are as follows:

- The research work has a significant impact by studying the required amount of soil strength and soil compaction at three selected experiment sites for the identification of soil seed relation and setting standards for seed type and required soil physical nature for the improvement of seed soil interaction.

- This work helps the Ethiopian farm mechanization system and farmers to understand the amount of specific soil resistance for different soil types and to know which types of soil properties affect soil compaction.
- This study also covers the way for future researchers to work in this direction in improving the design for measuring the soil resistance on tillage implements and soil compaction.
- Due to the hydraulic system for measuring system of soil compaction attached to a tractor, the power loss required for the operation is saved.
- This work helps the Ethiopian farm mechanization system and farmers to understand which types of soil properties are good for the different types of seeds.
- In this research work farmers, agricultural industries, agricultural research sectors, and the country as a whole will benefit.

1.6. Scope

This research work is enclosed in the design of the selected parts of the hydraulic system for measuring soil compaction by attaching a cone penetrometer at the tip of a double-acting cylinder road. The design mainly focused on the force and pressure required to insert the cone penetrometer into the soil at different depths of operation. After the design and development, the system can be integrated into a tractor to operate specific tasks. The system is dsigned to measure soil compaction in two different farming seasons. In addition, the research studied the effects of selected soil's physical and chemical properties on soil compaction. During the field experimental test,only 3 different depths were selected for taking soil compaction data and soil samples from three agricultural farm areas at two farming seasons. During the compaction test, only 15 sample point data were taken from 0.6 ha farm land.

1.7. Limitations

This study was restricted to evaluating specific soil physiochemical characteristics within the study region, including soil texture, moisture content, electrical conductivity, cation exchange capacity, total organic carbon, total nitrogen, organic matter, soil pH, and soil penetration resistance. Additional variables not taken into account during this investigation duel to luck of instruments included soil bulk density and the number of passes, both of which have an impact on soil compaction. The soil physiochemical investigation and soil compaction tests could only be conducted to depths of 100 mm, 200 mm, and 300 mm. The study's conclusions only apply to clay, clay loam, and sandy clay loam. The study looked at how depth, season, farm location, and various soil physical and chemical qualities affected soil compaction caused by large farm machinery and equipment. To prevent the cone penetrometer from breaking, the tractor's instrumental integration system did not monitor soil compaction on stony farmland. Moreover, this research addressed only computer modeling and simulations for predicting tractor performance without completing field tests.

1.8. Organization of Thesis

This dissertation is divided into five chapters that cover distinct topics. The introductory section of Chapter 1 includes subsections on the study's background, justification, problem statement, general and specific objectives, the significance of the research, the research's scope, and its limitations. The second Chapter includes a review of previous studies on the many components that contribute to soil compaction. It also describes the conclusions drawn from these studies and any research gaps that were identified. The methodology to be used, the materials needed to conduct the research, and the specifics of the data gathering and data analysis methodologies are all covered in Chapter 3. The theoretical underpinnings and framework of the study include mathematical and numerical models that were investigated with this study's title. Findings and discussion are articulated in Chapter 4, where the data are also evaluated and gathered from the output of the simulation and experiment. Chapter 5 concludes with conclusions and suggestions, which summarize the study's findings and provide guidance for further research.

1.9. Summary

In this chapter, a brief introduction to soil compaction of agricultural soil and what measures should be taken for compacted soil are addressed. The risk of compaction and factors depending on the soil tillage and crop rotations, soil physical and chemical properties, and working depth are also addressed. The background of the study contains an introduction of national and global scenarios related to soil compaction factors and the consequence of farm soil compaction is discussed. The research justification and issue that needs study and what problem is the research attempting to address are covered in this chapter. The focus area of the dissertation, variables to be measured and steps to be involved in the overall research work including the main research study achievement and methods are discussed. General and specific objectives, which show specific outcomes to achieve through research and the benefits of this research work were addressed under the objective and significance of the study parts. The extent to which this research area was explored the parameters of the study and the weaknesses of the study were explained briefly in this chapter with different subtopics.

CHAPTER 2

2. LITERATURE REVIEW

2.1. Background and History

The study of the interaction between soil and tillage implements and the impact of soil strength on tillage operation is a very complex and vital thing for the agricultural mechanization sector. The process of interaction between soil and tillage implements and soil and tire is continuing to be the main subject of study of researchers in connection with the necessity to considerably improve the performance characteristics of soil physical properties and pneumatic tires in different soil conditions. In this chapter, an effort has been made to discuss various studies related to the hydraulically operated soil resistance on tillage implements and soil compaction in a real field. The major study areas included are as follows.

- Soil compaction
- Constituent factors for soil compaction like :Soil physical properties, Soil chemical properties,Tractor density and Animals and human
- Soil compaction and draft resistance
- Soil Tire Interaction Modelling
- Traction Parameters
- Tractor dynamics
- Soil resistance on tillage implements
- Soil Compaction due to tillage operation and traction device
- Role of hydraulic power in soil resistance and compaction measurement

2.2. Soil Compaction

Pore space, size, distribution, and soil strength all change as a result of soil compaction. Bulk density measurement is one method for calculating the change. The bulk density of soil increases as the pore space decreases. Higher clay and silt content soils have a lower bulk density than sandy soils because they naturally have more pore space (Kim et al., 2010). Soil compaction, on the other hand, increases soil strength, which is the ability of soil to resist being moved by an applied force. To penetrate this layer of tightly packed soil in compacted soil, roots must exert more force.

Compaction of soil occurs during intensive agriculture due to the use of machinery and animals. Water and air movement, seedling emergence, and root penetration may all be hampered by the compressive effects (Marshall et al., 1996). One of the main issues with modern agriculture is soil compaction. Overuse of machinery, intensive cropping, short crop rotations, intensive grazing, and inappropriate soil management lead to compaction. Soil compaction occurs in a wide range of soils and climates. It is made worse by low soil organic matter levels, tillage, and grazing at high soil moisture levels. Because less water and nutrients can be stored and supplied in the soil due to soil compaction, the need for extra fertilizer rises along with production costs. Compaction also reduces soil physical fertility. A detrimental sequence then occurs of reduced plant growth leading to lower inputs of fresh organic matter to the soil, reduced nutrient recycling and mineralization, reduced activities of micro-organisms, and increased wear and tear on cultivation machinery (Hamza et al., 2005).

Although soil compaction is useful in other fields, it is disastrous for agricultural land because it prevents water from penetrating deeply into the soil and instead increases surface runoff, which leads to soil erosion and flooding as well as increased pesticide movement and indirect nutrient leaching (TONUI, 2015). These negative impacts lower fertilizer efficiency and crop output, increase waterlogging, runoff, and soil erosion, and cause unwanted environmental pollution (Hamza et al., 2005). Recent research has demonstrated that the usage of large and heavy machinery reduces the pore size distribution of the soil. It was discovered that heavy traffic had an impact on the form, size, and orientation of the soil's macroporosity features (porosity). In addition to having fewer large holes and a slower rate of drainage from the compacted layer, heavily compacted soils also have fewer large pores. This happens because saturated soil has wide pores that move water through it most efficiently (Lipiec et al., 2012). Compacted soils also have a slower rate of gas exchange, which increases the chance of aeration-related issues (Bottinelli et al., 2015).

2.3. Soil Physical Properties

Soils are frequently classified into different categories. These distinct varieties frequently also have various mechanical characteristics. Soil is composed of materials in all three states: solid, liquid, and gaseous. Both organic and inorganic materials make up the majority of the solid. The inorganic, or mineral, component of soil is composed of particles produced from the parent material, the rocks that weather to become soil. The organic component is made up of living and extinct plant and animal components, including worms and roots. Humus, a dark, amorphous organic substance, is the final by-product of decomposition. Soil water is a dilute but complex chemical solution that is formed by direct precipitation, run-off, seepage, and groundwater. When there is no water in the soil, the soil atmosphere fills the pore spaces. The movement of air, water, and dissolved compounds through the soil, as well as factors influencing germination, root development, and erosion processes, are all examples of soil physical attributes. Many chemical and biological processes begin with the physical characteristics of the soil, and these processes may be further influenced by the climate, position in the landscape, and kind of land use. As a result, changes to a variety of soil physical attributes brought on by climate change may set off a series of events that result in changes to the soil environment, which may have a significant impact on crop development and production (Jat et al., 2018).

2.3.1. Soil texture

The proportion in which the soil separates to form the mineral component of the soil is defined as soil texture. Sand, clay, and silt are the three types of separates as shown in Fig. 2.1. Sand and silt have no bearing on the soil's ability to replenish nutrients or water. Because of its tiny size, high surface area per mass, and ability to store ions and water, clay is an active component of soil texture.

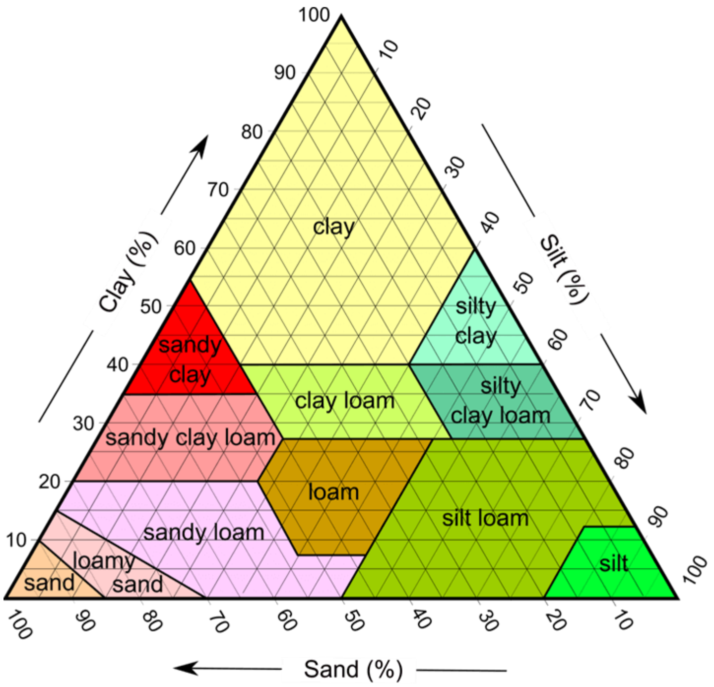

Figure 2.1: Soil texture triangle
Source:(Estefan, 2013)

The fineness or coarseness of the mineral particles in the soil is referred to as the soil texture. It is governed by the quantity of sand, silt, and clay particles. Loam is a mixture of all three. The soil's aeration, drainage, deformability, and ability to store water are all impacted by the texture of the soil. Sand has a particle size range of 0.05 to 2 mm, Silt ranges from 0.002 mm to 0.05 mm, and Clay ranges from 0.002 mm to less than 0.002 mm in diameter. When none of the three (sand, silt, or clay) predominates over the other two, the soil is said to be loamy. Around 40% sand, 40% silt, and 20% clay make up loamy soil.

2.3.2. Soil moisture content

One of the trickiest measurements needed in agriculture is the measuring of soil moisture. A variety of techniques are used to measure soil moisture, including feeling the soil and employing sophisticated electrical equipment that uses radioactive materials (van Verseveld & Gebert, 2020). Only the gravimetric, electrical-resistance, tensiometric, and radioactive approaches are routinely utilized. Every method has drawbacks as well as benefits, and the optimal approach that can deliver measures that are precise, dependable, and quick has not yet been established (Ganiyu et al., 2020). The gravimetric approach is the most appropriate for most soil moisture measurements that require one-time moisture-content data. Because the gravimetric approach delivers data directly, the effort and potential for mistakes associated with converting indirect values (electrical resistance, radioactive, and tensiometric) to moisture content are eliminated. Compared to the indirect approaches, the gravimetric method takes less skill but more work in many situations. Even if one of the indirect methods is utilised, significant gravimetric sample is required for calibration. Continuous or frequent moisture-content monitoring may necessitate the use of an indirect approach. In the field, repeated measurements of soil moisture are best obtained using radioactive techniques.

2.3.3. Soil structure

How clay, silt, and sand particles are grouped is known as the soil structure. Soil creatures like earthworms and bacteria, as well as organic matter (decaying plants and animals), have an impact on soil structure. Aggregates are created when clays, organic matter, and substances secreted by soil organisms bind soil particles together. Because it controls air and water flow, influences root development, and affects nutrient availability, soil structure is crucial for plant growth. Squeezing good-grade soil will quickly break it up since it is friable (crumbly) and has fine particles. Coarse, extremely solid clods or no structure at all are signs of poor soil structure (Bronick & Lal, 2005).

2.3.4. Soil permeability

The ability of the soil to convey water is known as soil permeability. Understanding the water dynamics and the water balance of the soil is crucial for effective irrigation management. It is influenced by soil management and partially by texture, with sandy soils having higher permeability than clay soils. Except for clay, which has pores that are so small that groundwater held by surface tension frequently fills them, most porous rocks are permeable. Granite is another exception, which is both non-porous and permeable. Soil with a high organic content tends to be more porous (Singh et al., 2020).

2.4. Soil Chemical Properties

Concentrations of particular chemicals (such as phosphorus, nitrogen, carbon, main cations (calcium, magnesium, sodium, potassium), sulfur, and trace metals and elements) are among the chemical characteristics of the soil. Other chemical characteristics include pH, cation exchange capacity, base saturation, salinity, sodium adsorption ratio, enzymes, and electrical conductivity (Andrews et al., 2004; Schoenholtz et al., 2000). The nutrient cycle, biological activity, soil formation, pollutant destiny, and erosion are all affected by these qualities. In Table 2.1, a summary of the chemical characteristics of soil and the related processes that have an impact on those characteristics and processes is briefly given. The total amount of negative charges in the soil that bind to cations such as calcium (Ca^{2+}), magnesium (Mg^{2+}), and potassium (K^{+}) for plant nutrition is known as the cation exchange capacity.

2.4.1. Cation exchange capacity

In the soil environment, certain plant nutrients and metals exist as positively charged ions, or "cations." Hydrogen (H^{+}), aluminum (Al^{+3}), calcium (Ca^{+2}), magnesium (Mg^{+2}), and potassium (K^{+}) are some of the more prevalent cations found in soils (Chapman & properties, 1965). The majority of heavy metals are also present in the soil as cations. Because the majority of the particles in clay and organic materials are negatively charged (anions), they can keep cations from being "leached" or washed away. The “cation exchange capacity (CEC)”, of soil, is a measurement of the magnitude of the negative charge per unit weight of soil or the number of cations a particular sample of soil can hold in an exchangeable form. The greater the clay and organic matter content, the greater the CEC, although different types of clay minerals and organic matter can vary in CEC.

Cation exchange is an important mechanism in soils for retaining and supplying plant nutrients and for adsorbing contaminants (Sumner & Miller, 1996). Factors affecting CEC are; Soil pH, soil organic matter, and Soil texture. The retention and supply of plant nutrients as well as the adsorption of pollutants are both facilitated by the significant role played by cation exchange in soils. Soil chemical properties and associated activities are indicated in the Table 2.1.

Table 2.1: Soil chemical properties and associated activities

Property	Effects	Desired value
Phosphorus	An essential nutrient for plants and animals	The optimum concentration is 30 to 50 mg-P/kg-soil (ppm)
Nitrogen	An essential nutrient for plants and animals	The optimum concentration is 25-50 mg-N/kg-soil
Major cations	Calcium (Ca), magnesium (Mg), and potassium (K) are essential nutrients for plants and animals; these cations may affect soil properties (e.g., crusting with excess sodium) or soil processes (e.g., buffering)	Ca: > 300 mg/kg-soil; Mg: > 35 mg/kg-soil; K: 40-80 mg-kg-soil; sodium: less than 15% of soil cation exchange capacity
Sulfur	An essential nutrient for plants and animals	The optimum concentration is 30-40 mg-S/kg-soil
Trace metals	Some trace metals and metalloids are essential for plants and animals (molybdenum (Mo), copper (Cu), boron (B), manganese (Mn), iron (Fe), zinc (Zn)); most trace metals are toxic above certain concentrations	Mo: 2 mg/kg-soil; B: 0.5-4 mg/kg-soil; Cu: 2-50 mg/kg-soil; Zn: 1-200 mg/kg-soil; Mn: 2-25 mg/kg-soil; Fe: 20-30 mg/kg-soil. For non-essential trace metals, toxic effects vary with vegetation.
CEC	Affects the availability of nutrients and pollutants	12-40 meq/100 g-soil
Electrical conductivity	An indicator of salt concentration in soil. Salts affect the availability and transport of nutrients and pollutants.	Less than 8 dS/cm is desirable
Organic matter (carbon)	Many important effects in the soil, including providing nutrients, improving soil physical properties	2-8 % of soil, by weight
Base saturation	An indicator of the extent to which cation exchange capacity is attributable to calcium, magnesium, and potassium.	40-80% for calcium, 10-40% for magnesium (Mg), and 1-5% for potassium (K)
pH	Affects many soil processes, such as microbial activity, affects the availability and mobility of nutrients and pollutants	6-8

source : (Mallarino et al., 2013; Miles et al., 2017; Pagani, 2011), (Dinkins & Jones, 2013; Maikhuri et al., 2012)

Soil pH, soil organic matter, and soil texture are all factors that have an impact on CEC. Here is a detailed description.

- **Soil pH:** Certain soil types' CEC and organic matter can be impacted by soil pH. Increased soil CEC can assist the soil act as a buffer by reducing cation leaching losses. A soil's ability to buffer helps it withstand chemical changes, such as pH, which have an impact on the availability of nutrients and microbial activity.
- **Soil organic matter:** In general, increased soil organic matter is linked to higher CEC. The organic matter's stage of decomposition can, however, cause variations in CEC. Humus is an example of a well-decomposed organic material that can be used to boost soil CEC. Microorganisms have a role in the transformation of nutrients in the soil as well as the breakdown of organic debris like thatch and leaf litter. Soil environmental conditions must be kept appropriate to support microbial activity.

- **Soil texture:** The proportions of sand, silt, and clay particles in the soil affect its texture. CEC is usually higher in soils with larger percentages of clay content. The addition of soil organic matter may be necessary for sandy textured soils since they often have lower CEC. Table 2.2 describes the cation and anion in the soil.

Table 2.2: Cation and anion in soil

Nutrient	Cation	Anion
Hydrogen (H)	H^+	
Nitrogen (N), Nitrate		NO_{3-}
Nitrogen (N), Ammonium	$NH4^+$	
Potassium (K)	K^+	
Calcium (Ca)	Ca^{2+}	
Magnesium (Mg)	Mg^{2+}	
Iron (Fe)	Fe^{2+}, Fe^{3+}	
Manganese (Mn)	Mn^{2+}	
Zinc (Zn)	Zn^{2+}	
Copper (Cu)	Cu^{2+}, Cu^+	
Boron (B)		H_3BO_3
Molybdenum (Mo)		MoO_4^{2-}
Chlorine (Cl)		Cl^-
Nickel (Ni)	Ni^{2+}	

Source: (Rhoades & properties, 1983)

2.4.2. Soil reaction (pH)

The concentration of active hydrogen ions (H+) in the soil is measured by its pH. The term "soil response" refers to this phenomenon, which shows how acidic or alkaline the soil is.

The pH scale runs from 0 to 14, with readings below 7.0 being acidic and those over 7.0 being alkaline. Neutrality is defined as a pH value of 7 (Spurway, 1941). The ion solubility of the soil, which in turn impacts microbial and plant growth, is the most significant consequence of soil pH. For most crops, a pH range of 6.0 to 6.8 is appropriate because it promotes the best solubility of the most vital plant nutrients. At lower pH levels, some minor elements (like iron) and most heavy metals are more soluble. Because of this, managing pH is crucial for preventing the migration of heavy metals in soil (Sharma et al., 2014).

Aluminum and hydrogen are the two main exchangeable cations in acidic soils. The latter is soluble in acidic solutions and creates hydrogen ions when it reacts with water (hydrolysis). Because they are basic cations, calcium, and magnesium cause a decrease in the proportion of acidic cations (McLean et al., 1983). Parent material, vegetation, and climate are all elements that have an impact on soil pH. Acidic sandstone and alkaline limestone produce soils that are more acidic than other types of sediment and rocks. Some plant species, especially conifers, create organic acids, which can reduce the pH of soil. Because rainfall replaces basic cations with hydrogen and washes them away, soils in humid regions like the eastern US tend to become more acidic over time. Hydrogen ions can also be created by adding specific fertilizers to the soil. The amount of liming material required to elevate the soil pH to a particular level, or the "lime demand," rises with CEC (cation exchange capacity). Sulfur can be applied to the soil, producing sulfuric acid, to lower the pH (Khaledian et al., 2017).

2.4.3. Soil electric conductivity

The ability of a material to transfer an electrical current is known as electrical conductivity, and it is frequently stated in units of milli Siemens per meter (mS/m) (Corwin et al., 2005). An indirect measurement that closely corresponds with some soil's physical and chemical characteristics is electrical conductivity. The quantities of nitrates, potassium, sodium, chloride, sulfate, and ammonia have been associated with EC, although it does not directly detect particular ions or salt compounds. A contact sensor and a non-contact sensor are the two types of sensors that may detect electrical conductivity (Rhoades et al., 1989).

To measure electrical conductivity, contact sensors should make touch with the soil. Two to three pairs of colters are typically utilized. As one pair supplies the soil with electrical current, the other pairs measure the voltage drop that occurs between them and utilize that drop to determine the electrical conductivity of the soil. The electrical conductivity of soil is often measured by contact sensors at two distinct depths. Among the soil parameters that affect crop productivity are soil texture, cation exchange capacity (CEC), drainage conditions, organic matter content, salinity, and subsurface features. Oil electrical conductivity (EC) is a measurement that corresponds to these factors (Grisso et al., 2005). Moderate salinity is defined as values above 8 dS/m, whereas high salinity is defined as values over 16 dS/m. Saline soils are most frequently found in arid regions, irrigated soils, soils that get a lot of manure or sludges, and soils that have been affected by a specific source, like road salt (Nackley & Kim, 2015).

2.4.4. Organic carbon

The importance of soil organic carbon to soil fertility in both managed and uncontrolled environments has long been recognized (Kucharik et al., 2001). The macronutrient nitrogen frequently restricts soil-based plant development (Michopoulos et al., 2008). Furthermore, soil organic matter, and consequently soil organic carbon, is one of the soil's most crucial characteristics since it influences water availability, soil structure, and nutrient cycling (Vitousek & Farrington, 1997).

2.4.5. Organic matter

The organic part of soil known as soil organic matter (SOM) consists of plant and animal remains in various stages of decomposition, soil organism cells and tissues, and compounds produced by soil organisms. The majority of our fertile agricultural soils contain 3 to 6% organic matter. Numerous factors, including soil organic content, influence soil production. Living things are typically considered to be a part of SOM, especially those that are smaller than 2 mm (Manson & Bulletin, 2018). Traditionally, SOM was assumed to be largely made up of a special category of cross-linked compounds known as human substances, and the extended residence durations of soil organic carbon in soils were attributable to these substances' capacity to resist microbial and enzyme breakdown (Rhoades et al., 1989). However, recent research has revealed that the majority of the organic matter in soil resides as complexes of molecules bound together by non-covalent connections. These bonds hold together the organic material pieces that result from the breakdown of biomolecules (Kannan et al., 2005).

2.4.6. Total nitrogen

Nitrogen contributes to the growth of internal plant tissues and cells as well as the production of chlorophyll, making up around 1% of a plant's dry weight (Nelson & Sommers, 1973).

Nitrogen is frequently a limiting component in soil, along with phosphorus. Nitrogen-deficient soils inhibit the growth and development of plants, whereas nitrogen that is in excess can be transferred from the soil and enter freshwater sources, including groundwater. Both organic and inorganic forms of nitrogen can be found in soil, with ammonium (NH^{4+}) and nitrate (NO^{3-}) being the two most common inorganic forms (Rhoades et al., 1989).

2.5. Biological Properties of Soil

The existence and activities of live plants and animals as well as their non-living organic products are all part of the overall biological involvement in soil formation. There are two main ways by which living plants influence the development of soil (Delgado & Gómez, 2016). The first is biomass or the formation of organic materials biomass both above the soil as stems and leaves and within the soil as roots. In the O horizon and lower horizons, it provides the organic matter's primary source material. The decomposer organisms break down this basic material, turning it into a humus and then back into its original carbon dioxide and water compositions. The second method includes cycling nutrients from the soil into the tissues of dead plants. By using a technique called nutrient recycling, excess soil water that might otherwise leech nutrients from the soil is kept from doing so (Elfeel et al., 2009). The biological processes of soil are significantly influenced by the animals that reside there. For instance, earthworms remodel the soil by both burrowing and traveling around it via their intestinal tracts (Gizachew & Smit, 2008).

2.6. Soil Resistance on Tillage Implements

In their experiment, (Patil et al., 2018) kept the speed of the earthing-up process constant while varying the widths and depths of the ridger plow in sugar cane plants. Two load cells were fixed to the surface of the ridger plow for their experimental research to quantify the draft forces delivered to the surface According to their experimental findings, the maximum force at a 26-inch width and 10-inch depth diminishes as depth and width increase. Also, it has been shown that the width of the cut is significantly affected by the cut's various widths. In various trials, the range of draft forces ranges from 8 to 42 kg. Kifle et al. (2018) assessed the impact of linked ridgers and mouldboard plows on wheat productivity in three chosen districts of Ethiopia's Tigray region.

Traditional farming practices make up Ethiopian agriculture, which is influenced by the moisture content of the soil (Kifle et al., 2018). On a single farm, they chose four test plots for the comparison, and this was repeated with six farmers. The remedies included mouldboard plows, local maresha for plowing, and tie-ridgers. They conclude their experimental study that the tied-ridger is more successful at retaining moisture than the native maresha. Moldboard, according to their claims, plows deeper so that leftovers and weeds are deeply buried and converted to compost.

An in-situ device that could assess horizontal soil strength in real time while moving over a soil bin was created and evaluated by (Cho et al., 2015). In the system, several cone-shaped penetrometers were joined horizontally at intervals of 50 mm at the front of a vertical plow blade. Each penetrometer has a direct connection to a load cell that could detect stresses between 0.01 and 2.54 kN. They employed a microprocessor built into the measurement system to process the digital signals from each transducer concurrently. This real-time horizontal soil strength measuring system moved at 0.5 m/s through an indoor experimental soil bin using a wireless data connection between a data storage device and the measurement equipment. In their research, they contrasted the cone index (CI), as determined by a conventional cone penetrometer, with the horizontal soil strength index (HSSI), as determined by the system they invented. According to their findings, the coefficient of determination between the CI and the horizontal soil strength index was substantially lower at depths of 50 mm and 100 mm ($r^2 = 0.67$ and 0.88, respectively) than it was at depths below 20 cm ($r^2 \geq 0.93$). They also took measurements of horizontal soil strength indices, which were ordinarily higher than the CIs for a specific number of compactor operations. The coefficient of determination for all depth regression was 0.94, and the RMSE was 0.23. In comparison to the traditional soil strength measurement technique, a horizontal soil strength index measurement system was assessed. The shortcoming of this study is there are no included field tests.

The design of a penetrometer, which can measure the instantaneous soil resistance on tillage implements in the soil horizontally, and data gathering software based on the global positioning system (GPS) were studied by (Topakci et al., 2010). Microsoft Visual Basic was used to create the data acquisition software. After the system was designed, it was manufactured and put together, and a field test was then conducted. Under this study, soil resistance on tillage implements was mapped in the field for a soil depth of 40 cm using the Kriging method by ArcGIS, and data from GPS and penetration resistance values were recorded in the Microsoft SQL Server database. They conclude that during operation, neither mechanical nor software defects were noticed. As a result, the minimum and maximum values for soil resistance on tillage implements were determined to be 200 kPa and 3000 kPa, respectively.

(Frantisek Varga et al., 2013) created the hydraulically controlled tractor three-point hitch that uses force, positional, and mixed control types to examine different soil and topographic circumstances. In this study, force control received special attention since it enhances the use of tractors with mounted implements but, on the other hand, harms the uniformity of the working depth of implements on soils with varied resistance.

According to the initial circumstances for the implementation, the paper's theoretical analysis and experimental measurements determined the impact of soil resistance on tillage tools on the depth of tillage. Tillage depth, soil resistance, and plow cutting width all serve as initial conditions for an implementation. According to research, soil resistance on tillage implements has a significant impact on tillage depth, and as soil resistance increases, tillage depth falls nonlinearly. A less drastic reduction in tillage depth is correlated with a gradual rise in soil resistance on tillage equipment.

To take simultaneous in-situ measurements of soil penetration resistance and shear stress, (Boon et al., 2005) designed and created a tractor-mounted, automated soil penetrometer and shearometer unit. Two high-torque stepper motors were utilized in their investigation to move the penetrometer and shearometer carriages in the vertical axis direction, and a third stepper motor with a lower torque was employed to move the shearometer's rotating spindle. During the field sample operation, a personal computer data capture and differential GPS on the tractor helped in real-time measuring, displaying, and recording the tractor location, soil penetration resistance, and soil shear stress.

The automated soil penetrometer-shearometer unit was field tested, as well as data on soil moisture content, terrain slope, and tractor-implement performance characteristics were collected. Their study makes use of spatial maps that revealed significant site-specific variance in the observed parameters across the field. The results of the statistical analysis the author conducted to demonstrate a significant relationship between soil penetration resistance and shear stress as well as a significant relationship between soil moisture content and penetration resistance and shear stress revealed a significant relationship between the two. There is a strong link between soil moisture content shear stress and penetration resistance(Bertonha et al., 2015). Using the stepwise analytic method, multiple regression equations were created to forecast travel speed, apply draught, and calculate fuel consumption for mouldboard plowing on Serdang sandy clay loam soil. According to the results of Stepwise multiple regression analysis, a three-variable equation with tractor travel speed square, soil penetration resistance, and soil moisture content as independent variables could be used to accurately represent mouldboard draught for Serdang sandy clay loam soil (Topakci et al., 2010).

(Bertonha et al., 2015) examined the amount of disturbed soil, tractor performance, and corn crop production using three hoe-type tillage instruments of planters at various operating depths. The findings demonstrated that at working depths of 105 mm, 120 mm, and 135 mm, the soil disturbance was at its maximum. The treatments had no impact on the crop's final stand, grain production, or biomass. At a working depth of 135 mm, the opener with the highest tip angle (29°) displayed a lower traction power demand and fuel consumption than openers with 27° and 17° but generally used more fuel per volume of soil disturbance. The geometry of the opener and the kind of soil have a direct impact on crop development, machine performance, and soil disturbance as indicated in Fig.2.2.

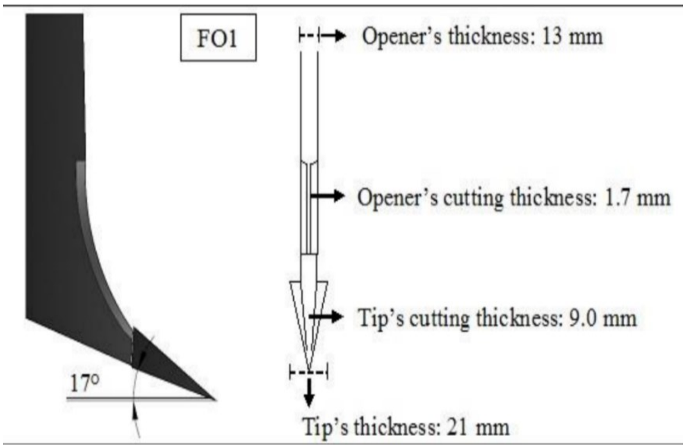

Figure 2.2: Characteristics and dimensions of tillage implements
Source: (Bertonha et al., 2015)

To cut through surface residue and plant seeds into undisturbed soil, (McLaughlin et al., 2019) designed and developed no-till grain drill tillage instruments; the opener performance might vary greatly under various soil and residue circumstances. With two no-till grain drills with different opener types, hoe, and triple disc, they undertake field experiments to assess seeding performance and implement draft and tractor fuel consumption for planting wheat under Atlantic Canada conditions.

The number of emerging plants and the actual depth of seeding were measured. An instrumented tractor was used to measure the drill draft and fuel consumption. Both opener types functioned equally well, as shown by the fact that ground speed and opener type had no impact on seeding depth, vertical seed scatter, or emergence rate. While seeding depth had a substantial impact on both opener types, ground speed had little bearing on the opener draft. At the same speed and depth, the hoe opener draft was roughly 200 N greater than the triple disc opener draft. When expressed on an area basis (Lha^{-1}), the fuel consumption at higher ground speeds was lower due to the enhanced tractor operating efficiency. Tractor fuel consumption was higher for higher ground speeds. The finding holds for globally comparable soil conditions, but it might not hold for unique or more challenging no-till seeding circumstances, such as fine-textured cohesive soil, compacted soil, or a significant amount of surface residue.

(Burce et al., 2013) conceptualized and created a special depth control system for zero tillage systems that are managed by separate tillage equipment. For soft, medium, and hard soils, the proper tillage for the control system was examined. Hoe, tine, and 2-disc tillage tools were assessed for uniformity in furrow shape, lateral and vertical seed distribution, soil penetration, and disturbance. According to the paper's summary, even in hard soils with high soil penetration, the hoe tillage implements exhibited no discernible difference in furrow form, and the variation in lateral and vertical seed distributions was reasonable.

2.7. Soil Compaction Measurement

Farm machinery is utilized for everything from land preparation to harvesting procedures by driving in fields in a mechanization system (FAO., 1990). In many parts of the world, the use of large farm equipment has led to extensive soil compaction. Compacted soil restricts plants' access to water and nutrients in the soil and is predicted to lower agricultural output (Liu et al., 2021). Farm equipment's weight compacts agricultural soil when in use, which can have both a good and a negative effect on the soil's physical and chemical characteristics (Ungureanu et al., 2015). Livestock trampling and farm machinery both contribute to soil compaction. Moreover, factors such as soil tillage, crop rotation, soil moisture, and working depth affect the danger of compaction (Bertonha et al., 2015). Even though they are crucial for preserving the soil quality of various agroecosystems, soil tillage, crop rotations, soil moisture, and working depth have consistently been ignored in the management of agricultural traffic (Guimaraes Junnyor et al., 2019). The main issue limiting agricultural production's potential output is soil compaction. Because of its increased strength and draft

resistance while being compacted, the soil is challenging to plow. The appropriateness of soil for agricultural, environmental, and engineering uses is significantly influenced by its physical characteristics (Phogat et al., 2015). Traditional soil cone penetrometers can be used to test soil strength (ASAE, 2013; Herrick & Jones, 2002; Topakci et al., 2010).
In agricultural studies, the soil CI is frequently used to evaluate the strength or compaction of the soil. Soil cone penetrometers are crucial measurement tools for characterizing the physical properties of soil in soil tillage research. A healthy root environment cannot be maintained if there is excessive compactness. Moreover, it causes runoff and erosion to rise and water penetration to decrease (Mudarisov et al., 2020). The soil depth, textural characteristics, bulk density, and moisture content all affect the CI value. According to research on agricultural fields with no-tillage and conventional tillage, the values of the CI decrease as clay fractions rise and rise as sand and silt fractions rise (Kumar, 2012).

In a split-split plot arrangement, (Mihretie et al., 2021) conducted a three-year study at the Aba Gerima watershed in north-western Ethiopia to examine the effects of two tillage practices (reduced tillage and conventional tillage), two planting methods (row planting and broadcast planting), and two compaction options with tillage and without tillage trampling on soil loss and teff yields.

Pore space, void ratio, dry volume weight, and bulk weight volume can all be used to represent the degree of soil compaction (Duiker, 2002; Koolen & Kuipers, 2012). To identify and describe the levels of soil compaction throughout the soil profile to employ the two important parameters, soil BD and PR (Duiker, 2002; Hatley et al., 2005; Raper, 2005; Soane et al., 1987). The PR of soils is measured using a soil cone penetrometer device with a 30° circular cone, and most published articles on soil compaction have adhered to a standard protocol for data recording and analysis(Agricultural & Engineers, 2006). When soil PR is presented, it is crucial to discuss soil characteristics and management information to describe and comprehend the impact of compaction (ASABE & Engineers, 2011; Standards, 2004). Soil texture, OM, soil moisture content (MC), BD by soil layer, cropping history, soil moisture retention curve, drainage condition, plasticity limit, and soil structural unit size are the most commonly collected data to investigate the soil physical and chemical properties (Standard, 2000).

The crucial soil PR ranges that potentially limit the growth of crop roots are thought to be between 1,500 kPa and 3,000 kPa (Hakansson, 2005). The lower threshold value, which was also reported to be 1,380 kPa, shows that this value is not constant (Kulkarni et al., 2010). This is true because several factors, including soil structure, soil texture, moisture, clay content, and SOM, have an impact on the degree of resistance (Reichert et al., 2009). Due to subsoil compaction in sandy clay loam soil, wheat and sorghum nutrient absorption was reduced, soil BD (+17%) increased from 1.65 to 1.93 mg/ m^3 and PR increased from 1,000 to 4,830 kPa (Ishaq et al., 2001). Crop root growth, development, and yield have all been proven to be restricted to variable degrees by cone index values of more than 2,000 kPa (Aase et al., 2001; Hamza et al., 2005). Crop yield and soil property ratio are inversely connected. For instance, as soil PR increased, soybean production declined (Sivarajan et al., 2018). An air-filled porosity of 10% (v/v) restricts soil aeration, and a soil PR of 3,000 kPa is frequently regarded as essential for crop root development (Håkansson et al., 2000; Lipiec & Hatano, 2003). Occasionally, visual inspection of the soil is employed to describe soil compaction.

2.7.1. Hand-held recording cone penetrometer

People used to probe the ground years ago while holding sticks, but they were solely used for support and weight balance. In recent years, scientific probing of sticks has been done in the fields of drawing and agricultural mechanization. Researchers began probing the ground with pointed rods in the early 1900s as they became more interested in understanding soil strength. To assess off-road vehicle mobility, (Swanson & Patin, 1973) created a hand-held manual cone penetrometer, and Waterways Experiment Station (1948) created a cone penetrometer. The penetrometer was a cone-shaped device with a base area of 161 mm^2 and a 300-degree apex angle. Their research was mounted on a graded shaft measuring 9.5 mm in diameter and 914 mm long. On the top of the shaft was a proving ring with a handle and a dial gauge to show the penetration resistance (Swanson & Patin, 1973). On the top of the shaft was a proving ring with a handle and a dial gauge to show the penetration resistance.

The proving ring was calibrated so that the dial gauge would display the force per unit area, or CI, of the soil resistance to tillage equipment. The WES standardized cone penetrometer was recommended for use in the field by the American Society of Agricultural and Biological Engineers (ASABE, 1968), and it is still in use today. These are a cone with a base area of 323 mm^2, a base diameter of 20.27 mm, a probe with a diameter of 15.88 mm for soft soil, and a cone with a base area of 130 mm^2, a base diameter of 12.83 mm, a probe with a diameter of 9.53 mm for hard soil. The size and form of the cone, the penetrometer's rate, and the degree of surface abrasion all affect the penetrometer resistance that is measured. Therefore, the American Society of Agricultural and Biological Engineers has established standards for soil cone penetrometer examinations to ensure testing consistency and ease in interpreting the data (ASABE, 1999). The dial indicator is first set to zero before conducting penetration tests. Dial gauge readings are taken every 25 mm of shaft penetration while the penetrometer is driven into the ground. Pushing the cone into the ground ought to be done consistently at a speed of about 30 mm/s.

To assess soil strength, a more sophisticated device known as a cone penetrometer was created in the Netherlands in the 1930s (Kees, 2005). When a cone-shaped device is steadily pushed into the ground, cone penetrometers measure the soil penetration resistance or soil strength that is encountered at different depths. Penetrometer features now include moisture and temperature sensors, soil structure analysis, and soil composition analysis thanks to advancements in electronics and software. The majority of the time, environmental and geotechnical site studies use these sophisticated penetrometers.

The hand-held electronic cone penetrometer was created by (Kees, 2005) to help identify compaction issues that might call for more thorough soil testing. It can also be used to examine variability or variations in soil strength brought on by machinery, automobiles, and foot traffic. The information from a penetrometer could be useful for this research project, which the agricultural sector has been using in forest tree nurseries. For example, it could help identify areas with high compaction, plow pans, and clay zones to help determine the best irrigation, fertilization, and cultivation practices. Finally, it is concluded that when the soil strength reaches roughly 1,500 kPa, soil compaction starts to hinder the root growth of the majority of plants (Swanson & Patin, 1973).

When the strength of the soil reaches roughly 2,500 kPa, the roots of many plants stop growing. Penetrometers can locate these locations more quickly and easily than conventional bulk density measurements. The penetrometer can pinpoint the problem regions, but further thorough soil testing may be necessary. The dynamic cone penetrometer was created by (Herrick & Jones, 2002), who defined it as an affordable, dependable, and long-lasting alternative to instruments that use strain gauges. It is especially suitable for almost all uses where a manually operated static penetrometer would be employed. It is especially beneficial for applications where the consistency of the operator or the soil conditions are unpredictable. Their study findings are readily implemented by farmers and ranchers because of their robust, all-steel construction and simplicity of usage. It cannot serve as a replacement for accurate measurements of soil bulk density because, like other penetrometer designs, it is sensitive to variations in soil moisture and texture. However, the penetrometer can be used to monitor changes in soil quality as a result of management and to pinpoint regions that need more precise readings. Additionally, it may be used to quickly find probable compaction zones in a profile and a field.

An integrated penetrometer was created by (Carter., 1968) to measure the typical soil strength. It was made up of a signal generator, an operational amplifier, and a force transducer. The circuitry's continuous recording and integrating capabilities made it possible to measure the penetrometer force by doing away with the time-consuming process of manual integration. A recording soil cone penetrometer with two components; one for measuring force and the other for detecting depth was created (Hendrick, 1969). A relative movement between an exterior barrel and the handle plunger was used to measure the force. The relative movement of the foot-plate shaft and penetrometer shaft as the tip was driven into the earth allowed for the measurement of depth. The penetrometer's tip was a round cone with a base area of 0.20 in^2 and a diameter of 300 degrees.

An electronic recording penetrometer operated by a solenoid was created by E. Rawitz et al.(1970). The cone had a 300-tip and a 0.2in^2 base area. They coupled a cone and shaft to a load cell that was housed in a sturdy casing and connected to a handle to measure the force. An unbounded strain gauge load cell with a 200 lb maximum capacity and a 0.12 mm total displacement was used to measure the force. The results of their experiment indicate that the output signal is proportionate to the force applied to the cone and that there is little to no cone deflection caused by the penetrometer handle.

2.7.2. Hydraulic-operated soil resistance on tillage implements

Because of the stresses generated by agricultural equipment, soil particles compact closer together and arrange into a smaller volume. The amount of space in the soil that is available for air and water decreases as soil particles are pushed closer together, reducing the amount of pore space. To evaluate soil resistance on tillage implements in the field up to a maximum CI value of 2,000 kPa, Kumar et al. (2019), created and constructed a mechanical soil cone penetrometer that is hydraulically powered.

According to standard ASABE S313.3. R2013, the system is primarily built using the hydraulic principle and a tractor hydraulic system, and it consists of a drive unit for inserting the probe into the soil at the specified speed (Kumar et al., 2019). The system is primarily built using a tractor-hydraulic system and is based on the hydraulic principle. It consists of a driving unit to drive the probe into the soil at the desired speed, a sensor unit to measure penetration resistance, and an acquisition system to automatically log data to the computer. According to ASABE's advice, the design of the penetrometer probe and cone tip was chosen. The system was controlled by a standard value penetration rate of 30 mm/s and a maximum depth of penetration of up to 150 mm. Overall, the device was created to work in a variety of field settings and was able to quickly gather data on soil strength.

To save time, labor, and potential measurement mistakes when collecting data on soil compaction for study, (Tekin & Okursoy, 2007) designed a three-point hitch-mounted hydraulic soil cone penetrometer. The typical penetrometer cone is pushed into the soil at a steady speed by a hydraulic piston as the hydraulic penetrometer is mounted on the three-point hitch. A computer-based 16-bit data acquisition system that includes a load cell, a portable computer, signal amplification, and the necessary control software for the sampling is used to record forces operating on the cone base. The hydraulically powered standard soil cone penetrometer was designed and built to attach on a three-point hitch and detect soil compaction in clay soil under large loads quickly and accurately.

2.8. Soil Strength and Compaction in Traction

The most significant variables that affect traction are soil type and conditions. More than modifications to tire loading or tire dimensions, changes in soil conditions have a significant impact on tire performance. The shear strength and normal strength of the soil both have an impact on the traction performance. Shear strength generally has more of an impact on slip and gross traction than normal strength does on motion resistance. To evaluate traction performance, soil cohesion, internal soil frictional angle, shear modulus, and sinkage characteristics (Bekker, 1967) determined the strength of the soil using CI or stress-strain equations.

To determine soil sinkage and shear properties, the Bevameter technique developed by (Bekker, 1966) is frequently employed. Therefore, the CI continues to be a "best guess" to determine the strength and consistency of cohesive-frictional soils. According to (Défossez et al., 2003), penetration resistance can be used to quickly assess the mechanical state of the soil on a given day. The penetrometer is a widely used tool for determining the strength of the soil. Cone penetrometers were created by (Vaz et al., 2011) based on ASABE criteria for determining soil strength, which is seen in (Fig. 2.3).

The force needed to drive the cone into the earth is recorded by depth. Dividing this force by the cone's base area gives the pressure measurement CI, usually in kN/m². For tillage and compaction, CI can be measured up to 500 mm deep, though the top 100-150 mm is often used for traction with the depth reference as shown in Fig.2.3. The soil density, moisture content, and type all have a significant impact on the CI, a measurement of the penetrating resistance of the soil (Busscher, 1990). According to experimental investigations, the CI declines when the soil moisture level rises (Voorhees & Walker, 1977) (Wells & Treesuwan, 1978).

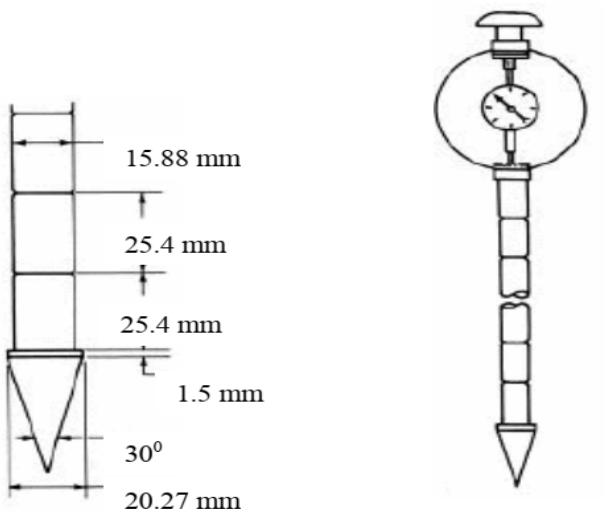

Figure 2.3: ASABE standard cone penetrometer
Source: (Vaz, et al.,2017)

Results of penetration tests conducted in sandy clay loam and clay loam soils showed that the dependency of maximum penetration resistance on bulk density was greater at lower moisture levels than at higher moisture levels. As a general rule, previous studies indicate that the soil CI increased with an increase in soil density. Similar conclusions were drawn from penetration test outcomes in clay loam and loamy sand as researched by (Hayes & Ligon). The effect of moisture content on intelligent soil compaction was examined by (Hu et al., 2020). It has been proven that intelligent compaction (IC) technology is a potent instrument for soil compaction. The effect of various moisture contents on soil modulus was determined using the compaction curves from the gyratory compactor and field compaction.

2.8.1. Soil strength

The evaluation of traction performance, soil cohesion, internal soil frictional angle, shear modulus, and sinkage characteristics are used to calculate the soil's strength using CI or stress-strain relationships. To measure soil sinkage and shear properties, Bekker (1956, 1960, and 1969) invented the Bevameter technique. It is, however, relatively pricey and inconvenient. Therefore, the CI continues to be a "best guess" to determine the strength and consistency of cohesive-frictional soils. According to research done by Defossez et al. (2003), the use of penetration resistance offers value for quickly assessing the mechanical condition of the soil on a given day.

2.8.2. Factors affecting soil cone index

The soil type, moisture content, and density all have a significant impact on the cone index (CI), which is a measurement of the soil's penetration resistance. Ayers and Perumpral (1982); Busscher (1990); Sojka et al. (2001); Vaz and Hopmans (2001); Dexter et al. (2007); Santos et al. (2012); Quraishi and Mouazen (2013) are a few examples of the numerous researchers that have studied related subjects. Based on the findings of researchers like Turnage (1970), and Turnage (1977), experimental tests have demonstrated that the CI decreases with rising soil moisture levels.

Collins (1971), and others found that the anticipated and experimental results values were very close in agreement due to the logarithmic connection between CI and moisture content. According to earlier studies, the soil CI rose as soil density increased, as discovered by (Melzer, 1971; Turnage, 1974). According to the findings of penetration experiments done on sandy clay loam and clay loam soils, maximum penetration resistance is more dependent on bulk density at lower moisture levels than it is at higher moisture levels. Similar findings were drawn from the findings of penetration experiments carried out in clay loam and loamy sand by (Hayes and Ligon, 1977).

Ayers and Perumpral (1982) looked at the effects of soil type, moisture content, and density on the CI. Zircon sand and Fire clay were combined in known amounts to represent five different soil types. Eight moisture levels ranging from 2 to 25 percent and density levels were taken into consideration. Based on the test results, the following empirical model was created to depict the CI as a function of density and moisture content as shown in Equation 2.1.

$$CI = \frac{C_1 \times \rho^{C4}}{C_2 + (MC - C_3)^2} \tag{2.1}$$

Where, CI= cone index in (kPa), ρ= dry bulk density in (kg/m^3), MC= moisture content C1-C4 = constants based on soil type.

Equations were created by Upadhyaya et al. (1982) to forecast CI in certain agricultural soils in Delaware. For silt loam, they suggested the following prediction Equation 2.2 using the dimensional analysis technique.

$$\alpha\left(\frac{CI}{BM}\right) = a\left(\frac{\rho}{\rho_s}\right)^n e^{-bMC} \tag{2.2}$$

Where: BM= bulk modulus in (N/m^2); ρ_s= soil particle density in (Kg/m^3); and e= nondimensional factor.

The impact of additional factors on the CI measurement, including the cone's base diameter, apex angle, and size of the penetrometer shaft to the cone's base diameter, cone surface finish, and penetration rate, has been researched in the past (Freitag (1968a); Gill (1968); Nowatzki and Karafiath (1972); Perumpral (1987). By employing a regular cone penetrometer, the impact of these parameters on the soil CI can be ignored. Table 2.3 ASABE standards (2011) and Table 2.4 provide typical CI values for a variety of soil situations (Brixius, 1987).

Table 2.3: Values of CI under different soil conditions

Soil	CI (kPa)
Hard	1800
Firm	1200
Tilled	900
Soft, sandy	450

Source: (Brixius, 1987)

According to the review in this section, it is clear that many studies have used CI to describe the soil for tractor traction performance in both laboratory and real-world settings. Although some researchers in the field have used hydraulically powered cone penetrometers, manual cone penetrometers have been the most widely used instrument to measure CI. According to Table 2.4, the typical CI values proposed by (Brixius, 1987) provide a solid foundation for sustaining the CI under various soil conditions.

Table 2.4: Cone index values

Soil Class	CI (kPa)	Typical Operating Conditions
Soft or Sandy soil (CI = 450)	0	
	350	Rice harvest
	480	Disking on the plowed ground or Low-land logging
	700	Spring plowing or Earthmoving on moist soil
Medium or Tilled soil (CI = 900)	850	Planting, field cultivation
	1000	Corn Belt harvesting, fall plowing
	1200	Wheat harvesting

Source: (Brixius, 1987)

2.9. Traction Prediction Approaches

The soil thrust is the horizontal propulsion force caused by the ground's shearing strength beneath a traction device. The remaining thrust, known as the tractive effort or drawbar pull, is used to accelerate the vehicle, climb a slope, or pull loads. A portion of this push is spent trying to overcome motion resistance (Bekker & terramechanics, 1960). To anticipate the traction properties of a wheel, numerous strategies have been created and utilized by different research researchers over time. The way these methods characterize terrain behavior varies generally.

2.9.1. Stress and strain of soil

(Bekker, 1956; Bekker & terramechanics, 1960) determined the maximum thrust force necessary to shear the ground along the ground contact area (A) and under load (W) based on Coulomb's Equation 2.3.

$$F = \left(Ac + W\tan\phi\right) + F_{sh} \tag{2.3}$$

Where: F_{sh} is the shearing force in (N) produced by tire treads or spuds of a track.

Spud action force in the (Equation 2.3) it takes the form

$$F = blc\left(1+\frac{2h_t}{b}\right) + W\tan\phi\left[1+0.64\left\{\left(\frac{2h_t}{b}\right)\cot^{-1}\left(\frac{2h_t}{b}\right)\right\}\right] \tag{2.4}$$

Where: h_t is the height of the tread or grouser in (m).

(Bekker, 1956; Bekker & terramechanics, 1960) suggested a solution for defining the relationship between soil properties, the geometry of the ground contact area, load, slippage, and soil thrust in terms of distance between the front end of the ground contact area and the point where the unit thrust is to be determined. This is because soil thrust reaches a maximum at a certain amount of optimum slip. (Janosi & Hanamoto, 1961) created a less complicated equation to describe peripheral force or thrust in Equation 2.5 since the original relationship was too complex.

$$F = \left(Ac + W\tan\phi\right)\left(1 - e^{\frac{-j}{k}}\right) \tag{2.5}$$

Where: j= Sx soil displacement in (m); K= a constant, for a particular soil; S= slip (%); and x= distance from the front of the contact area in (m).

Upon integration over the whole length l of the ground contact area, the total soil thrust is given by

$$F = \left(Ac + W\tan\phi\right)\left(1 + \frac{Ke^{-Sx}}{Sx} - \frac{K}{Sx}\right) \tag{2.6}$$

To investigate the impact of ply rating on tire performance on grassland, stubble, and plowed land characterized the soil using Bekker's sinkage displacement coefficients, bulk density, moisture content, particle size classification, soil-to-steel, and soil-to-rubber friction coefficients, cone penetrometer readings (Dwyer et al., 1990). He concluded that ply-rating did not seem to have a significant impact on the thrust obtained at typical working slip levels. The stiffer, higher ply rating tires have more rolling resistance, especially on the softer soils, thus it does have a significant impact on that.

A semi-empirical model developed by (Roşca et al., 2014) predicts the traction force for a 2WD farm tractor under the assumption that the tire-ground contact area is shaped like a super elliptical as indicated in Fig.2.4. The value of the super elliptical exponent was set to k = 3.5 to produce the best match between model data and experimental data. After reviewing the stress-strain relationship technique, it is clear that Bekker's way of forecasting tractive performance provides a good understanding of the effects of different factors and allows different ground-drive system designs to be assessed on paper.

Although applicable to any soil, it is too complicated to be used in real life. Although simpler, the Janosi-Hanamoto equation is only applicable to soils that exhibit asymptotic shear diagrams. Both formulas hold for tracked vehicles. However, it was modified for pneumatic tires (Bekker, 1985). These equations also take into account the tire-soil contact area for the prediction of tractive force under dynamic situations, which calls for highly technical field instrumentation. As a result, it is challenging to employ these equations for a traction device with reasonable simplicity.

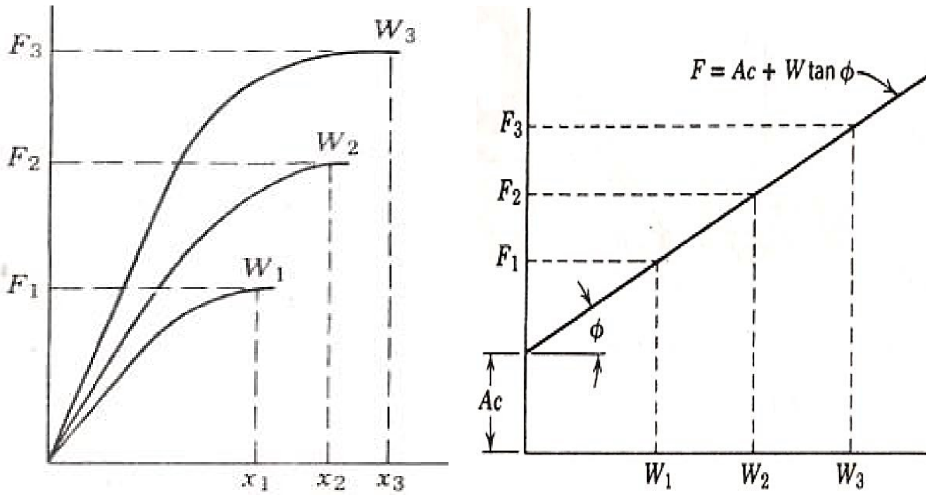

Figure 2.4: Force vs. soil displacement, for different values of normal load
Source: (Dwyer et al., 1990).

2.9.2. Techniques for single-wheel testing

The moving wheel must be supported, the necessary torque must be applied, and the net traction must be measured to create a basic traction wheel test equipment. But this can be done in several ways, each with a different amount of intricacy. Some equipment can only be used in dirt bins, while other equipment is used outside. In other instances, testing is carried out using whole cars, with the driving wheels or tracks acting as the tractive device.

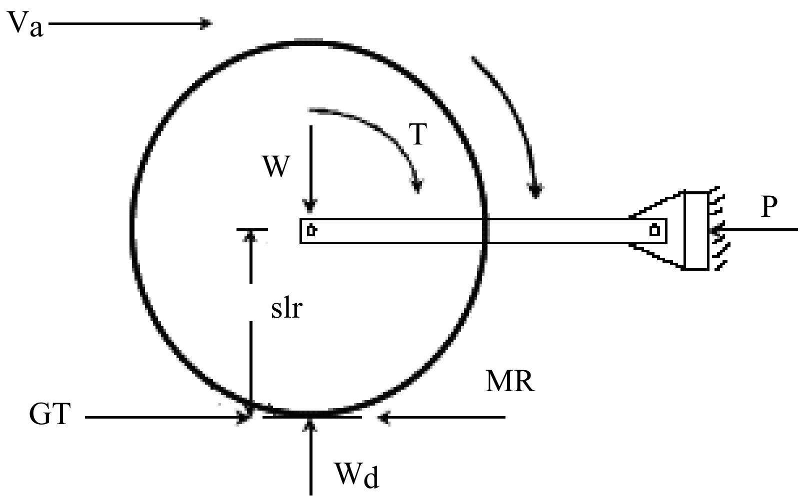

Figure 2.5: The simplest form of single-wheel tester
Source: (Tiwari et al., 2010), (Zoz and Grisso, 2003b)

Numerous tire testing instruments have been created globally since experimental approaches virtually totally dictate tire design (Tiwari et al., 2010). For single-wheel testing, (Zoz & Grisso, 2003b) have identified three fundamental apparatuses. A change in input torque causes a change in vertical force reaction, which may be dynamically evaluated during the test with the single-link device as shown in Fig. 2.5.

As indicated in Fig. 2.6 a change that eliminates the weight transfer effect may make it more challenging to quantify pull and torque. The torque may be computed as the difference between the forces multiplied by the distance between the arms, and the pull can be calculated as the sum of the response forces. The mechanism used by most single-wheel tests is depicted in Fig. 2.7. The input to the wheel is where torque is measured. As torque is applied, a vertical reaction with parallel arms remains constant (W = Wd).

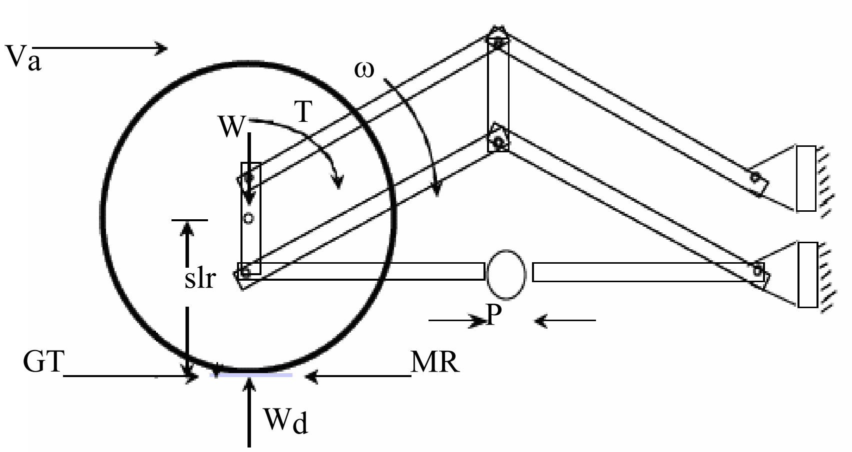

Figure 2.6: Single-wheel tester with parallel arms
Source: (Tiwari et al., 2010), (Zoz and Grisso, 2003b)

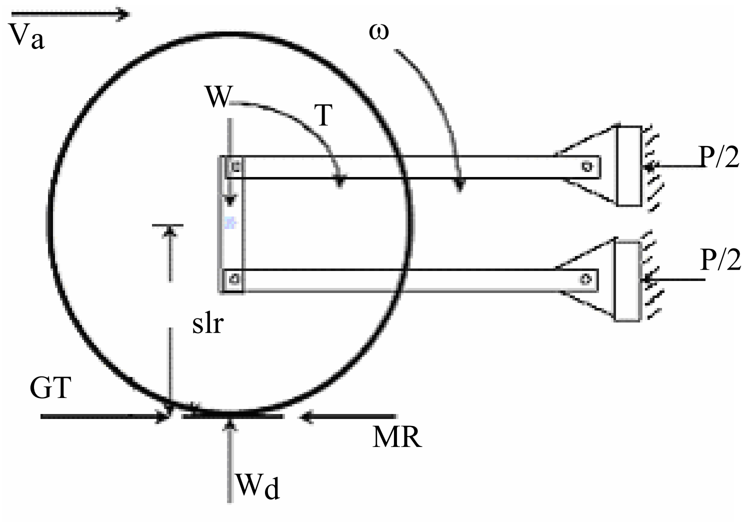

Figure 2.7: Parallel arm single-wheel tester with direct measurement of pull
Source: (Tiwari et al., 2010), (Zoz and Grisso, 2003b)

A mechanism for interior soil bins was created by the National Soil Dynamics Laboratory (Burt et al., 1980). The tester may carry out either variable slip tests (while maintaining the dynamic load constant) or variable dynamic load tests since it is possible to independently change the testing device's speed and the angular speeds of the test tire (while maintaining the slip constant). There is a control system for each key operation, including vertical load, test tire angular velocity, and device forward velocity. The test tires' ranges are 12.4-28 to 30.5-32, and the applied vertical load and draft force can reach 71.2 kN and 44.5 kN, respectively.

The NSDL unit has a high degree of control over all required tire tests. To conduct controlled field tests, the single wheel tester was created in 1986 at the University of California in Davis in the United States by (Upadhyaya et al., 1986). Between the rails is a driven test tire that is being towed by the tractor. Slip is created by the discrepancy between the forward speed of the entire apparatus and the angular speed of the test tire. The test tires have a diameter range of 0.46 to 2 m, a vertical force limit of 26.7 kN, and a draft force limit of 13.2 kN. The Davis field single-wheel tester combines a field testing instrument with a dirt bin. This tester has the benefit of working in controlled environments outside.

Additionally, a fully instrumented tool has been created to gauge traction-related characteristics of the soil (Upadhyaya et al., 1997). The instrument could measure soil shear parameters with grouser plates and sinkage parameters with sinkage plates. The soil CI can also be measured using this tool. To compare the tractive ability of several tires, (Upadhyaya, 1988) emphasized consistent test methodologies and zero circumstances. They claimed that the degree to which various testing methodologies (constant slip, constant draft, variable slip, and varying slip) affect scatter in traction data varies.

A constant slip test process produces reproducible and consistent findings, whereas a variable slip test procedure produces significant data scatter. During tire testing, they noticed that changing slips seemed to have a significantly greater impact on the system dynamics than changing drafts. They recommended forecasting the real slip and rolling radius under the presumption of zero. A rig attached to a four-wheel trailer served as the foundation for the tester (Ambruster & Kutzbach, 1989) created at the University of Hohenheim. Throughout the test run, a tractor was used to haul the trailer. The tester could accommodate tires with a diameter of up to 2 m and could apply a vertical force of up to 40 kN. This tester's capacity to test driven inclined wheels is its key benefit.

A brand-new field single-wheel testing apparatus was created by (Shmulevich et al., 1996) to conduct tire traction tests under varied slip or vertical load circumstances. A heavy-wheeled tractor with a unique soil property testing device was installed at the front and a tire-testing device was mounted at the rear. While the torque was measured by a different linkage method, the vertical, horizontal, and side forces could be monitored inside a frame that holds the test wheel. The tire testing apparatus could test tires with a diameter of up to 2 m and could exert vertical forces of up to 50 kN and torques of up to 31 kNm. According to the review, single-wheel testers may evaluate a variety of tire sizes, typical loads, drafts, and speeds. A single-wheel tester needs to be equipped to be able to continuously measure the forward speed, tractive force, and torque. Both the continuous slip and constant draft test protocols produced reliable results, therefore traction investigations can employ either of the two techniques. A description of the mobility number technique for traction prediction modeling is provided in the following section.

2.9.3. Mobility number approach

Accurate modeling of the intricate interplay between a pneumatic tire and the terrain is challenging. Empirical techniques based on mobility numbers and a dimensional analysis approach have been developed to address this issue. Generally speaking, these models are based on the testing outcomes of several chosen pneumatic tires on a variety of relevant terrains. Then, using basic measurements and observations, the measured vehicle performance is empirically associated with the terrain. This can result in the creation of a scale that compares the ability of the topography to support traffic on one side and vehicle mobility on the other.

(a) Mobility number model

From the U.S. Army Engineer Waterways Experiment Station's (WES) trafficability analysis, one of the first empirical models for soil-tire performance was developed. This analysis, which was initially created to provide a method to analyze vehicle trafficability and mobility of the military vehicle, was based on the cone penetrometer description of soil quality. The technique is continually being updated and validated after being established empirically from the outcomes of several field experiments with a variety of vehicles in fine-grained soils. To forecast the tractive performance of treadle pneumatic tires on soft soils, (Freitag, 1996) proposed a mobility number method based on dimensional analysis, which is how the mobility number idea was initially developed. The following two mobility numbers, or dimensionless ratios based on CI, were created, one for sand and the other for clay. The clay mobility number, sand mobility number, and soil cone index gradient (G_{CI})

were defined using the following Equation.

$$N_{CC} = \frac{CIbd}{W}\left(\frac{\delta}{h}\right)^{\frac{1}{2}} \tag{2.7}$$

$$N_S = \frac{G_{CI}\left(bd\right)^{\frac{3}{2}}}{W}\left(\frac{\delta}{h}\right) \tag{2.8}$$

Where: N_{cc}= clay mobility number; N_s = sand mobility number; CI = soil cone index in (kPa); G_{CI} = soil cone index gradient in (kPa); B = unloaded tire section width in (m); D = unloaded overall tire diameter in (m); W = dynamic load on the tire in (kg); δ = tire deflection in (m) and H = tire unloaded section height in (m).

The CI gradient (G_{CI}) was defined as:

$$G_{CI} = \frac{CI - CI_{surf}}{\frac{1}{2}\ depth\ of\ \text{int}\,erest} \tag{2.9}$$

Where: CI= average cone index in (kPa) and CI_{surf} = Cone index at the surface in (kPa).

The cone index was measured over a depth of 150 mm to characterize the topography, and it was found that CI is a reliable indicator of soil consistency. To evaluate the applicability and validity of the analysis technique, the predicted vehicle cone index (VCI) and measured VCI for a chosen vehicle at various inflation pressures were compared (Turnage G. W., 1972).

$$N_{CI} = \frac{CIbd}{W}\left(\frac{\delta}{h}\right)^{\frac{1}{2}}\left(1+\frac{b}{2d}\right)^{-1} \tag{2.10}$$

In an additional effort to match the wheel laboratory data from the vehicle field test, Turnage offered a modification: rating penetration resistance (RCI) was employed in place of CI. More accurately than any other soil parameter that has been examined in WES trafficability tests, RCI characterizes the soil strength that predominates during multipass tire traffic. The new definition of the clay mobility number was defined as

$$N_{RCI} = \frac{RCI.b.d}{W}\left(\frac{\delta}{h}\right)^{\frac{1}{2}}\left(1+\frac{b}{2d}\right)^{-1} \tag{2.11}$$

(Wismer & Luth, 1973) employed a straightforward wheel numeric as

$$C_n = \frac{CI.b.d}{W} \tag{2.12}$$

(Rowland & Peel, 1975) wheel numeric (N_R), used for determining the mean maximum pressure (MMP) is analyzed using Equation 2.13.

$$N_R = \frac{CI.b^{0.85}d^{1.15}}{W}\left(\frac{\delta}{h}\right)^{0.5} \tag{2.13}$$

In Rowland's wheel numeric (NR), (Maclaurin, 2007) replaced the factor δ/ h with δ /d and claimed that this made the model simpler to use without compromising its accuracy.

$$N_M = \frac{CI.b^{0.8}d^{0.8}\delta^{0.4}}{W} \tag{2.14}$$

(Maclaurin, 2007) also examined the basic wheel numeric provided by

$$W_{Ni} = \frac{CI}{P_i} \tag{2.15}$$

(Maclaurin, 2007) determined that a basic wheel numeric C_n, as proposed by (Wismer & Luth, 1973), was preferable for expressing the tire/soil interaction. (Brixius, 1987) provided various wheel numbers known as mobility numbers. By incorporating the deflection-to-height ratio and section width-to-diameter ratio, he adjusted the Wismer and Luth wheel numerical. This mobility number is suggested to be

$$B_n = \frac{CIbd}{W}\left(\frac{1+5\frac{\delta}{h}}{1+3\frac{b}{d}}\right) \tag{2.16}$$

The Wismer and Luth (1973) wheel numeric is the mobility number that has been most frequently used in the literature among those that have been proposed. This wheel number is not appropriate for tires with varied tire inflation pressures because it does not take deflection into account as an input variable. Due to its greater working range, the Brixius mobility is superior in this regard.

(b) Traction models

Traction models based on the mobility number approach are as follows:

Models based on Turnage and Freitag mobility numbers

(Turnage G., 1972) created models based on field tests of military vehicles and dirt bin tests. Military tires were installed on the test vehicle to determine the minimal soil cone index (CI) in a no-go scenario. Because they are based on outdated technologies, the models may provide low mobility predictions for contemporary automobiles. These are examples of field test models:

$$COT = \frac{P}{W} = 0.8 - \frac{1.3}{\left(N_{CI} - 2.45\right)} \tag{2.17}$$

$$MRR = \frac{MR}{W} = 0.04 + \frac{0.2}{\left(N_{CI} - 2.5\right)} \tag{2.18}$$

Laboratory test models

$$COT = 1.51 - \frac{12.37}{\left(N_{CI} + 594\right)} \tag{2.19}$$

$$MRR = 0.04 + \frac{0.2}{\left(N_{CI} - 1.5\right)} \tag{2.20}$$

Dwyer et al.(1985) examined a variety of tires at varied loads and inflation pressures operating under diverse field circumstances using the mobility number of Turnage. The manual was developed using the empirical relationships between performance metrics and the mobility number that are shown below.

$$(COT)_{20\%} = 0.56 - \frac{0.47}{N_{CI}} \tag{2.21}$$

$$MRR = 0.07 + \frac{0.2}{N_{CI}} \tag{2.22}$$

$$(TE)_{\max} = 78 - \frac{55}{N_{CI}} \tag{2.23}$$

$$\left(COT\right)_{TE(\max)} = 0.41 - \frac{0.21}{N_{CI}} \tag{2.24}$$

$$\left(S\right)_{TE(\max)} = 9 + \frac{19}{N_{CI}} \tag{2.25}$$

where, $(COT)_{20\%}$ = coefficient of traction, MRR= motion resistance ratio, TE (max) = maximum tractive efficiency in (%), $(COT)_{TE\ (max)}$ = coefficient of traction at maximum tractive efficiency, and $(S)_{TE\ (max)}$ = slip at maximum tractive efficiency.

Gee-Clough et al. (1978) identified the following relationships after analyzing a wider variety of data.

$$(COT)_{\max} = 0.796 - \frac{0.92}{N_{CI}} \quad (2.26)$$

$$k\left(COT\right)_{(\max)} = 4.838 + 0.061 \times N_{CI} \quad (2.27)$$

$$COT = \left(COT\right)_{(\max)}\left(1 - e^{-ks}\right) \quad (2.28)$$

$$MRR = 0.049 + \frac{0.287}{N_{CI}} \quad (2.29)$$

Where: K = a rate constant, and N_{CI} = Turnage mobility number.

These equations were used in the prediction of vehicle performance ((Gee-Clough, 1980). (Pandey et al., 2001) studied bias-ply tractor tires in soil bins using sandy clay loam soil. (Freitag, 1966) developed empirical equations based on the mobility number suggested by narrower tractor tires (b=0.280 to 0.350 m, b/d=0.23 to 0.25) with deflection (δ/h=0.18 to 0.26).

$$COT = \frac{P}{W} = 0.76\,(1 - e^{-0.07 N_{cc}.S}) \quad (2.30)$$

$$GTR = \frac{T}{r.W} = 0.36\left(1 - e^{-0.35 N_{cc}.S}\right) \quad (2.31)$$

Were: $N_{CC} = \frac{CI.bd}{W}\left(\frac{\delta}{h}\right)^{0.5}$; COT = coefficient of traction; GTR = gross traction ratio, and S = slip, decimal.

(i) Models based on Wismer and Luth's approach

For cohesive-frictional soils, (Wismer & Luth, 1973) developed empirical relationships for the tractive performance of tires. Equations were derived to characterize the tractive properties of driven and towed farm tires. For bias-ply pneumatic tires with the standard tread designs having a b/d ratio of 0.3, /h ratio of 0.2, and r/d ratio of 0.475, his prediction equations are appropriate. The calculated equations for the gross traction ratio (T/rW) and the motion resistance ratio (MR/W) are as follows.

$$\frac{MR}{W} = \frac{1.2}{C_n} + 0.04 \quad (2.32)$$

$$\frac{T}{r.W} = 0.75\left(1 - e^{-0.3 C_n.S}\right) \quad (2.33)$$

where, C_n = wheel numeric, $C_n = \frac{CI.bd}{W}$; P = wheel pull in (N); W = dynamic wheel load in (kg); T = wheel torque in (Nm); R = wheel rolling radius in (m)

To define the traction characteristics of tractors tested on the concrete surface at the University of Nebraska, (Leviticus & Reyes, 1983) used a generalized form of the (Wismer & Luth, 1973) model. The equation was the same as Wismer and Luth's, but the motion resistance was ignored. They also noted that the rubber hardness would be the CI for a wheel operating on soil, but according to Wismer and Luth's equation, this factor is equivalent to 0.3 times the CI. Clark and Dahua (1995) proposed a modification to the Wismer and Luth (1973) model, yielding the following two equations:

$$\frac{MR}{W} = \frac{C_1}{C_n} + C_2 \tag{2.34}$$

$$\frac{P}{W} = C_3\left(1 - e^{-(C_4 C_n .S}\right) - \left(\frac{C_1}{C_n} + C_2\right) \tag{2.35}$$

Where: C_n = wheel numeric; $C_n = \frac{CI.bd}{W}$; MR= motion resistance of wheel in (N); P= net pull or traction of a driving wheel in (N); W= dynamic load on the wheel in (N); b= unloaded tire section width in (m); d= unloaded overall tire diameter in (m); CI= cone index in (kPa); C_1, C_2 = constants depending on the soil surface; C_3= constant, a function of the maximum net tractive ratio; and C_4= constant, a function of the soil surface and tires.

The generalized constants C_1, C_2, C_3, and C_4 may allow the model to be used for a broader range of actual field conditions than Wismer and Luth's equation which was only valid when the tire deflection to the undeflected section height ratio (δ/h) was limited to a 0.20 value (Clark & Dahua, 1995). (Rummer & Ashmore, 1985) developed the following rolling resistance coefficient model for skidders operating on firm soils.

$$MRR = 0.24\left(\frac{W_W}{CI.b.d}\right) + 0.06\left(\frac{W_W}{4W_R}\right) \tag{2.36}$$

The model was modified for one wheel, with certain accuracy, as follows:

$$MRR = \frac{1.15}{C_n} + 0.06\left(\frac{W}{4W_R}\right) \tag{2.37}$$

Where: W= wheel load in (kN); W_W = vehicle total weight in (kN) and W_R= rated a load of tire defined by the tire and rim association in (kN).

(Ashmore et al., 1987) created traction equations for pneumatic log-skidder tires that were tested in a soil bin under various loading and soil conditions. American clays and silts were the soil types. The following are the developed equations for gross traction ratio and motion resistance ratio:

$$GTR = 0.47\left(1 - e^{-0.2C_nS}\right) + 0.28\left(\frac{W}{W_R}\right) \tag{2.38}$$

$$MRR = -0.1\left(\frac{W}{W_R}\right) + \frac{0.22}{C_n} + 0.2 \tag{2.39}$$

Where: C_n= wheel numeric as described by (Wismer & Luth, 1973).

The dynamic load ratio (W/WR, was added by Ashmore to the empirical model developed by Wismer and Luth. The dynamic load ratio accounts for the varying dynamic loads that occur frequently during skidding operations. When compared to (Wismer & Luth, 1973), found that while both equations show similar trends, quantitative differences resulted from testing a less flexible tire over a range of dynamic loads. If a tire is operated near its rated load under ideal conditions, the asymptotic constant will approach 0.75, as shown in the (Wismer & Luth, 1973) equation. (Kumar, 2015) used empirical equations for the coefficient of traction and gross traction ratios to develop generalized forms of Wismer-Luth equations.

$$\frac{P}{W} = C_1\left[1 - \exp(-C_2S)\right] \tag{2.40}$$

$$\frac{T}{r.W} = C_3\left[1 - C_4\exp(-C_5S)\right] \tag{2.41}$$

Where: C_1 to C_5 are coefficients from the non-linear regression technique

With good correlation, (Kumar, 2015) and Upadhyaya *et al.* (1988, 1989) used these equations to evaluate the tractive performance of a variety of tire sizes, inflation pressures, dynamic loads, soil conditions, and loading procedures. With limited success, the challenge of relating traction coefficients to soil and tire parameters was attempted. (Gu & Kushwaha, 1994) discovered that (Equation 2.40 and 2.41) fit their experimental data very well as well.

(iii) Models based on the Brixius approach

Brixius presented new equations that improved tractive performance predictions and broadened the range of application over Wismer and Luth's equations (Brixius, 1987). These equations are now the most widely used traction equations. Brixius models are based on farm tractor drawbar pull tests conducted by John Deere Co. in the United States. As a function of soil strength, tire load, slip, tire size, and tire deflection, tire torque, motion resistance, net traction, and tractive efficiency are predicted. The following equations can only be used with tires that have a b/d ratio between 0.1 and 0.7, static radial-ply tire deflections between 10% and 30% of the height of the undeflected tire section, and W/(bd) values between 15 and 55 kN/m^2 (ASABE Standards, 2011).

$$GTR = \frac{T}{r.W} = 0.88\left(1-e^{-0.1B_n}\right)\times\left(1-e^{-7.5.S}\right)+0.04 \tag{2.42}$$

$$MRR = \frac{MR}{W} = \frac{1}{B_n} + 0.04 + \frac{0.5\times S}{\sqrt{B_n}} \tag{2.43}$$

$$B_n = \frac{CI.b.d}{W}\times\left(\frac{1+5\frac{\delta}{h}}{1+3\frac{b}{d}}\right) \tag{2.44}$$

Where, B_n= Mobility number, b= unloaded tire section width in (m), d= unloaded overall tire diameter in (m), h= tire section height in (m), δ= tire deflection in (m).

(Evans, 1991) used a TK Solver to develop a traction prediction and ballast selection model based on (Brixius, 1987) traction equations. To improve traction predictions for a specific tractor operating on a grass surface, the coefficients of tractive equations were modified. The slip parameter in the gross traction equation was decreased from 7.5 to 4.15, while the slip parameter in the motion resistance equation was increased from 0.5 to 0.0.

$$GTR = 0.88\left(1-e^{-0.1B_n}\right)\times\left(1-e^{-4.1.S}\right)+0.04 \tag{2.45}$$

$$MRR = \frac{MR}{W} = \frac{1}{B_n} + 0.04 \tag{2.46}$$

(Al-Hamed et al., 1994) employed a broad form of Brixius equations. These equations for tires include six coefficients (C1-C6) and two constants (K1 and K2).

$$B_n = \frac{CI.b.d}{W}\times\left(\frac{1+K_1\frac{\delta}{h}}{1+K_2\frac{b}{d}}\right) \tag{2.47}$$

$$GTR = C_1\left(1-e^{-C_2B_n}\right)\times\left(1-e^{-.C_3S}\right)+C_4 \tag{2.48}$$

$$MRR = \frac{C_5}{B_n} + C_4 + \frac{C_6S}{\sqrt{B_n}} \tag{2.49}$$

As shown in Table 2.5, they changed the numerical values of these coefficients and constants for radial tires.

Table 2.5: Coefficients tires parameters

Coefficients	Brixius for bias-ply tires	Brixius for radial-ply tires	Al-Hamad et al. for radial-ply tires
K_1	5	5	5
K_2	3	3	3
C_1	0.88	0.88	0.88
C_2	0.10	0.10	0.08
C_3	7.5	8.5 to 10.5	9.5
C_4	0.04	0.03 to 0.035	0.032
C_5	1.0	0.9	0.9
C_6	0.5	0.5	0.5

Source: (Al-Hamed et al., 1994)

These modifications were made to more accurately represent the results of recent radial-ply tire tests. To predict the tractive performance of bias-ply tires used in India, (Tiwari et al., 2010) proposed the following model.

$$GTR = 0.66\left(1-e^{-0.09B_n}\right)\times\left(1-e^{-5.2.S}\right)+0.035 \quad (2.50)$$

$$MRR = \frac{1.2}{B_n}+0.035+\frac{0.77\times S}{\sqrt{B_n}} \quad (2.51)$$

According to the literature, bias-ply tires on rear wheel-driven tractors have been used frequently to predict traction performance using the Brixius model. This model is also included in the ASABE standards. However, the coefficients of this model can be changed to account for large differences between predicted and observed field results.

2.10. Tire and Soil System Parameters

The interaction of soil and tires is a very complex process. Tire tractive ability is affected by tire type (radial versus bias), tire geometry (width, overall diameter, and section height), lug design, inflation pressure, dynamic load on the axle, and soil type and conditions (Upadhyaya et al. 1989).

2.10.1. Inflation pressure

(Zombori, 1967) looked at the effect of inflation pressure on drawbar pull and tractive efficiency. According to the findings of his research, a decrease in inflation pressure caused an increase in drawbar pulls at constant travel reduction. According to Zoz (1972), lowering the ground contact pressure is typically a good way to improve tractive efficiency.

Wulfsohn et al. (1988) used a dimensional analysis procedure to test four tires (18.4×38, 18.4×R38, 14.9×28, 14.9×R28) at two different inflation pressures and three different vertical loads in a well-tilled Yolo loam soil. They found that larger tires outperformed smaller tires, that increased dynamic load improved performance and that large radial-ply tires had an average tractive efficiency of 27.23 percent versus 25.37 percent for large bias-ply tires over the 0-30 percent slip range. (Arvidsson & Ristic, 1996) discovered that as inflation pressure increased, so did rut depth, penetration resistance, and soil stress. Low-profile tires did not reduce compaction when used at low inflation pressures. Bailey et al. (1996) measured soil stresses under a radial-ply tractor tire at two different dynamic load and inflation pressure levels. Peak soil stresses and bulk density increased as dynamic load and inflation pressure increased. (Lee et al., 1997) studied the effect of inflation pressure on the tractive performance of bias-ply tires used on agricultural tractors. The test results showed that when the inflation pressure was reduced from 250 kPa to 40 kPa by a decrement of either 30 kPa or 50 kPa depending on the test surfaces, the traction coefficient and tractive efficiency increased maximally by 14 and 6 percent, respectively, at 20 percent slip.

2.10.2. Wheel-soil parameters

Taylor et al. (1967) investigated the effect of tire diameter on tractive performance. At the same normal load and inflation pressure, increasing tire diameter resulted in increased pull and tractive coefficient. Gill and Vanden Berg, (1968), Zoz, (1972), and Burt and Lyne, (1985) discovered that the normal range of travel speeds used by farm tractors did not affect traction performance. Greenlee et al. (1986) reported that the net pull-to-dynamic weight ratio decreased as speed increased. Dwyer et al. (1976) investigated tire tractive performance under various soil conditions. They discovered that in good tractive conditions, increasing increase in the drawbar pull developed and an increase in inflation pressure. (Burt & Goudie, 1979) examined how dynamic load affected tractive effectiveness. They emphasized that, at constant travel reduction, an increase in dynamic load increased tractive efficiency on compacted soil but decreased tractive efficiency on uncompacted soil. This supports the findings of Kliefoth (1966), who found that on soils with low bearing capacity, the coefficient of traction decreased as the load on the tire increased. (Gee-Clough, 1980) reported that the diameter had to be increased by 50% but the width by 60% to achieve good performance. (Dwyer & Heigho, 1984) compared the tractive performance of single tires and dual tires in a variety of field conditions. The widest tires' tractive performance was generally inferior to that of more conventional sizes.

2.11. Conceptual Frame Work

A silent contributor to the systematic destruction of soil structure and the ongoing decline in yield per unit area is soil compaction. Natural causes of soil compaction, such as raindrops and animal trampling, can prevent seeds from germinating. The main contributor is field traffic, including farm tractors, combine harvesters, and forage harvesters, to name a few. In Fig. 2.8, the causes and effects of soil compaction are listed.

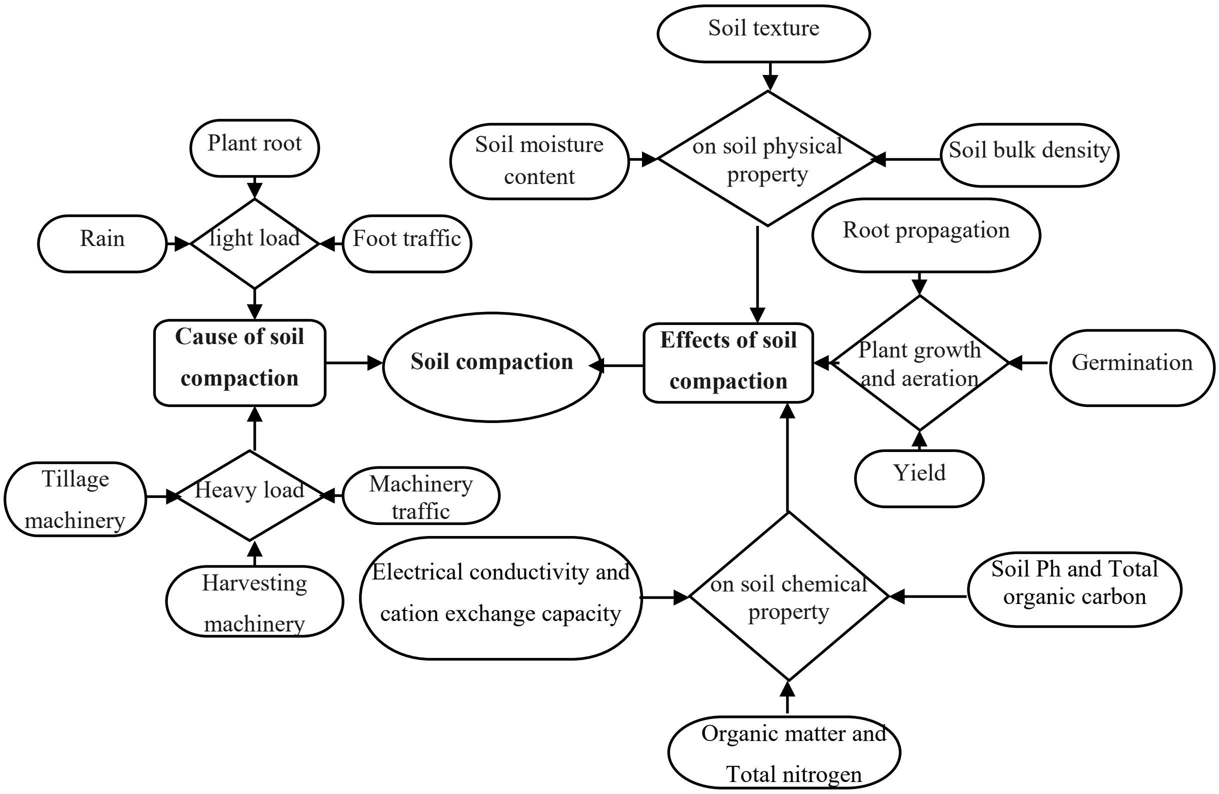

Figure 2.8: Cause and effects of soil compaction

Farm trafficking causes both topsoil compaction and, more importantly, subsoil compaction. Another cause of soil compaction is a lack of crop rotation in the soil. Soil physical properties include soil texture and moisture content, while soil chemical properties include inorganic soil matter, organic soil matter, cation exchange capacity, soil pH, and soil electrical conductivity. Soil physiochemical properties and machinery traffic during farm operations such as land preparation, harvesting, and even post-harvest activities are causes of concern for this study.

2.12. Summary

Related studies about soil compaction and causes for soil compaction were briefly discussed in this chapter**.** Physical characteristics of soil, such as moisture content and texture addressed. The soil's moisture content is important for soil compaction study, and soil structure, and water transmission ability were discussed. The chemical characteristics of soils were discussed, including inorganic and organic soil components, colloidal soil particle properties, soil reactions, and the buffering effects of basic and acidic soils. Studies linked to the CEC were discussed, which is a measure of the total negative charges in the soil that absorb plant nutrition cations like calcium, magnesium, and potassium.

A measure of soil pH, an important soil chemical property that influences plant adaptability, nutrient availability, soil microbial activity, chemical cycle, and the mobility of contaminants like metals, was briefly described. Plants, animals, insects, earthworms, nematodes, arthropods, protozoa, fungi, and bacteria that dwell in the soil are also discussed as part of the biological component. The most important factors that influence traction and traction prediction modeling were explained. Soil tire interaction parameter, and inflation pressure that affect tractive performance was discussed.

CHAPTER 3

3. MATERIALS AND METHODS

3.1. Geographical Locations

In this study, farm areas Bishoftu, Kulumsa, and Awash Melkasa were chosen for the experiment.

Bishoftu is a town in the East Shewa Zone of the Oromia Region in Ethiopia (Kebede et al., 2016). This area is 1,920 meters above sea level and 47.9 kilometers southeast of Addis Ababa with the GPS coordinates from 8° 25' 4.7400" to 8° 54' 6.500" N and 39° 0' 30.7188" to 39° 1' 12.7188" E. The texture of the soil in this experimental area is loam.

The second location is Kulumsa, which is about 170 km to the southeast of Addis Ababa and from 8º00' to 8º 02' northern latitude and from 39º 07' to 39º 10' eastern longitude. This woreda is located at the elevation from 1980 to 2230 meters above sea level (Haile et al., 2011).

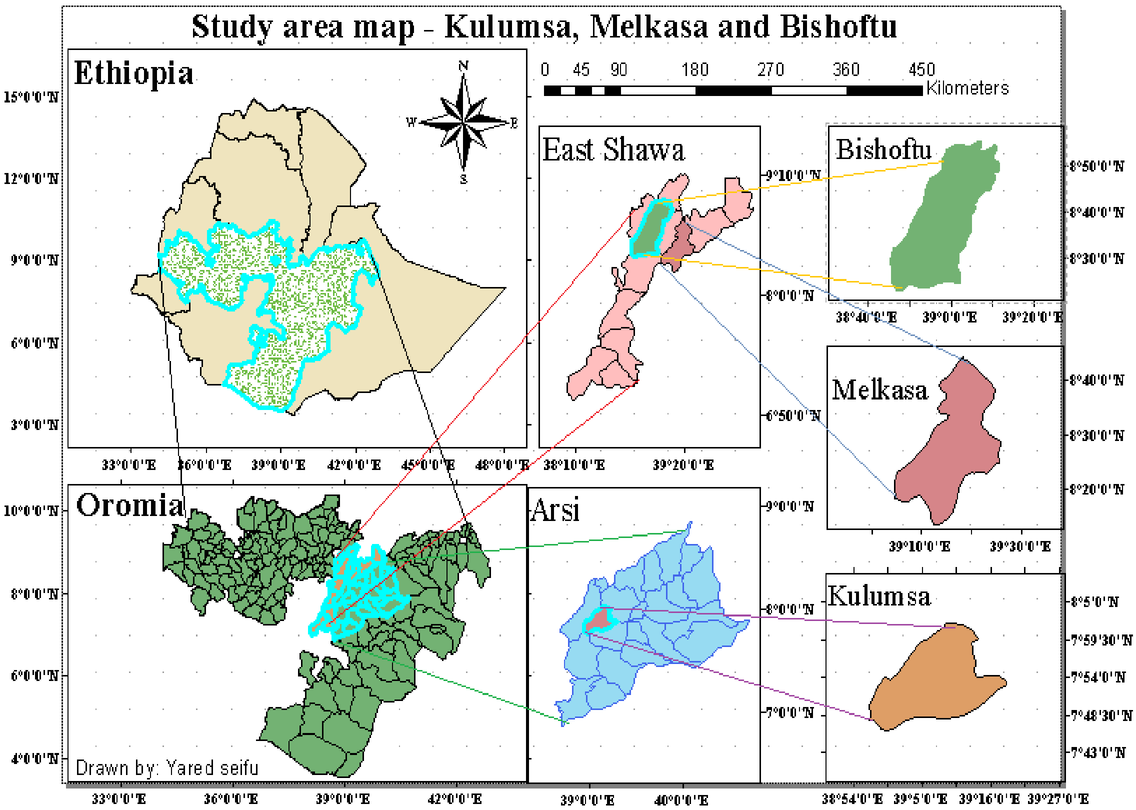

Figure 3.1: The geographical location of the experimental site
Source: ArcGIS drawn by researcher

Awash Melkasa in Ethiopia's Oromia Region was chosen as the experiment's third site. This woreda is located between 1400 m and 2500 m above sea level and from 8º24' to 8º 45' northern latitude and from 39º 21' to 39º 54' eastern longitude of (1,300 – 1,800 m+MSL (mean sea level). According to a survey of the land in this woreda, 23.2% of it is arable or cultivable, 10.6% of it is used for pasture, 4.3% for forest, and the remainder 42% is mountainous (Ham, 2008). The geographical map of the experimental sites is shown in Fig. 3.1

This study was initiated by the rise in the number of tractors and the involvement of foreign private investors, primarily from China and India, in large-scale commercial agriculture in Ethiopia (IMWIC, 2014). The criteria for choosing the expermental site are based on the tractor density and the specific type of soil that has been studied by other researchers. The field under study had a size of 0.6ha and was separated into three areas with different soil physical properties and tilled since 1989.

3.2. Experimental Design

The experiment was conducted in Randomized Complete Block Design (RCBD) in a real field to study the effect of different depths and soil compaction. Hence, the principle of local control is brought to reduce the experimental error due to unknown sources of variations such as soil heterogeneity to some extent. In short, in RCBD, the experimental area is divided into regular blocks of equal area. In each block, the treatments are distributed at random in such a way that each treatment should occur only once in each replication.

There were 3 tillage depths in cm (TD10, TD20 and TD30). All the tillage parameters were replicated three times and the soil compaction in the plot for two seasons was analyzed. The reason why those two seasons were selected is based on the maximum and minimum soil moisture found. Because the selection was not random, non-probability sampling does not allow for the assessment of sample errors and may be vulnerable to sampling bias. To collect data on soil compaction in the field, experimental tests at three different depths are chosen. (100 mm, 200 mm, and 300 mm). To gather data on soil compaction, all depth parameters will be reproduced fifteen times at the farm field (point A to point O) depicted in Fig 3.2. Three different experimental farmlands were chosen, and an experimental design with three replications in a row and three treatments in each row was modeled. The replications' random distribution is illustrated in Table 3.1 and Fig. 3.2.

The presence of a research center and the density of tractors serve as the selection criteria for the experimental area. The 0.6-hectare field under investigation at all experimental sites has been tilled continuously for more than 20 years. This long-term tillage provides a consistent and well-established environment for experimental analysis, ensuring that the soil conditions and any potential compaction effects are well-developed and can be accurately assessed. The materials, machinery, and instruments used, including tractor specifications, hydraulic components, hydraulic circuits, soil compaction measuring instruments, and all other materials necessary for the dissertation, are discussed in the following section.

Table 3.1: Experimental design with some treatment and replication

Treatments	R_I	R_{II}	R_{III}
Replications	$TD_{(A)}$	$TD_{(B)}$	$TD_{(C)}$
	$TD_{(D)}$	$TD_{(E)}$	$TD_{(F)}$
	$TD_{(G)}$	$TD_{(H)}$	$TD_{(I)}$
	$TD_{(J)}$	$TD_{(K)}$	$TD_{(L)}$
	$TD_{(M)}$	$TD_{(N)}$	$TD_{(O)}$

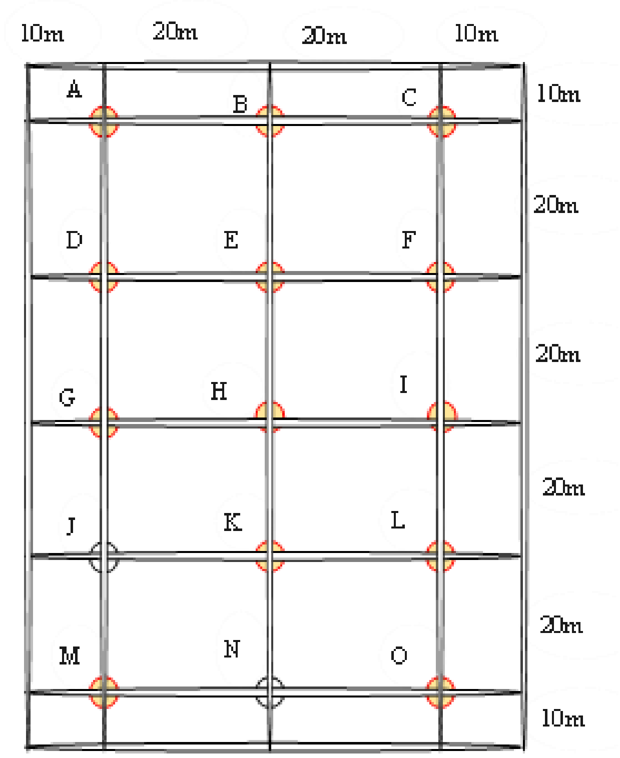

Figure 3.2: Data sampling plot with numbering replication

3.3. Materials, Machinery, and Instruments Used

The materials, machinery, and instruments used during soil compaction measurement and field performance are listed below with detailed specifications.

3.3.1. Materials

The entire discussions have been made under the following headings:

I. Selection of penetrometer shaft and cone tip
II. Development of frame structure to support the components of the cone penetrometer
III. Development of the hydraulic system
IV. Experimental procedure for field test

According to ASABE standard S313.2, a soil cone penetrometer was chosen, and the specifications are shown in Fig. 3.3. Among the five cone tips 12mm Dia. with a 30° included angle was selected for this research work.

stainless steel stick (D = 15 mm, L = 760 mm)

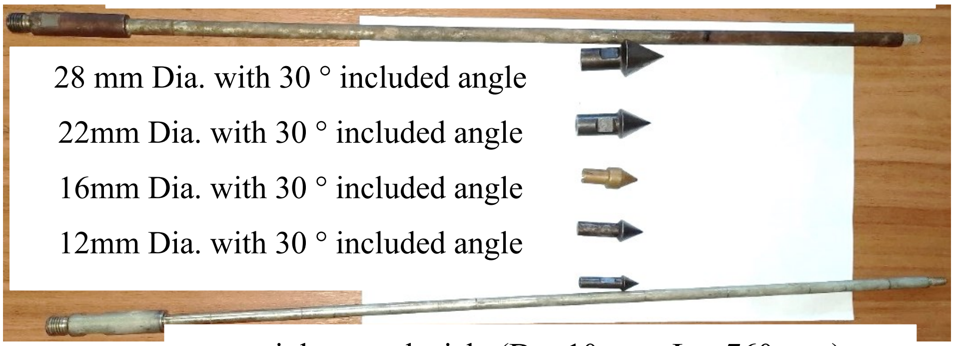

stainless steel stick (D = 10 mm, L = 760 mm)

Figure 3.3: cone penetrometer rods and cone tips specification

Using ASAE S217.11, (1999) as a guide, the frame was designed to support the system's weight as well as the force needed to operate the cone penetrometer. It was constructed primarily from MS bar solid section components and fastened to the slot bar fixture tractor. The frame was designed using a vertical hydraulic cylinder attachment arrangement for the front end. The frame was fixed at a height of 1,026 mm above the ground using a tractor slot bar fixture, as shown in Fig. 3.4.

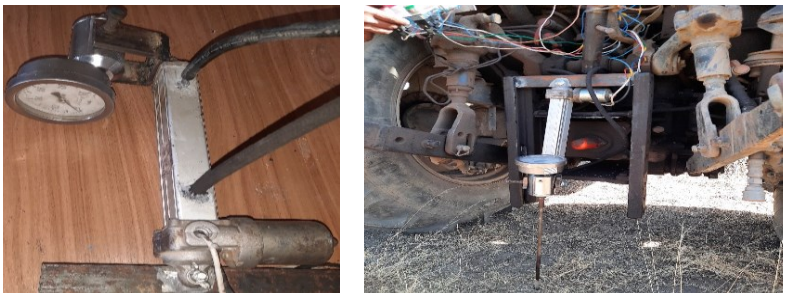

Figure 3.4: The integrated cone penetrometer on the tractor

3.3.2. Tractor specifications

In this study, data from a Chery tractor (Model RM750) with four-wheel drive was collected using a traditional tillage system that included a mounted mouldboard plow and three bottoms. A test tractor of about 75 hp was used for holding the overall components of the hydraulic cone penetrometer for measuring the soil compaction measurement system to experiment. The detailed specification of the tractor is described in Table 3.2.

Table 3.2: Specification of tractor

Parameter	Size
Fuel	Diesel
Front tires size	6.5-20 in
Rear tires size	14.9-30 in
Weight	2669 kg
Length	3.98 m
Width	1.65 m
Wheelbase	2.18 m
Ground clearance	0.42 m
Rear tread size	15.291m
Front tread size	1.3995 m
Engine capacity	4900 cc
Number of cylinders	4 cylinders
Horsepower	55.9 kW
Power RPM	2200 rpm
Engine torque	320.0 Nm
Engine torque RPM	1600 rpm
Bore stroke	(108 x 135) mm

3.3.3. Hydraulic component used

This section deals with the approaches made for designing a hydraulically operated instrumented soil cone penetrometer for predicting CI in a given soil condition. The hydraulic cone penetrometer consists of two main parts: a driving mechanism for inserting the penetrometer probe into the soil and a digital display unit for showing the measured penetration resistance.

3.3.3.1. Hydraulic circuit

The double-acting hydraulic cylinder in the hydraulic circuit was managed by a solenoid-operated 4/3DCV. The tractor's hydraulic power unit, which includes a reservoir and pump, is used to operate the system that gates hydraulic power. To control excessive pressure, the hydraulic fluid leaving the pump can be connected to the pressure relief valve. As shown in Fig. 3.5, the pump pressure line is initially connected to the 4/3 DCV's center position in the ideal configurations. In this position, the double-acting cylinder is not under pump pressure, allowing fluid to return to the tank via the pressure relief valve.

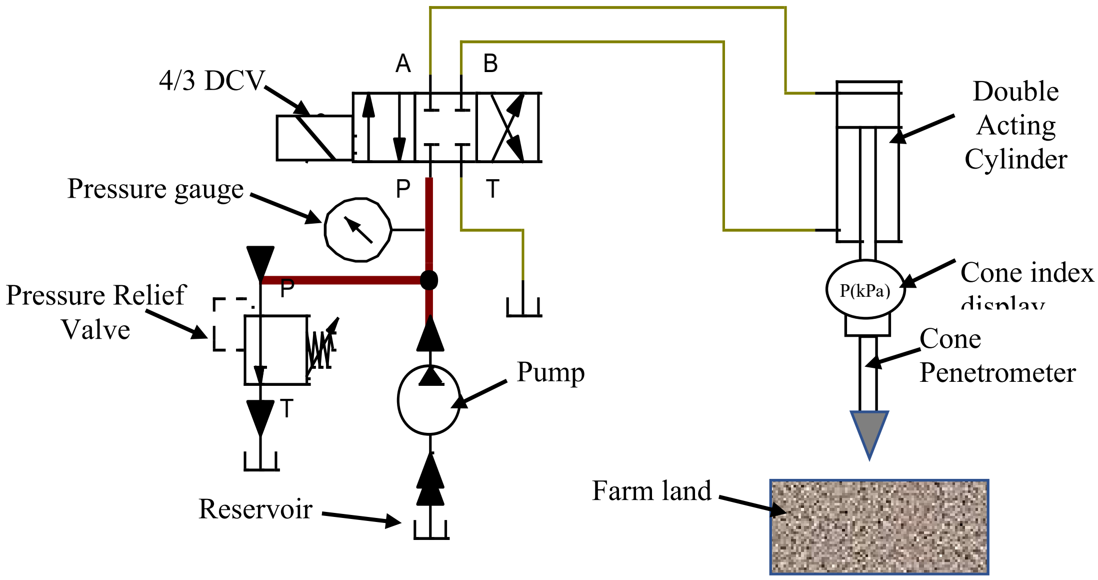

Figure 3.5: The ideal position of the hydraulic circuit of the system

As illustrated in Fig. 3.6, when the 4/3 DCV permits the fluid from the tank to pass through the pump, it expands the cylinder road and inserts a cone penetrometer into the soil, with the digital cone penetrometer showing the value of the soil CI. The arrangement in Fig. 3.7 demonstrates how the cone penetrometer is removed from the ground and the cylinder road is retracted when the 4/3 DCV permits fluid from the tank to pass via a pump and through the third position.

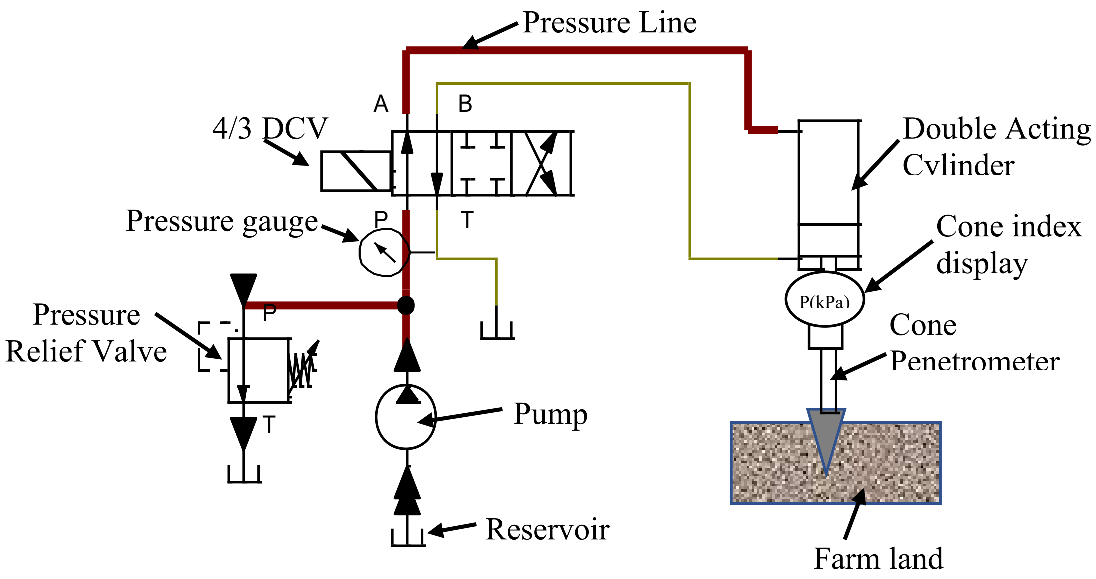

Figure 3.6: Working position of the hydraulic circuit of the system

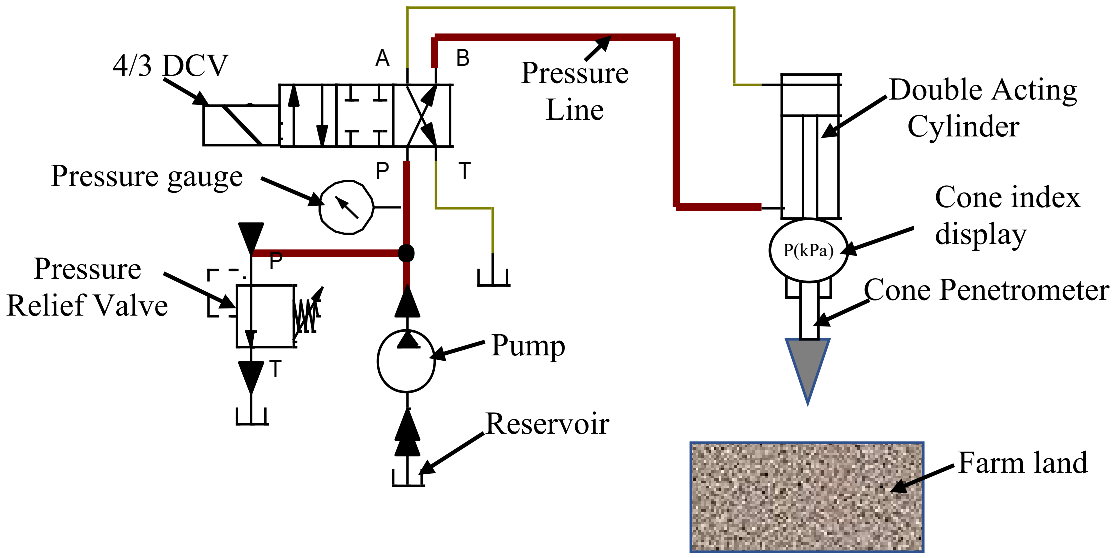

Figure 3.7: Retract the position of the hydraulic circuit

3.3.3.2. Components used in the hydraulic system

- **Directional control valve:** The cylinder must expand, retract, and be in a neutral position for the proposed system to operate satisfactorily. So a two-way, four-port directional control valve with three spring-centered positions and solenoid operation was chosen. The valve has three positions, the first of which, when the lever is pressed forward, expanding the piston rod, allows flow to enter the cylinder's complete bore. When the lever is released from its stationary position, the loaded spring forces the lever to instantly return to its neutral state. When the lever is pulled back, the piston rod retracts to a lower position where the flow enters the cylinder's annulus end.
- **Pressure control/ relief valve**: Relief valve selection is based on the highest operating pressure of the system. The relief valve size is generally 10 –25 percent more than the operating pressure, as the operating pressure is 180 bar, therefore, a direct-acting relief valve of range 182 –215 bar was selected.
- **Hydraulic hoses**: Hydraulic hose pipes with a 207 bar pressure rating are used to link the tractor's hydraulic system, cylinder, and control valves. The output pressure of the pump and a few safety factors were taken into consideration while choosing the hose pipe pressure rating. To link the various parts, the necessary lengths of hoses with high-pressure end connectors were built. Special care was taken to make the connections leak-proof. In the end, Teflon tape was used for additional safety.
- **Hydraulic cylinder**: The selection of the hydraulic cylinder is based on the force required to insert the penetrometer into the soil and is controlled by the electrical limit switch for

the maximum and minimum linear movement. For measuring soil compaction hydraulics, the component used and their specification are listed in Table 3.3.

Table 3.3: Hydraulic component used

Sl No.	Item	Qty	Specification
1.	Hydraulic power unit	1	25 Gallon
2.	Pump from tractor	1	30 lpm
3.	Connecting pipe(hoses)	6	1.5 m length
4.	Pressure relieve valve	1	Standard
5.	Throttle valve	1	Standard
6.	4/3 direction control valve	1	Standard
7.	Double acting cylinder	1	Cylinder diameter 70 mm Rod diameter 40 mm Stroke length 300 mm

3.3.4. Soil compaction measuring instrument used

The SpotOn digital soil compaction meter complies with ASABE S313.3 soil compaction standard and features a 12.8 mm steel cone diameter for long-lasting performance. For simple depth reference, the stainless-steel shaft has markings every 10 cm. The 760 mm probe length automatically displays the maximum compaction value when the probe is removed from the soil, and the entire specification is shown in Table 3.4.

Table 3.4: Specifications of soil compaction meter

Parameters	Specification
Usable Probe length:	760 mm
Range	0 to 5690 kPa
Accuracy:	+/- 100 kPa
Meter Size:	890 mm L x 280 mm W x 76 mm D
Weight:	0.6 kg
Cone Size	12.8mm Dia. with 30 ° included angle

3.4. Method

The entire discussion of the methodology includes the following stages and the overall dissertation is summarized under the methodology flow chart as shown in Fig. 3.8.

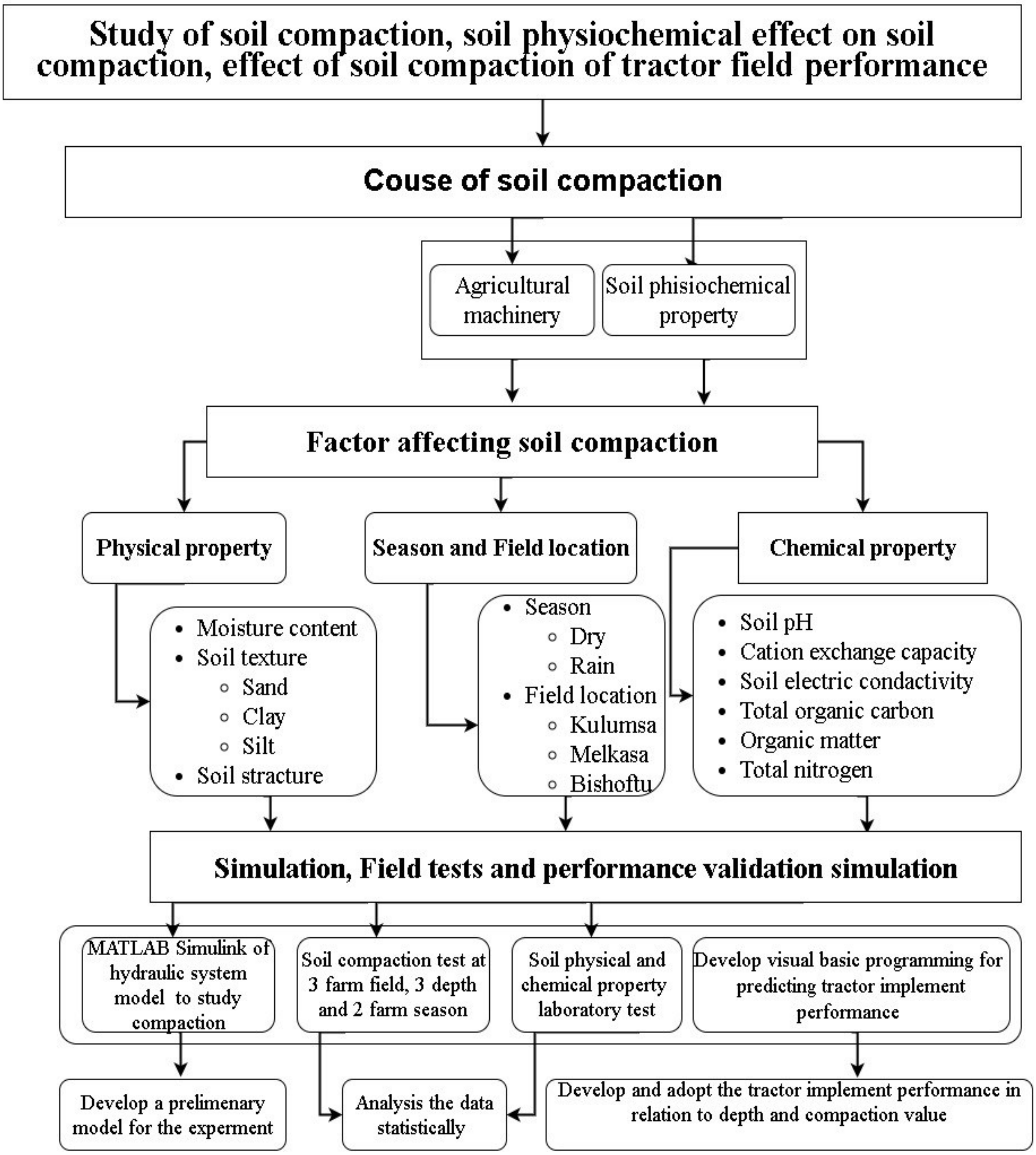

Figure 3.8: Effect of soil compaction on tractor field performance

1. Collection of the data: Primary and secondary data were collected by reviewing the documents available, and visiting the local farmers, agricultural machinery industries, and agricultural research centers by interviewing selected people from each sector.
2. Studying the design and assembly of hydraulically operated cone penetrometer for measuring soil compaction measurement system. A critical study of the design and constructional aspects of the hydraulic structure was done.

3. Selecting cone penetrometer geometry cone penetrometer shaft and cone tip used for measuring soil compaction measurement system.
4. Development of frame structure to support the overall components of the hydraulic system and cone penetrometer.
5. Development of the hydraulic system includes hydraulic lines from the tractor, hydraulic flowmeter, and pressure sensors like a pressure relief valve for reliving the excess pressure coming from the pump.
6. Preparing Instrumentation for measurements and recording desired data like depth measuring unit for cone penetrometer inserted into the soil.
7. Make a field test of compaction measuring at different depths controlled by the hydraulic actuator at different fieldwork in tillage and make on the data obtained.

3.5. Soil Compaction Experimental Procedure

A test tractor of about 55.9 kW was used for conducting experiments. Two persons were required to operate the prototype cone penetrometer, first to operate the tractor, operate the cone penetrometer through the limit switch. The second one takes the reading from the cone penetrometer. The detailed specification of the tractor and hydraulic system of the tractor is given in Table 3.2. All the components were fixed at their desired location and the input hose pipes were connected to the output of the auxiliary hydraulic system of the tractor as indicated in (Fig. 3.9).

The step-by-step procedure from cone penetrometer fixing to the field experiment test for collecting the cone index value from three experimental fields is as follows.

- The cone penetrometer fixture was fixed to the piston rod at its top position and to the penetrometer probe at the bottom.
- The circuit from the limit switch cell was connected to the hydraulic cylinder system through a voltage excitation circuit. The limit switch cell was energized by the the battery of the tractor was through an inverter and the excitation circuit was powered by an external 24V battery.
- Before conducting field experiments, the pressure and flow rate were adjusted by manual method.
- The output at the designed load during calibration was used as a basis for adjusting pressure in the pressure relief valve. The pressure, at which the relief valve opened

for maximum designed load, was kept fixed and this setting pressure is the system working pressure.

- After setting of pressure relief valve the piston rod without the probe was lowered and total time for complete lowering was noted by stopwatch. For any valve beyond the desired time and depth, the flow control valve was adjusted manually. This process was repeated till getting the desired value and the flow control valve was kept fixed there.
- Then the system was taken to the field for conducting experiments.
- The lever of the direction control valve was operated to give forward movement to the penetrometer and the limit switch control the depth of operation. When the base of the cone just touched the surface the data process was started and at the end i.e., when there was no movement the penetrometer was stopped. Just after completion of taking data the limit switch was operated in the reverse direction to retract the piston to its original position.

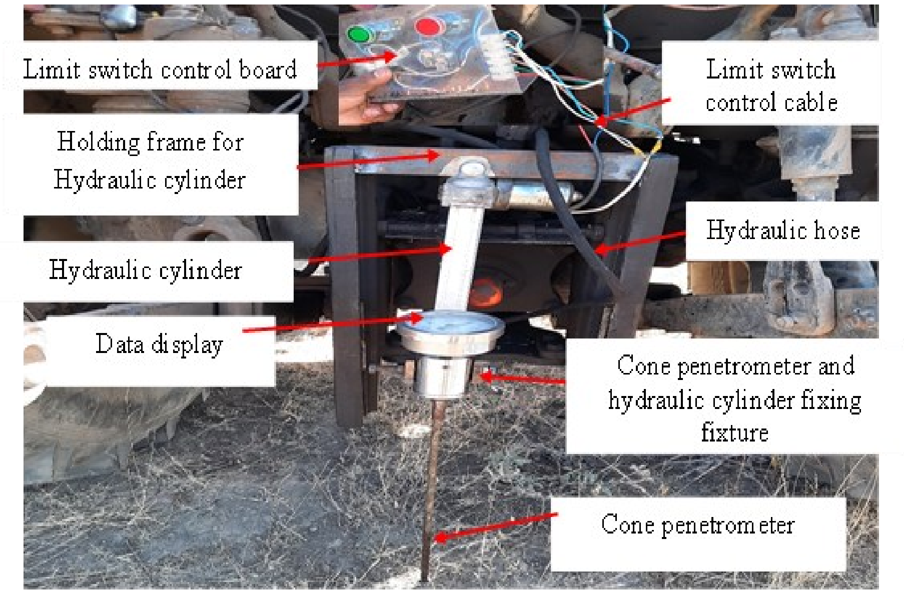

Figure 3.9: Cone penetrometer and tractor integration

3.6. Soil Physical Properties

Numerous chemical and biological processes are supported by the physical characteristics of soil, and these processes may be further influenced by the climate, position in the landscape, and kind of land use. Thus, when climate change affects a variety of soil physical qualities, it might set off a chain of events that creates a soil environment, which may have a significant impact on soil compaction and crop development (Jat et al., 2018). The three field sample soils with their stamp names are indicated in Fig. 3.10.

Figure 3.10: Soil samples collected from three experimental farm fields

3.6.1. Moisture content

One of the trickiest measurements needed in agriculture is the measuring of soil moisture. Equipment used in laboratories includes a non-corrodible container, a digital scale with a mass accuracy of 0.04%, and an electric oven that maintains a temperature between 105^0 C and 110^0 C. Moisture content is calculate using Equation 3.1 below.

$$W(\%) = \frac{(W_2 - W_3}{W_3 - W_1} \times 100 \qquad (3.1)$$

Where, W1 = Container's weight (gm)

W2 = Weight of container plus moist soil (gm)

W3 = container weight + dry soil (gm)

3.7. Soil Texture

The amount of sand, silt, and clay in the soil was measured using various sieves, and a hydrometer was used to measure how quickly the particles settled in an aqueous solution (Alexander, 1978). Gravel and sand are common terms to describe coarse and fine granular materials, respectively. Internationally, it has been decided to classify particles larger than 2 mm but smaller than 63 mm as gravel to have a consistently applicable language. Sand is made up of particles that are smaller than 2 mm but greater than 0.063 mm. Silt is defined as particles that are larger than 0.002 mm and less than 0.063 mm. Clay or luthum is the term for soil that contains even smaller particles than 0.002 mm; for further information, see Table 3.5.

Table 3.5: Grain sizes

Soil type	Min.	Max.
Clay	----	0.002 mm
Silt	0.002 mm	0.063 mm
Sand	0.063 mm	2 mm
Gravel	2 mm	63 mm

Source: (Li et al., 2020)

3.8. Soil Chemical Properties

In the following section summary of soil chemical characteristics and the related processes that have an impact on soil compaction are given.

3.8.1. Soil pH

A tabletop pH meter (HI 2210) was used to measure pH. The pH scale has a total range of 0 to 14. A pH reading that is lower than 7.0 is acidic, whereas one that is higher than 7.0 is alkaline. The pH of 7.0 is regarded as neutral for soil. Most plants thrive in slightly acidic to neutral soil (pH 6.0 to 7.0).

Figure 3.11: a)soil pH, b)soil electric conductivity, and c)soil organic content test

3.8.2. Soil electric conductivity test

Using a JENWAY 4310 Conductivity Meter, the electrical conductivity of soil was measured. Using a conductivity meter, the soil's electrical conductivity was assessed in the water extract filtrate. In Fig. 3.11, a picture of a soil pH test, a soil electric conductivity test, and a soil organic content test used in a lab is displayed.

3.8.3. Organic carbon and organic matter

According to Walkley and Black's standard protocol, the proportion of total organic carbon is measured using the chromic acid wet digestion method. Total organic matter was calculated using gravimetric weight change linked to high-temperature oxidation of organic matter (Ramamoorthi, 2018). The alkaline permanganate method was used to assess the amount of available total nitrogen.

3.8.4. Cation exchange capacity

The NCR-13 Standard was used to measure the cation exchange capacity (CEC) of soils. The CEC value, which is given by almost all soil testing laboratories, is calculated and represents an assessment of the soil's capacity to draw in, hold onto, and exchange cation elements.

3.9. Soil Compaction System Design and Modeling

The soil CI value design of the cone penetrometer is done based on the force acting in the system as indicated in Fig. 3.12. Forces acting on the soil are a hydraulic force in a vertical direction. In the case of the cone penetrometer since the operation is done at static conditions only downward hydraulic force and upward soil resistance are incorporated into the design process.

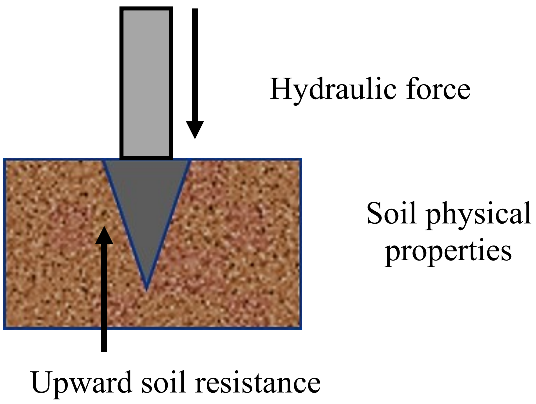

Figure 3.12: Factors affecting tillage operation

Design of Cylinder: The greatest force necessary for inserting the penetrometer probe in the ground is used to guide the hydraulic cylinder's design. You can determine the penetrometer's maximum necessary thrust using the formula of (Woldeyohannis, Hiremath, Tola, Wako, & Development, 2022):

$$F = CI \times A \tag{3.2}$$

Where: F = required thrust; CI = maximum cone index to be measured; and A=base area of a cone in case of a cone penetrometer.

Assume the system's maximum CI for the soil is 3,000 kPa. The WES standardized cone penetrometer was recommended for use in the field by the American Society of Agricultural and Biological Engineers (ASABE, 1968), and it is still in use today. The first cone has a base area of 323 mm^2, a base diameter of 20.27 mm, and a probe for soft soil that is 15.88 mm in diameter. The second cone has a base area of 130 mm^2, a base diameter of 12.83 mm, and a probe for soft soil that is 9.53 mm in diameter. The maximum force needed to operate the penetrometer can be estimated using the first standard as shown below.

Maximum Force (F) = $3\times10^6\times3.23\times10^{-4}$= 967N

Using Euler's formula, the piston rod diameter is examined for buckling. Euler's strut theory is thus employed to resist buckling. The equation for column buckling by Euler is given in Equation 3.3.

$$d_{(m_i n)} = 4\sqrt{\frac{F \times K^2 L^2 \times 64}{\pi^2 E}} \tag{3.3}$$

Where: F= buckling load; E= Young's modulus of elasticity (200 GPa); σ= Yield stress (380 MPa); d= diameter; L=length of cylinder rod; and K=constant.

$$d_{(m_i n)} = 4\sqrt{\frac{967 \times 2^2 \times 0.2^2 \times 64}{\pi^2 \times 200 \times 10^9}} = 0.008418\, m = 8.42\, mm$$

The cylinder rod is calculated using the following formula. Taking the factor of safety =2 cylinder rods become

$$d = \sqrt{\frac{4F}{\pi\sigma}} = \sqrt{\frac{4 \times 967 \times 2}{\pi \times 380}} = 6.48\, mm \tag{3.4}$$

The cylinder rod is offered in a 32 mm size. The cylinder can therefore withstand the load. The following formula can be used to determine the pressure needed to provide thrust on the annular side of the cylinder.

$$P = \frac{F}{A} = \frac{F}{\frac{\pi}{4}(d_c^2 - d_r^2)} \frac{967}{\frac{\pi}{4}(100^2 - 32^2 d)} = 1.3724\, bar \tag{3.5}$$

Where: P is pressure coming from the hydraulic system; d_c and d_r are cylinder and road diameter respectively.

Taking into account the pressure loss in the pipes and other components, the relief valve pressure should be set at a pressure that is 25% higher than needed to provide a thrust. Equations 3.6 and 3.7 are used to determine the bore side and annual side area.

Full bore area, $A = \frac{\pi}{4}(d_c^2) = \frac{\pi}{4}(0.1^2) = 0.007854 m^2$ (3.6)

Annulus area, $(A-a) = A = \frac{\pi}{4}(d_c^2 - d_r^2) = \frac{\pi}{4}(0.1^2 - 0.032^2) = 0.00705 m^2$ (3.7)

To satisfy the required standard cone penetration velocity as per ASAE S313.3, the piston velocity must be 0.03 m/s to enter the soil. Velocity can be computed as follows when the piston rod is extending:

$$V = \frac{Q_E}{A} = \frac{q_E}{A-a} = 0.03\ m/s \quad (3.8)$$

Where: Q_E= flow rate of the full bore end of the cylinder and q_E= flow rate of the annulus end as indicated in Fig. 3.14a and 3.14b.

$$Q_E = A \times V = 0.007854 \times 0.03 = 0.000024 m^3/s \quad (3.9)$$

$$q_E = (A - a) \times V = 0.00705 \times 0.03 = 0.000212 m^3/s \quad (3.10)$$

The piston velocity during retraction can be calculated as:

$$V = \frac{Q_R}{A} = \frac{q_R}{A-a} = \frac{235.62}{70.5} = 3.34 m/s$$

where Q_R= 235.62= Q_E

$$Q_R = A \times V = 78.54 \times 3.34 = 262.324\ cm^3/s = 0.01574\ m^3/min = 15.74 lpm$$

The summary specifications of the double-acting cylinder are indicated in Table 3.6.

Table 3.6: Specifications of the double-acting cylinder

S. No.	Parameters	Value
1	Cylinder diameter	100 mm
2	Rod diameter	32 mm
3	Stroke length	300 mm
4	Stroke speed	30 mm/s
5	Return stroke speed	33.4 mm/s
6	Oil flow required in the forward stroke	14.14 lpm
7	Oil flow required in the return stroke	15.74 lpm
8	Full bore area	7854 mm^2
9	Annual area	7050 mm^2

Source: Researcher design output

3.10. Tractor and Implement Mathematical Modeling

Traction concepts have developed to analyze the traction force obtained from the soil to pull a load as a result of tractors operating off-road in analyses of the soil and wheel dynamics. To overcome the motion resistance, torque at the axle generates gross thrust at the dirt wheel contact.

3.10.1. Soil tire interaction modeling

Wheel thrust (or gross tractive force), wheel rolling resistance, net tractive force (or pull or drawbar pull), and tractive efficiency are some of the forces and words that can be used to study traction (Zoz & Grisso, 2003a). Due to the torque at the axle, gross thrust develops at the earth-wheel interface. The net traction is the remaining portion of the gross thrust that is used to overcome motion resistance and can be put to use for meaningful work. This type of traction performance is explained by the laws of mechanics, and the parameters used in this modeling are shown in Fig. 3.13 below. Consider an engine driving the drive wheels with a rotational speed of "Ne." As the speed is decreased, the torque increases. When the engine's rotational speed, Ne, and torque, Te, are reduced, the torque increases and the engine drives the drive wheels. The following equation can be used to determine the engine power (Macmillan, 2003).

$$P_e = \frac{2\pi N_e T_e}{60} \tag{3.11}$$

Considering the overall transmission ratio 'q' which is (N_e/N_w) or (T_w/T_e) (Macmillan, 2003).

$$q = \frac{N_e}{N_w} = \frac{T_w}{T_e} \tag{3.12}$$

The axle power 'P_{ax}' can be calculated by (Equation 3.13) (Macmillan, 2003)

$$P_{ax} = \frac{2\pi N_w T_w}{60} \tag{3.13}$$

Drawbar power: Drawbar power is obtained using the relation between pull (net traction capacity) and actual travel speed as (Equation 3.14) (Kim et al., 2020):

$$P_{db} = P \times V_a \tag{3.14}$$

where P_{db} is drawbar power (kW).

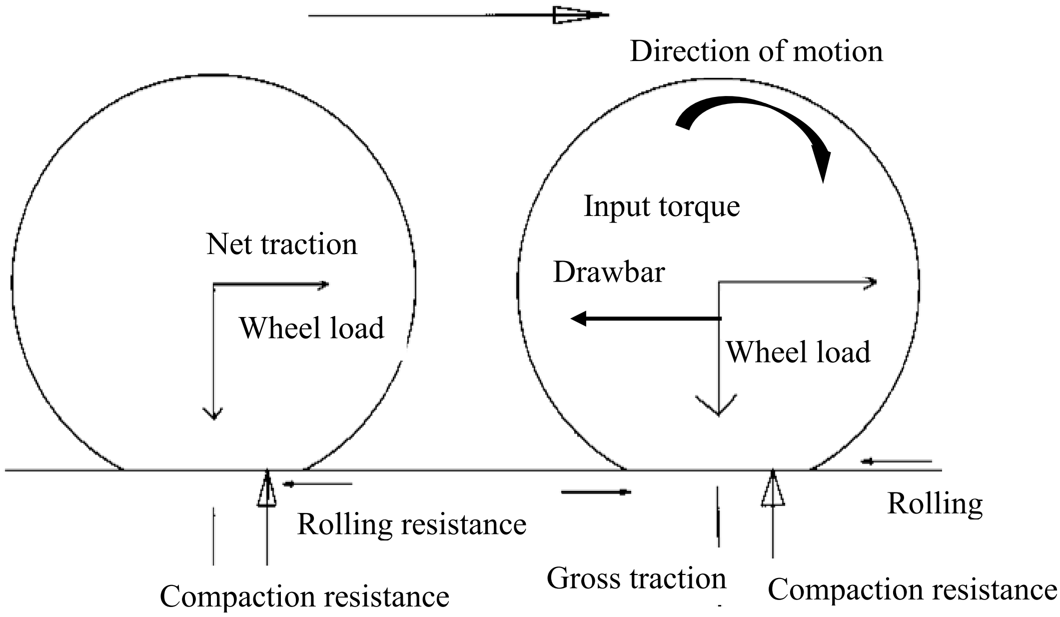

Figure 3.13: Factors that are significant in the study of the performance
Source: (Zoz & Grisso, 2003a)

3.10.2. Tire parameters

Bias ply and radial ply are two different ways that tires are constructed. The layers, or plies, that make up a bias ply tire's carcass are arranged diagonally to the tread and crisscrossed at an angle known as a bias angle. Plies on radial ply tires are perpendicular to the tread. The radial-ply tire's strength and stability are provided by a belt surrounding it. The result is a tire with more rigid tread but flexible sidewalls. Fig. 3.14 and 3.15 depict the design of a radial-ply tire as well as a description of tire specifications.

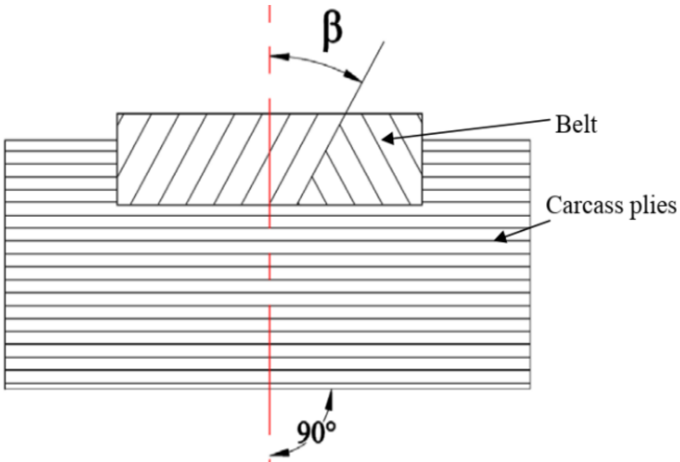

Figure 3.14: Arrangement of belt and plies in the radial-ply tire
Source: (Lindenmuth, 2006)

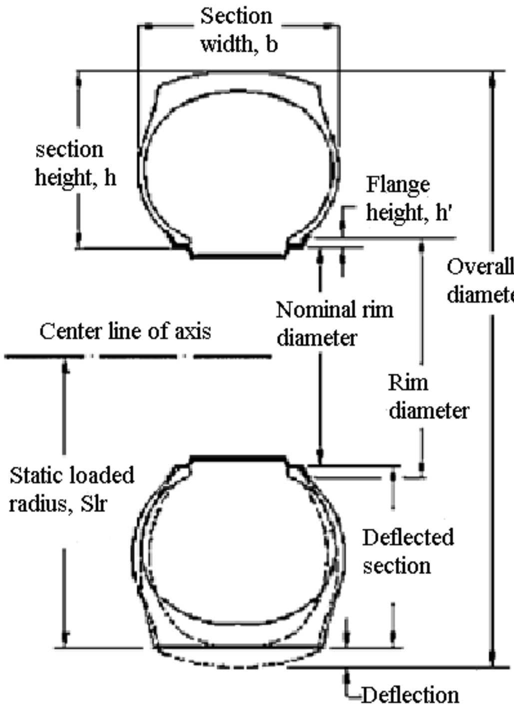

Figure 3.15: Description of tire parameters
Source: (Brixius, 1987)

Overall width (b): The overall width of a tire is the undeflected width of a fresh tire, including expansion brought on by inflation for 24 hours. The tire size indication starts with this number.

Overall diameter (d): The overall diameter of a tire is calculated by dividing the tire circumference by pi (π).

Section height (h): It can be represented as

$$h = \frac{d - nominal\ \ rim\ diameter}{2} \tag{3.15}$$

Deflection (δ): Tire deflection is defined as the difference between a tire's empty and loaded section heights at a specific load and inflation pressure. It can be represented as

$$Deflection\ (\delta) = \frac{Overall\ diameter(d)}{2} - static\ loaded\ radius\ (slr) \tag{3.16}$$

Static loaded radius (slr): The distance between the tire axle center line and the supporting hard surface for a tire mounted on an acceptable rim and carrying a load at a given inflation pressure.

Deflection, (%): The ratio of tire deflection to the amount of tire section height over the rim flange is known as the percent deflection.

$$Tyre\ deflection,\ percent = \frac{Vertical\ tyre\ deflection\,(\delta)}{\left(Tyre\ section\ height\,(h) - Flange\ height\right)} \times 100 \tag{3.17}$$

3.10.3. Tire deformation and ground contact characteristics

The investigation of the deflection of a moving tire under various inflation pressures and soil conditions is the first step toward understanding the vehicle-soil relationship. A pneumatic tire deflects to create a point of contact when loaded against a flat, rigid surface. All of the forces created between the tire and the ground are transmitted through this area. The tire will behave as a rigid wheel when its effective stiffness is more than the maximum sustainable normal stress for the soil, and as a flexible wheel when its effective stiffness is lower (Plackett, 1984). Hence, the tire contact area on the stiff surface can be useful in determining tire ground pressure. A hard surface also has the benefit of being a widely accepted standard, which creates a foundation for accurate and reproducible data.

3.10.4. Pneumatic wheel traction mechanics

Fig. 3.16 and 3.17 depict the forces operating on a pneumatic wheel traveling through the soil surface. It is possible to suppose that the torque (T) applied to the wheel is equal to the gross traction (GT) acting at an effective moment arm (r). A portion of the GT is necessary to overcome the resistance to the wheel's passage in the soil.

$$GT = MR + Net\ traction\ (P) \tag{3.18}$$

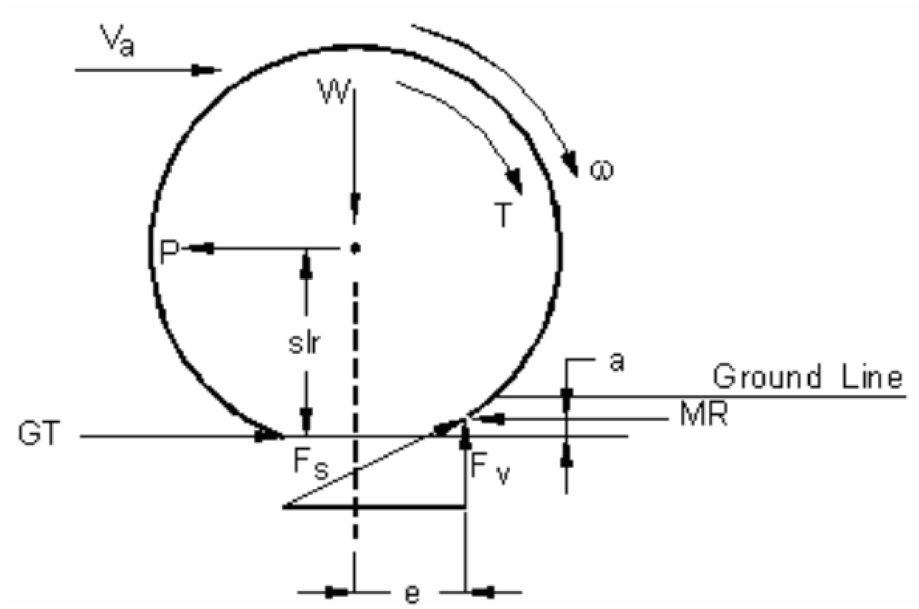

Figure 3.16: A pneumatic traction wheel's force profile on a deformable surface
Source: (Wismer & Luth, 1973)

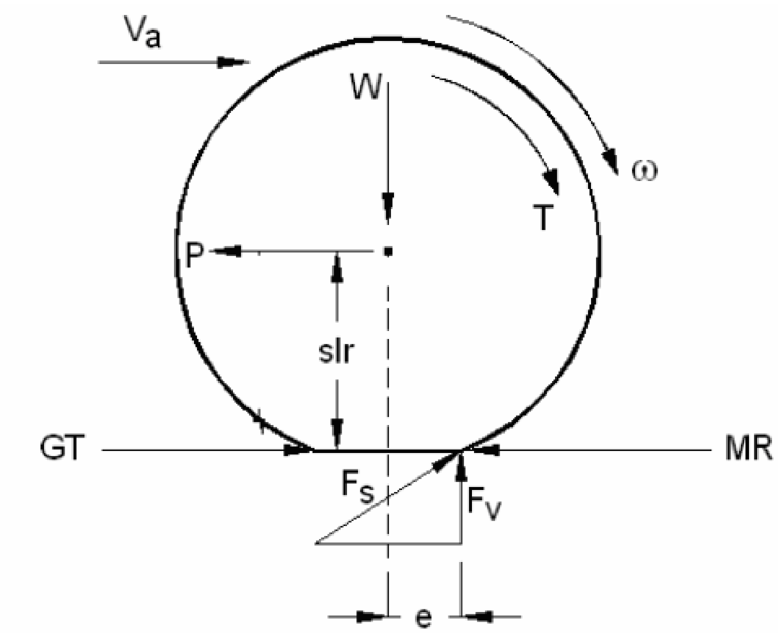

Figure 3.17: A pneumatic traction wheel's force profile on a hard surface
Source: (Wismer & Luth, 1973)

The representation of Fig. 3.16 and 3.17 was a= vertical offset distance in (m), e= horizontal offset distance in (m), Fs= resultant soil reaction force in (N), Fv= vertical component of resultant soil reaction force in (N), slr= static loaded radius in (m), Va= actual forward velocity in (m/s), W = weight on wheel in (N) and ω= angular velocity in (rad).

For a pneumatic wheel moving on hard or soft surfaces, the vertical reaction force is not directly under the axle center line but is offset by a distance designated “e”. The amount of the offset on a hard surface as indicated in Fig. 3.16 is given by Equation 3.19.

$$e = \frac{slr \times MR}{F_V} \tag{3.19}$$

A soft surface (Fig. 3.20) is given by

$$e = \frac{(slr - a) \times MR}{F_V} \tag{3.20}$$

The motion resistance, the radius of the static loaded object, and the vertical force all influence how much the horizontal offset is. The rolling circumference is used to calculate the rolling radius. Axle torque and rolling radius are typically used to derive the GT force because they cannot be measured directly. There are three different force states identified: a towed wheel, a self-propelled wheel, and a driving wheel (Wismer & Luth, 1973). A wheel that is being towed is not being powered and has zero torque. When the slip is less than zero, a towing condition takes place. When the pull is equal to zero and the gross thrust is equal to the motion resistance, a self-propelled wheel is a traction wheel. A traction wheel that creates pull and has positive slip is referred to as a driving wheel.

3.11. Traction Parameters

Traction performance parameters like the gross traction ratio (GTR), net traction ratio (NTR), pull ratio, or coefficient of traction (COT), motion resistance ratio (MRR), wheel slip (S), or travel reduction ratio, expressed in percent, as well as tractive efficiency (TE) or (η_t), typically expressed in percent, are included in the traction parameters for a tractor and its implements. These parameters are discussed in the following section.

3.11.1. Specification tractor and mouldboard

A Chery tractor with four-wheel drive, model RM750, was used to gather data for this study using a traditional tillage method with a mounted mouldboard plow and three bottoms. A test tractor of about 75 hp was used for holding the overall components of the hydraulic cone penetrometer for measuring the soil compaction measurement system to experiment. The detailed specifications of the tractor and implementation are shown in Table 3.7 and Table 3.8.

Table 3.7: Chery RM750 Tractor Specification

Parameters	Size
Fuel	Diesel
Front tires size	6.5-20 in
Rear tires size	14.9-30 in
Weight	2669 kg
Length	3.98 m
Width	1.65 m
Wheelbase	2.18 m
Ground clearance	0.42 m
Rear tread size	1.5291m
Front tread size	1.3995 m
Engine size	4,900 cc
Number of cylinders	4 cylinders
Horsepower	55.9 kW
Power RPM	2,200 rpm
Engine torque	320.0 Nm
Engine torque RPM	1,600 rpm
Bore stroke	(108 x 135) mm
PTO claimed power	49.5 kW
Rear PTO RPM	540 rpm

Table 3.8: Specification of tillage implement

NO.	Parameters mould board Parameters	Value
1	Total weight	305 kg
2	Furrow slice width	400 mm
3	No. of bottom	3
4	Width of bottom	300 mm

3.11.2. Wheel slip

Slips in traction devices occur between the device and the medium. This is defined as

$$S = 1 - \frac{V_a}{V_t} \tag{3.21}$$

$$S = 1 - \frac{V_a}{r\omega} \tag{3.22}$$

Where: r= rolling radius in (m); S= wheel slip in (%); Vt= theoretical speed in (m/s); Va = actual speed in (m/s); and ω= angular velocity in (rad.).

Slip is a reduction in distance traveled and/or speed that occurs because of flexing of the tractive device and shear within the soil. The theoretical speed of the wheel is calculated using Equation 3.23

$$V_t = \omega \times r \tag{3.23}$$

3.11.3. Net traction ratio

The net traction ratio is the ratio of pull (P) to the dynamic weight (W) of a powered wheel.

$$NTR = \frac{P}{W} \tag{3.24}$$

The net traction force (P) must be horizontal and perpendicular to the reaction force (Fv) to maximize tractive efficiency (Dwyer & Heigho, 1984).

3.11.4. Tractive efficiency

The ratio of output power to input power, or drawbar power to wheel power, is known as tractive efficiency (η_t). According to the study conducted by (Kim et al., 2020), tractive efficiency solely takes into account the losses that occur between the axle and drawbar.

$$\eta_t = \frac{Output\ power}{Input\ power} = \frac{P/W}{T/rW} \times (1-S) \tag{3.25}$$

$$\eta_t = \left(1 - \frac{NTR}{GTR}\right) \times (1-S) \tag{3.26}$$

The overall efficiency of the tractor is given by:

$$\eta_0 = \frac{Engine\ \text{Power}}{Fuel\ \ power} \times \frac{Wheel\ Power}{Engine\ \text{Power}} \times \frac{Drawbar\ power}{Engine\ \text{Power}}$$

$$\text{Overall efficiency}(\eta_0) = \text{Engine efficiency} \times \text{Transmission efficiency} \times \text{Tractive efficiency}$$

$$\eta_0 = \eta_e \times \eta_{tr} \times \eta_t \tag{3.27}$$

Losses in velocity and pull result in a reduction in tractive efficiency. A "slip" is a popular term used to describe the decrease in travel speed. Because motion resistance lowers the amount of GT that is translated into net traction.

3.11.5. Torque ratio

The GTR is the ratio of GT to dynamic weight (W) and is given by

$$GTR = \frac{GT}{W} = \frac{T}{rW} \tag{3.28}$$

GT is usually calculated from the axle torque (T) and the rolling radius.

3.11.6. Motion resistance ratio

A pneumatic tire's motion resistance is affected by the normal load, tire size, inflation pressure, and soil strength. A traction wheel's motion resistance is the sum of the horizontal components of soil reaction forces acting in the opposite direction of travel (Vandenberg et al., 1961). The MRR of a traction device is the ratio of motion resistance to dynamic weight. This proportion is also written as:

$$\text{MRR} = \text{GTR} - \text{NTR} \tag{3.29}$$

By dividing (Equation 3.29) by the weight on the wheel (W), the following equation results, (Kim et al., 2020)

$$\frac{MR}{W} = \frac{T}{rW} - \frac{P}{W} \tag{3.30}$$

3.11.7. Power delivery efficiency:

A power loss from the engine to the drawbar, including both hydraulic and drivetrain power losses, is known as power delivery efficiency (PDE). Engine or PTO power can be employed for comparing computations when utilizing PDE as a performance comparison tool, depending on what is available and practical (Kim et al., 2020).

$$PDE = \frac{P_{db}}{P_e} \tag{3.31}$$

3.11.8. Fuel economy:

The annual average fuel consumption from Farm Machinery Management engineering practice is the basis for the fuel consumption utilized in machinery budgets. For determining the fuel consumption of diesel engines in letters per hour (L/h), the most used relation is given by (Equation 3.32) (Grisso et al., 2004):

$$FC = 0.223 \times P_{pto} \tag{3.32}$$

Where, FC= Fuel consumption in (l/h) and P_{pto} = PTO power in (kW)

The equation used to estimate specific fuel consumption is given in (Equation 3.33) (Grisso et al., 2004):

$$SFC = (2.64X + 3.91 - 0.203\sqrt{738X + 173}) \times X \times P_{pto} \tag{3.33}$$

Where, X = equivalent PTO power/ rated PTO power

3.11.9. Implement draft:

The implement draft is estimated based on break horsepower, implement type, depth of tillage, furrow slice width, and angle of share. The implement draft is calculated using (Equation 3.34) below (Sharma & Mukesh, 2019)

$$D_i = 3.6 \times P_{db} / V_a \tag{3.34}$$

Where P_{db} = Drawbar power in (KW), Va = Working speed of tractor in (m/s), and D_i = implement draft in (N).

Also, the implement draft can be calculated in terms of tillage parameters using (Equation 3.35) (Sharma & Mukesh, 2019):

$$D_i = k.n.a.b \tag{3.35}$$

Where: K = specific draft in (N/mm^2); n = number of bottoms; a = depth of plough in (m); and b = width of furrow slice in (m)

Based on the mould board implement geometry as indicated in Fig. 3.18 the forces on the implement for the pull can be derived (Sharma & Mukesh, 2019).

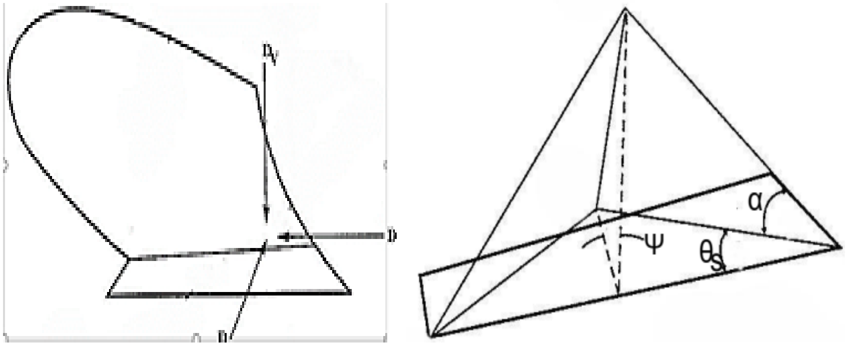

Figure 3.18: Mould board geometry with force components
Source: (Sharma and Mukesh, 2019)

$$D = P\cos\theta_s \cos\alpha \,,\; D_s = P\cos\theta_s \sin\alpha \,,\; D_v = P\sin\theta_s \cos\alpha \tag{3.36}$$

Where: D = Horizontal draft in (N); D_v = Vertical draft in (N); D_s = Side draft in (N); α = Load angle in (deg.); Ψ= Cutting angle in (deg.) and θ_s =Shear angle in (deg.)

3.12. Tractor Dynamics

To evaluate the field performance of the tractor implement, the dynamic weight on the tractor axles is necessary. Fig. 3.19 displays a free-body diagram of the tractor implementing the arrangement.

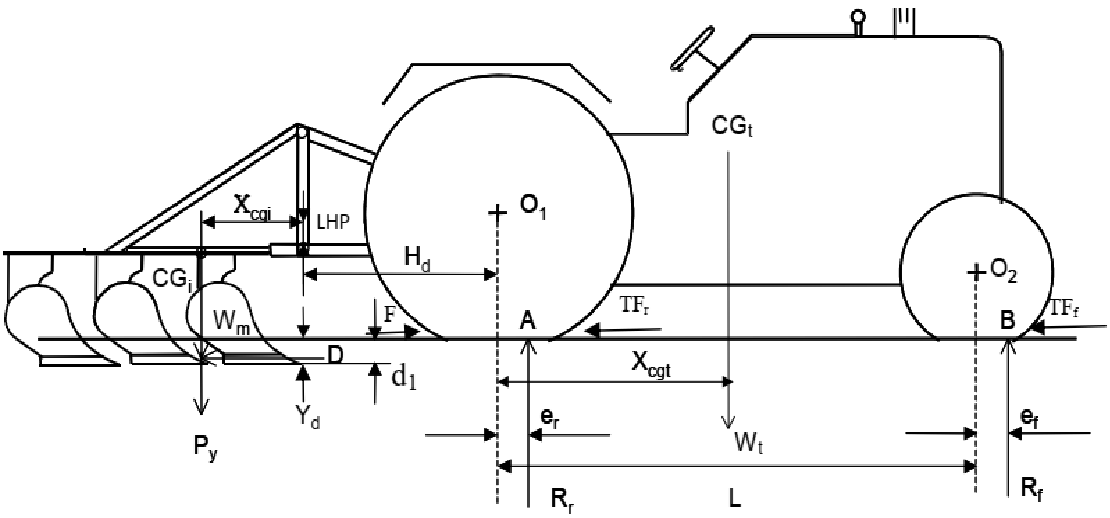

Figure 3.19: Forces acting on a tractor-mold board plow combination

The following equation can be used to express the force and moments of the dynamic reaction acting on the tractor's front and rear wheels, respectively.

$$R_r = \frac{W_t\left(L+e_f-X_{cgt}\right)+\left(W_m+P_y\right)\left(X_{cgi}+H_d+L+e_f\right)-DY_d}{L-e_r+e_f} \tag{3.37}$$

$$R_f = W_t + W_m + P_y - R_r \tag{3.38}$$

The following GTR and MRR expressions were created by (Brixius, 1987), (Tiwari, 2006), and (Tiwari et al., 2010) as a function of mobility number (Bn) and wheel slip (S).

$$GTR = A_1\left(1-e^{-A_2B_n}\right)\times\left(1-e^{-A_3S}\right)+A_4 \tag{3.39}$$

$$B_n = \left(\frac{CI.b.d}{W}\right)\times\left(\frac{1+A_5\,{}^{\delta}\!/_{h}}{1+A_6\,{}^{b}\!/_{d}}\right) \tag{3.40}$$

Where; b = Tire width in (m); d = Tire diameter in (m); δ = Tire deflection in (m); and h = height in (m)

$$MRR = \frac{A_7}{B_n}+A_4+\frac{0.5\times S}{\sqrt{B_n}} \tag{3.41}$$

$$NTR = GTR - MRR \tag{3.42}$$

Substituting Equation 39 and Equation 41 into Equation 42

$$NTR = \left(A_1\left(1-e^{-A_2B_n}\right)\times\left(1-e^{-A_3S}\right)+A_4\right)-\left(\frac{A_7}{B_n}+A_4+\frac{0.5\times S}{\sqrt{B_n}}\right) \tag{3.43}$$

3.13. Dimensional Analysis

Dimensional analysis is an effective tool because it gives a way to combine factors that affect the process and a way to simplify complex physical issues.

Tire deformation: According to Equation. 3.44, the tire deformation system has six relevant variables. The parameters are displayed in Table 3.9.

 $$\delta = f\ (d,\ b,\ h,\ P_g,\ W) \tag{3.44}$$

Bekker, (1960) and Wong, (1989) define ground pressure as the sum of tire inflation pressure and carcass pressure. The Buckingham theorem states that four dimensionless ratios are required to express the deflection phenomenon as shown in Table 3.9.

Table 3.9: Tire deflection model parameters

Parameter	Symbol	Dimension
Tire section width when unloaded	b	L
Tire diameter when not loaded	d	L
Tire deflection	δ	L
Tire section height	h	L
Vertical wheel load	W	MLT^{-2}
Ground pressure	P_g	$ML^{-1}T^{-2}$

Source: (Bekker, 1960) and (Wong, 1989)

Traction potential of agricultural tires: The traction study includes eleven relevant variables and two dimensions. Table 3.10 shows a set of parameters, and wheel torque can be written as:

$$T = f\,(d, b, r, \delta, h, W, S, MR, NT, CI) \qquad (3.45)$$

The Buckingham theorem states that nine dimensionless ratios are required to express a relationship between the variables in the traction phenomenon.

Table 3.10: Wheel-soil model parameters

Parameter		Symbol	Dimension
Wheel			
Unloaded tire section width		b	L
Unloaded tire diameter		d	L
Tire rolling radius		r	L
Tire deflection		δ	L
Tire section height		h	L
System			
Vertical wheel load		W	MLT^{-2}
Slip		S	–
Wheel torque		T	$ML^{2}T^{-2}$
Motion resistance		MR	MLT^{-2}
Net traction		NT	MLT^{-2}
Soil	CI	CI	$ML^{-1}T^{-2}$

Source: (Bekker, 1960) and (Wong, 1989)

3.14. Modeling of the Soil Compaction Measuring System

In Fig. 3.20 of the Simulink hydraulic system model, a tractor auxiliary hydraulic system is depicted. It consists of hydraulic oil, a hydraulic pump for generating pressure and velocity, and a hydraulic motor for generating mechanical rotation. After receiving power from the tractor unit and passing through the pump, the system is connected to a pressure relief valve for regulating excess pressure, a hand operated four port three positions directional control valve, a double-acting cylinder for creating linear movement, and a cone penetrometer for measuring vertical soil pressure.

The system receives hydraulic power from the tractor's hydraulic power unit, which includes a reservoir and pump. The soil is modeled as a solid particle that retains its spring and damping properties, while the pressure applied from the cylinder is simulated as a variable mass.

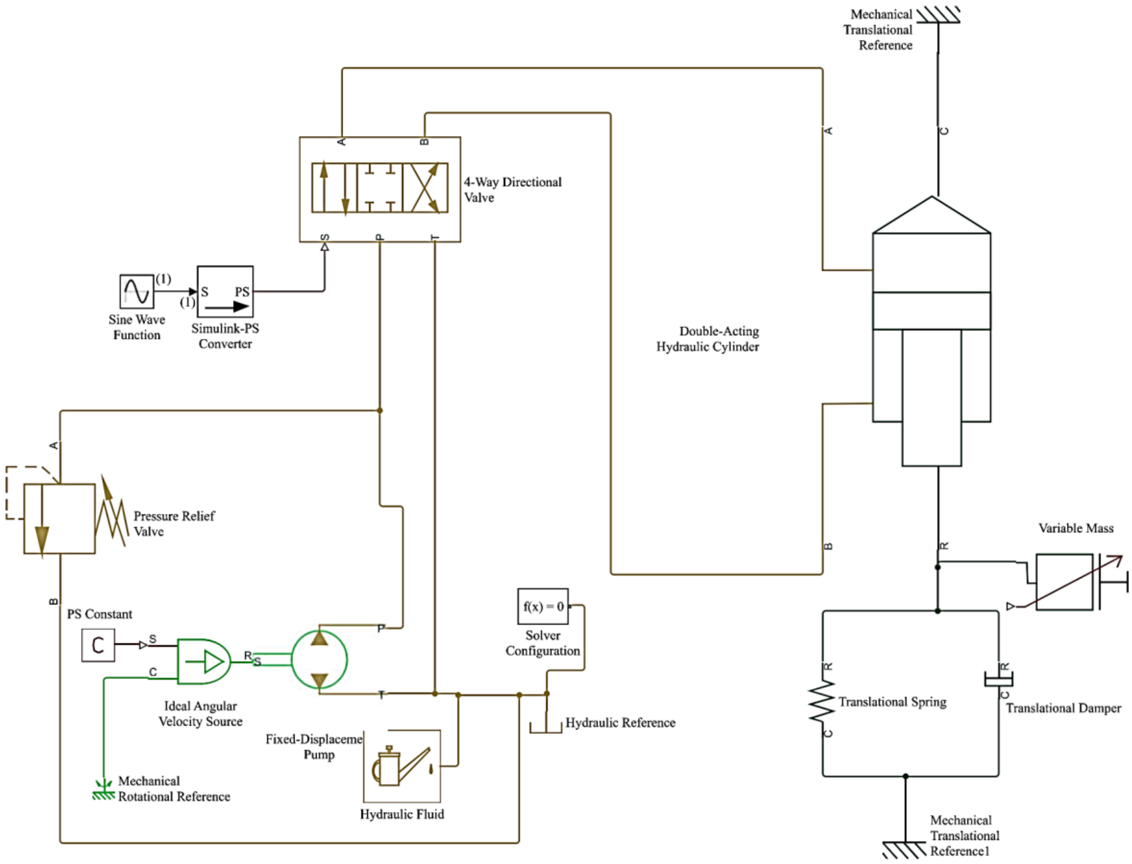

Figure 3.20: MATLAB Simulink hydraulic system modeling
Source: (Woldeyohannis, Hiremath, Tola, Wako, & Development, 2022), MATLAB Simulink 2018

3.15. Data Analysis

Hydraulic circuit modeling and data analysis were done by using Simulation X and MATLAB Simulink software for analysis of the amount of pressure required for the insertion of the cone penetrometer into the soil. AutoCAD and Catia were used for modeling the cone penetrometer. These experimental data were analyzed using Minitab and SPSS data analysis statistical software. According to (Marczyk et al., 2010), linear regression is a technique for forecasting a value on some dependent variables given the values of one or more independent variables. Analyzing relationships between variables using statistical regression is similar to looking at correlations. To examine the impact of each independent variable on the variability of the overall soil compaction, the standard regression coefficient (beta weight) is calculated using the multiple regression equation. This study's regression analysis aims to identify an equation that might be applied to determine how soil physiochemical characteristics affect soil CI value. The specified regression equation for this study takes the following form;

$$Y = \alpha + \beta_1X_1 + \beta_2X_2 + \beta_3X_3 \ldots\ldots\ldots\ldots\ldots + \beta_nX_n \qquad (3.46)$$

In the above equation, predictor variables xi may represent independent variables (Bhattacherjee, 2012).

$$Y=19689 + 201.4\, X_1 + 462\, X_2 + 279.9\, X_3 - 4898\, X_4 - 58.2\, X_5 - 103.7X_6 - 2488\, X_7 - 947X_8 + 22325\, X_9$$

Where:

Y= Soil CI, x_1= Moisture content, x_2= Sand percentage, x_3= Clay percentage, x_4 = Soil pH value**,** x_5= Soil EC, x_6= Soil CEC, x_7= Total organic carbon, x_8 = Soil organic matter and x_9= Soil total nitrogen

3.16. Summary

In this chapter, the location of the study where the experiment was conducted on three farm fields; Kulumsa, Melkasa, and Bishoftu was explained. The experimental design and data collection for all the experiment locations of the study were designed and the RCBD method of experimental design was selected. Nonprobability sampling was used as a sampling technique. The materials, machinery, and instruments used were hydraulically components and systems, and soil compaction measuring instruments.

The detailed methods required starting from design, the experimental set-up, instrumentation, and experimental procedure followed for measurement of soil compaction at different field conditions and laboratory procedure associated with soil physical and chemical properties to the present study are discussed.

The theoretical considerations and methods of experimental, the development of different components, and the procedure followed for measurement of soil compaction in the different fields were discussed. The laboratory procedure associated with soil physical properties like soil texture (grain size) and soil moisture content and chemical properties like; soil pH, cation exchange capacity, soil electric conductivity, soil organic carbon, and soil organic matter were also discussed. Soil compaction system design and modeling starting from the hydraulic force at the power hydraulic cylinder to the soil where the compaction takes place was modeled and discussed.

Tractor and implement mathematical modeling considering soil tire interaction, tire parameters, tire deformation and ground contact characteristics, and mechanics of pneumatic traction wheel were discussed. The traction parameters like tractor and implement specification geometry, wheel slip, pull ratio or the coefficient of traction, tractive efficiency, torque ratio, motion resistance ratio, power delivery efficiency, fuel economy, and implement draft were addressed. The software used for data analysis were SAS, Minitab, MATLAB Simulink, and Origin for analysis of the result of the experiment. The overall simulation and experimental result data and discussion will be addressed in Chapter 4 below.

CHAPTER 4

4. RESULTS AND DISCUSSIONS

4.1. Simulation Results and Discussion

A tractor hydraulic system with an oil, pump, and engine is included in the Simulink hydraulic system model in Fig. 3.22. A pressure relief valve, a solenoid-operated directional control valve, and a double-acting cylinder are all connected to a hydraulic fluid that was used to insert a cone penetrometer into the soil. The soil is represented as a solid particle that holds its spring and damping properties, while the pressure generated by the cylinder is represented as a variable mass. The hydraulic cylinder simulation's output reveals the amount of time needed and pressure variation during cylinder extension and retraction, soil compaction resistance in the shape of a damper and soil stiffness in the shape of a spring property, flow rate through the pump to the hydraulic cylinder, hydraulic power, and torque.

4.1.1. Hydraulic cylinder speed

The cylinder model in Fig. 4.1 was built using the translational hydro-mechanical converter and translational hard stop blocks. The cylinder extension maximum speed was 0.3 mm/s to move the cone penetrometer into the soil in 3.3 seconds

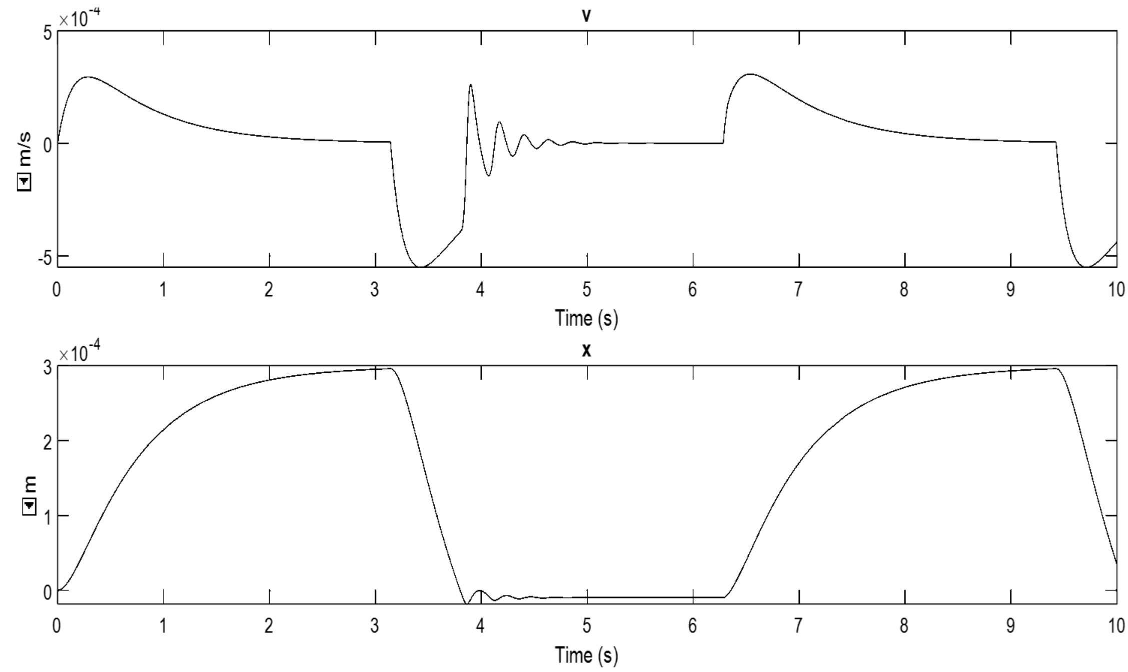

Figure 4.1: hydraulic cylinder speed and single-stroke distance

Hydraulic cylinder pressure: The simulation output graph in Fig. 4.2 shows the pressure variation along the pressure line and returning line. The findings show that during the first three seconds, the pressure in port A changes from 24 to 38 Pa as shown in Fig.4.2a, while the pressure in port B varies from 0 to 13 Pa as shown in Fig.4.2b.

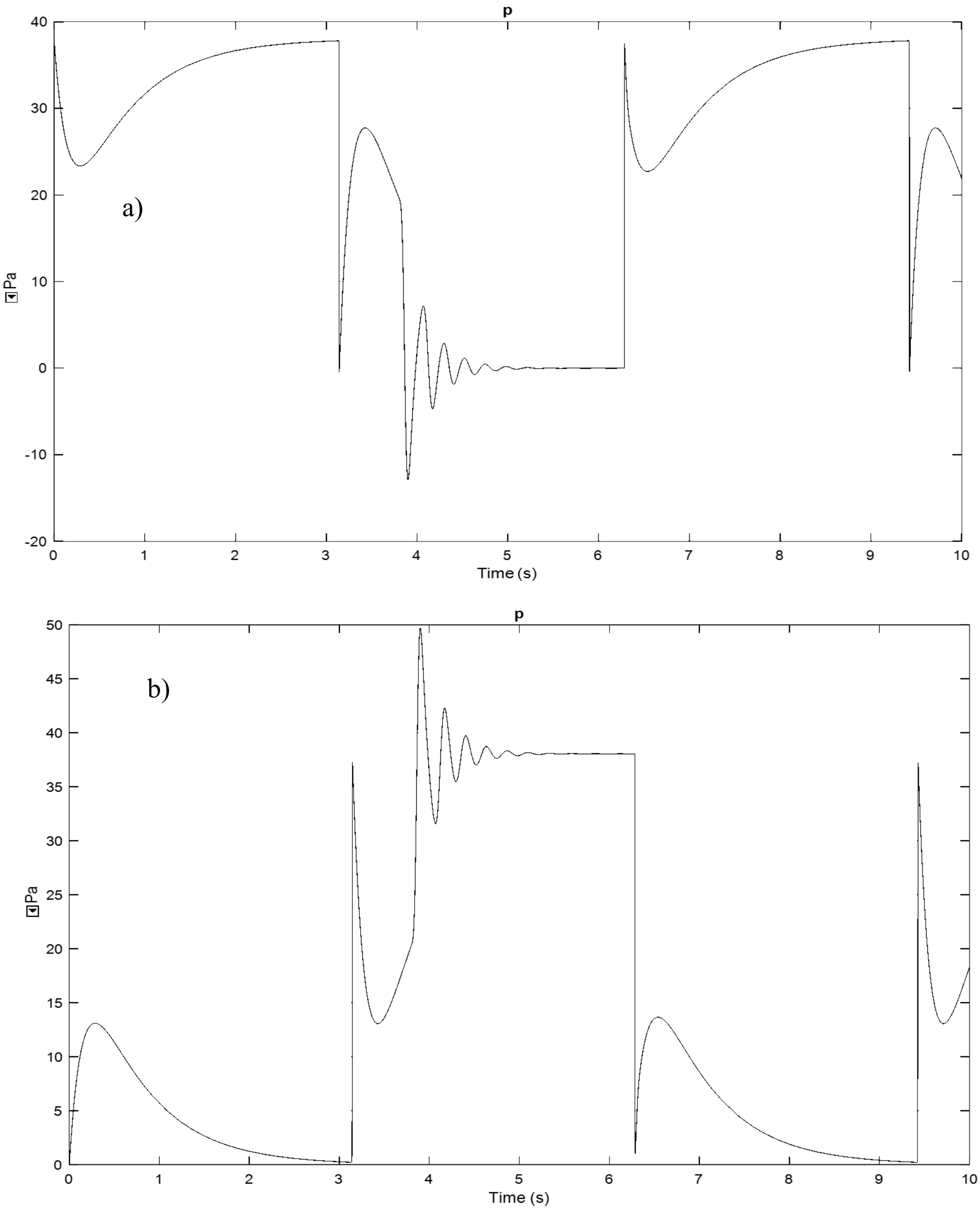

Figure 4.2: Pressure variation in the hydraulic cylinder at Port A and Port B

4.1.2. Translational spring

The graph in Fig. 4.3a and 4.3b displays a maximum downward penetration resistance force of 0.3 N and a maximum penetration speed of 0.032 mm/s.

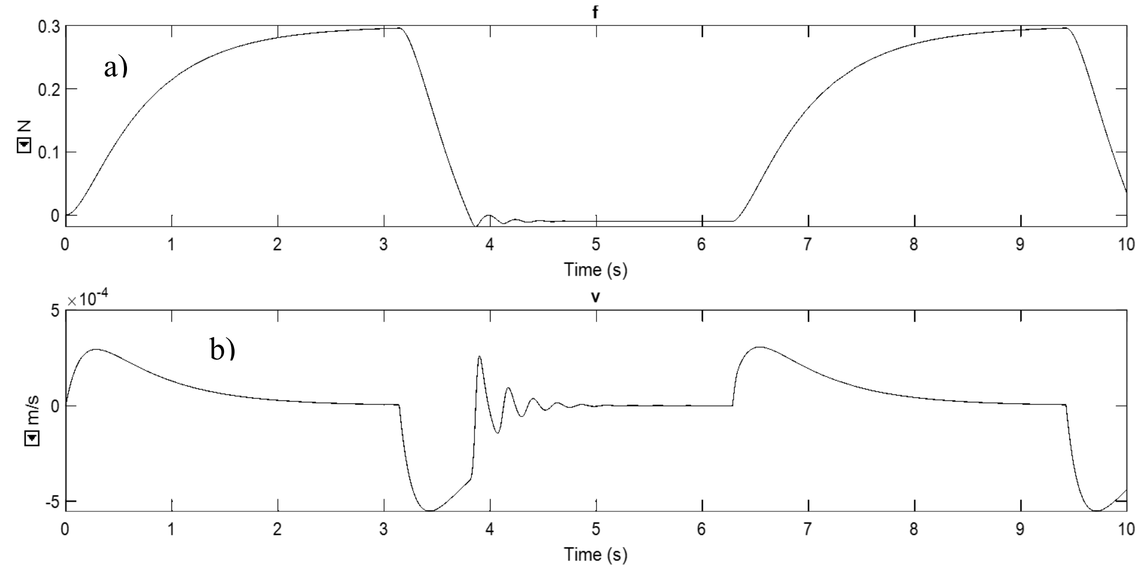

Figure 4.3: Translational spring

4.1.3. Flow rate

The flow rate of oil from the pump utilized to generate linear motion for the cylinder road is displayed in Fig. 4.4. The greatest flow rate, as seen on the plot, is 3.8 X 10^{-6} m^3/s. After the cone penetrometer begins to enter the earth, the flow rate property starts to decline for up to three minutes during the cylinder extension. It achieves its maximum flow rate during penetration once again, completes the extension of the road, and then begins retracting the cylinder rod.

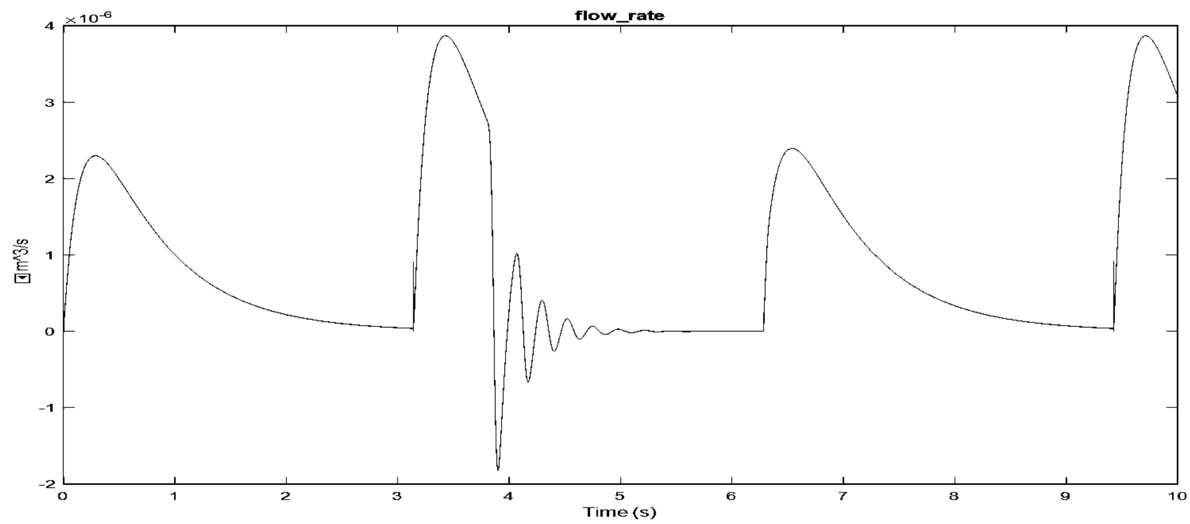

Figure 4.4: Pump flow rate

4.1.4. Hydraulic power and torque

The hydraulic power and torque graph used in the soil compaction measurement model is shown in Fig. 4.5. It shows that the hydraulic power and flow rate have a direct proportional relationship, meaning that as the flow rate increases, hydraulic power also rises. On the other hand, the hydraulic torque and flow rate have an inversely proportional relationship.

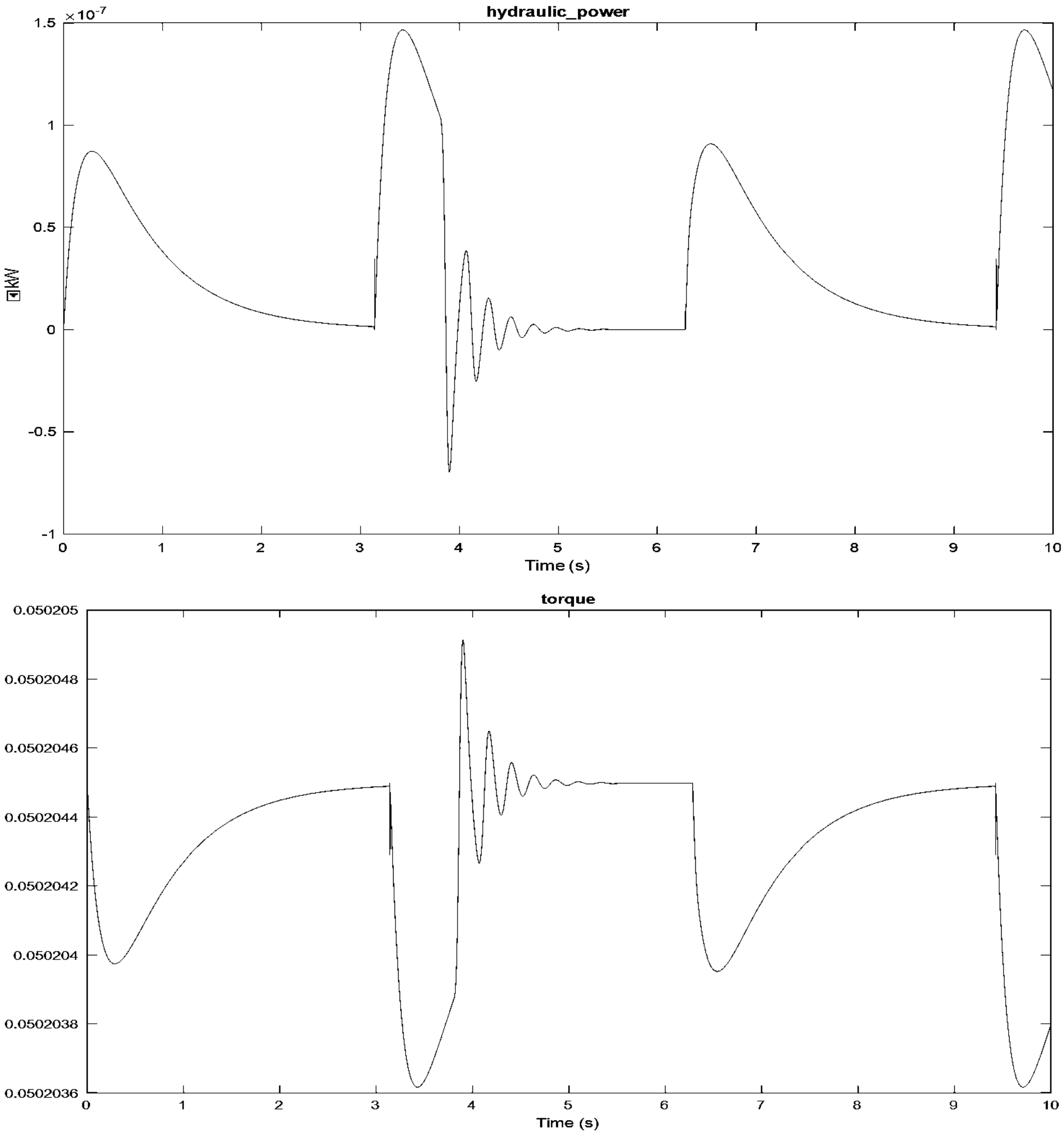

Figure 4.5: Pump hydraulic power and torque

4.1.5. Pump pressure difference

The pressure variation via the pump is depicted on the simulation output graph in Fig. 4.6. The outcome reveals that the pressure drops from 38.05 Pa to 37.90 Pa in a couple of seconds before starting to rise again and reaching 38 Pa. The pressure drops to a minimum pressure of 37.8 Pa when the cone penetrometer comes into contact with the soil. The pressure variation graph displays a sine wave and completes the first cylinder extension cycle as a result of the interaction between the soil and cone penetrometer.

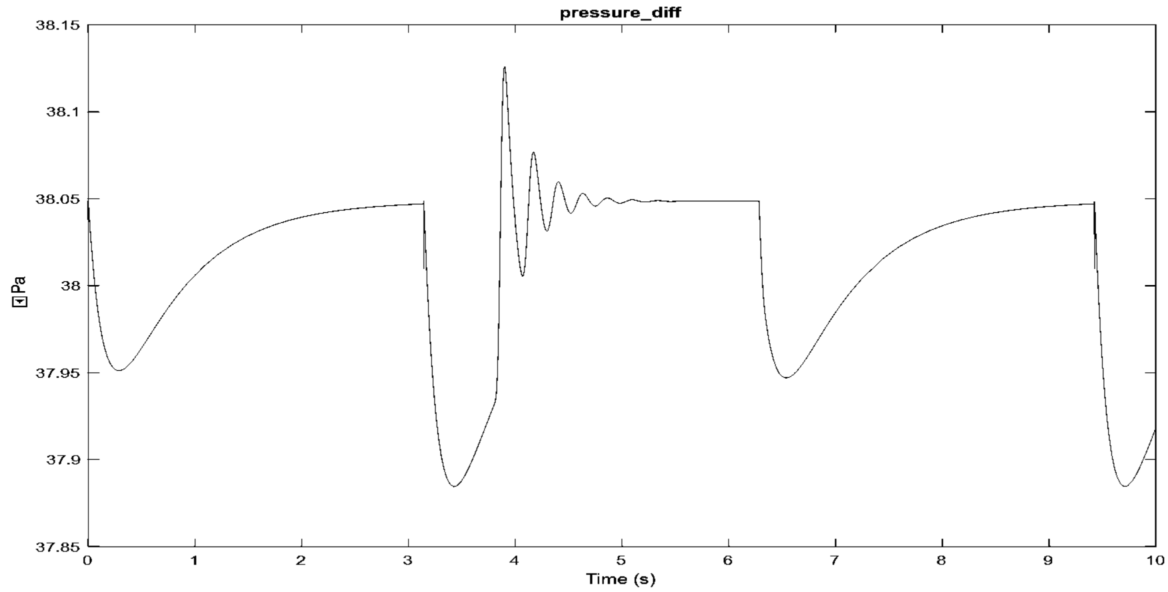

Figure 4.6: Pump pressure difference

4.2. Soil Compaction Field Experimental Results and Discussion

The result of this study covers soil penetration resistance collected from three farm fields (Kulumsa, Melkasa, and Bishoftu) with different geographical locations and different soil properties. The influence of season and depth during harvesting and seeding season on soil compaction for all sampling points was evaluated during the compaction test.

4.2.1. Kulumsa farm field

Plots of the soil compaction which are measured by hydraulic system integrated on a tractor are made for each sampling point and depth as indicated in Fig. 4.7. According to the graph, soil compaction during the harvest season was higher than during the seeding season due higher foot traffic from animals and machinery. During the harvesting and seeding seasons, the maximum soil compaction values were 5,900 kPa and 2,076 kPa at sample locations C and J at a depth of 200 mm, respectively., as shown in Fig. 4.7, the minimum soil compaction value from the fifteen sample locations during the harvesting and sowing seasons was 1,600 kPa and 612 kPa at sample points F and M at a depth of 300 mm, respectively.

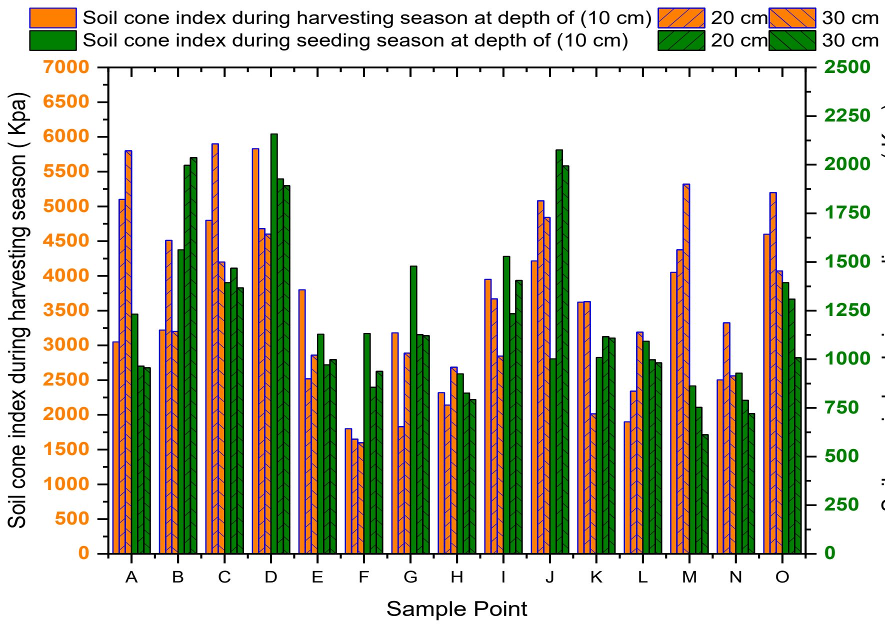

Figure 4.7: Soil CI vs. field sample point for the Kulumsa field test

The soil compaction was measured both using manually with a sopton soil compaction meter and hydraulically powered by integrating on the tractor. In both experimental seasons averages all sample points result of manually measured soil cone index values were higher than the hydraulically powered soil cone index measured value for the Kulumsa field experiment as indicated in Fig.4.8. This is due to the improper handling of the cone penetrometer and ergonomic nature of human.

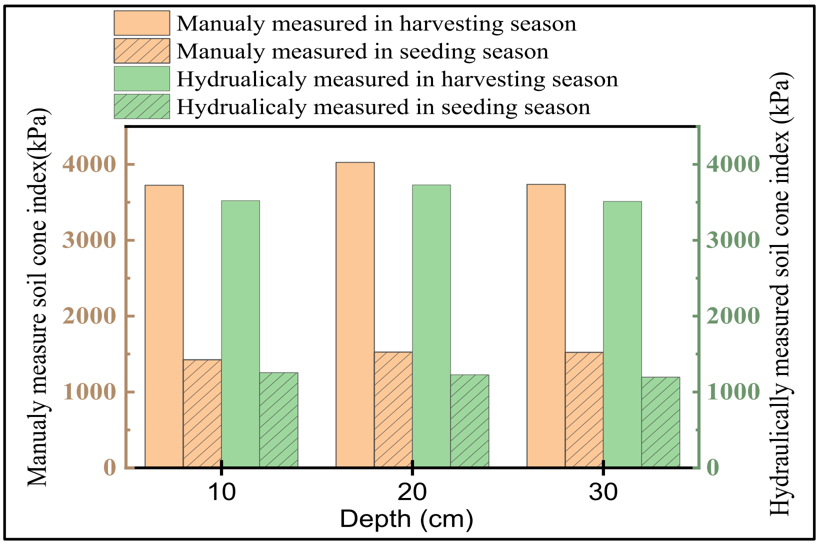

Figure 4.8: Manually and hydraulically measured CI vs. depth for Kulumsa field

Overall, the study highlights significant variations in soil compaction within the examined field.

4.2.2. Melkasa farm field

At sample locations A and F for the harvesting season, the study's results showed that the maximum and lowest soil compaction values were 6,159 kPa and 327 kPa, respectively. Sample points B and K showed the highest and lowest soil compaction values during the sowing season, 3,052 kPa and 563 kPa, respectively, as shown in Fig. 4.9. The average maximum and minimum soil compaction results of the three experimental locations are summarized in Table 41.

Table 4.1: Average maximum and minimum soil CI value

Ex. Site	Season	Max/Min	CI (kPa)	depth	Sample point
Kulumsa	Harvesting	max	5,900	20	C
		min	1,600	30	F
	Seeding	max	2,076	20	J
		min	612	30	M
Melkasa	Harvesting	max	6,159	30	A
		min	327	30	F
	Seeding	max	3,052	30	B
		min	563	10	K
Bishoftu	Harvesting	max	3,958	30	M
		min	502	10	M
	Seeding	max	2,018	30	L
		min	279	30	D

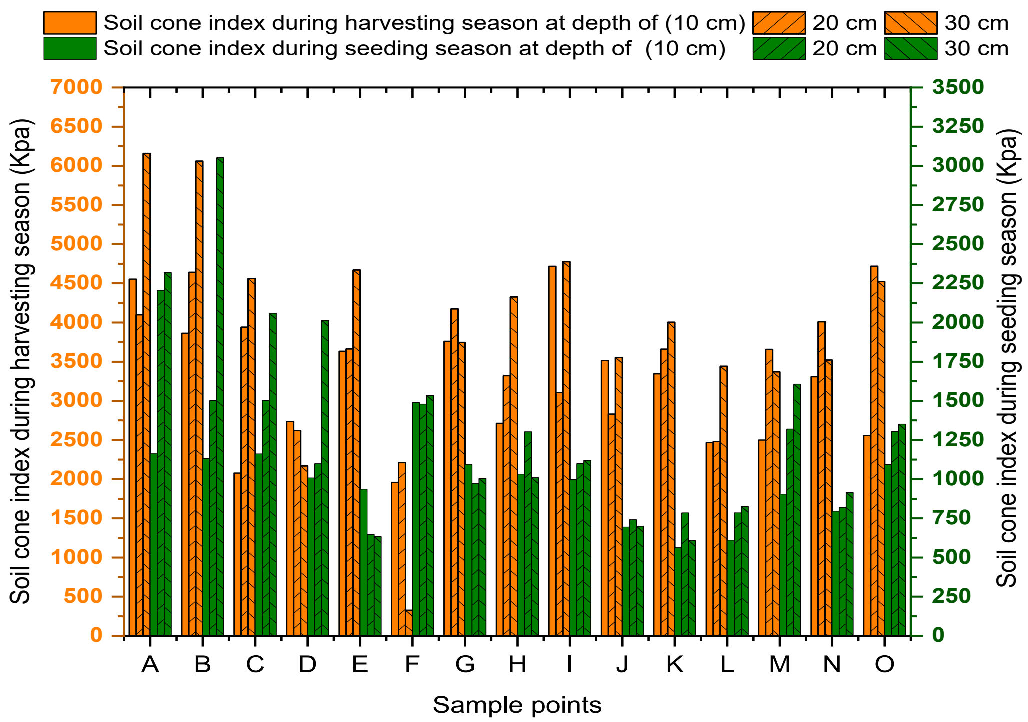

Figure 4.9: Soil CI vs. field sample point for the Melkasa field test

As depicted in Fig.4.10 the soil compaction results in both experimental seasons, manually measured soil cone index values were higher compared to hydraulically powered soil cone index values as indicated in Fig.4.10. in both measurement methods at 10 cm depth, the soil compaction value was less.

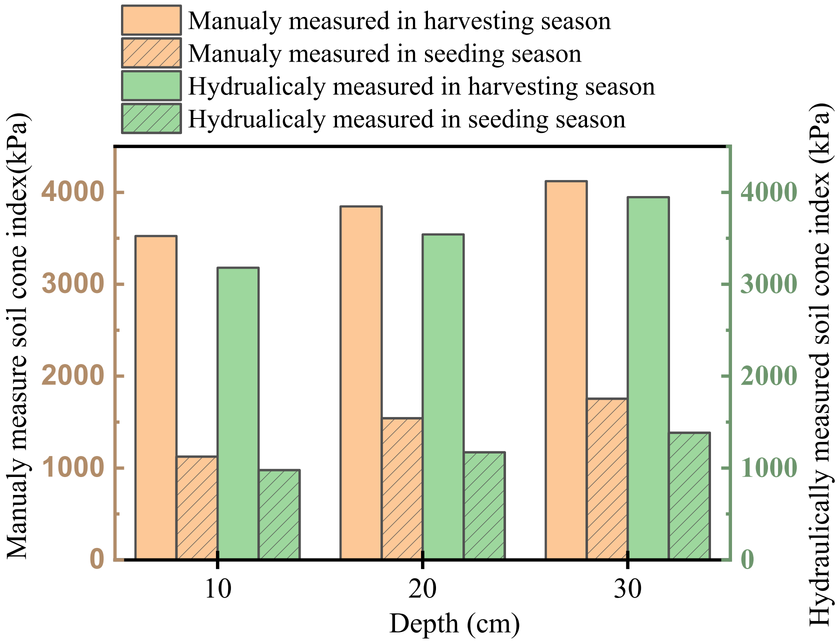

Figure 4.10: Manually and hydraulically measured CI vs. depth for Melkasa field

4.2.3. Bishoftu farm field

At sample points M and L, the soil compaction was highest throughout the harvesting and seeding seasons at 3958 kPa and 2018 kPa, respectively, while it was lowest at sample points M and D at 502 kPa and 279 kPa. As shown in Fig. 4.11, soil compaction increased with soil depth at the research experimental farm. The average soil compaction results of the three experimental locations for the seeding and harvesting season are summarized in Table 4.2.

Table 4.2: Average maximum soil CI value for three experimental locations

Depth	Season	Kulumsa	Melkasa	Bishoftu
10	Harvesting	3,522.6	3,180.3	1,011.2
	Seeding	1,255.4	978.3	630.1
20	Harvesting	3,730.3	3,542.3	1,918.1
	Seeding	1,227.4	1,171.0	549.3
30	Harvesting	3,511.8	3,947.3	1,838.3
	Seeding	1,195.5	1,383.5	548.2

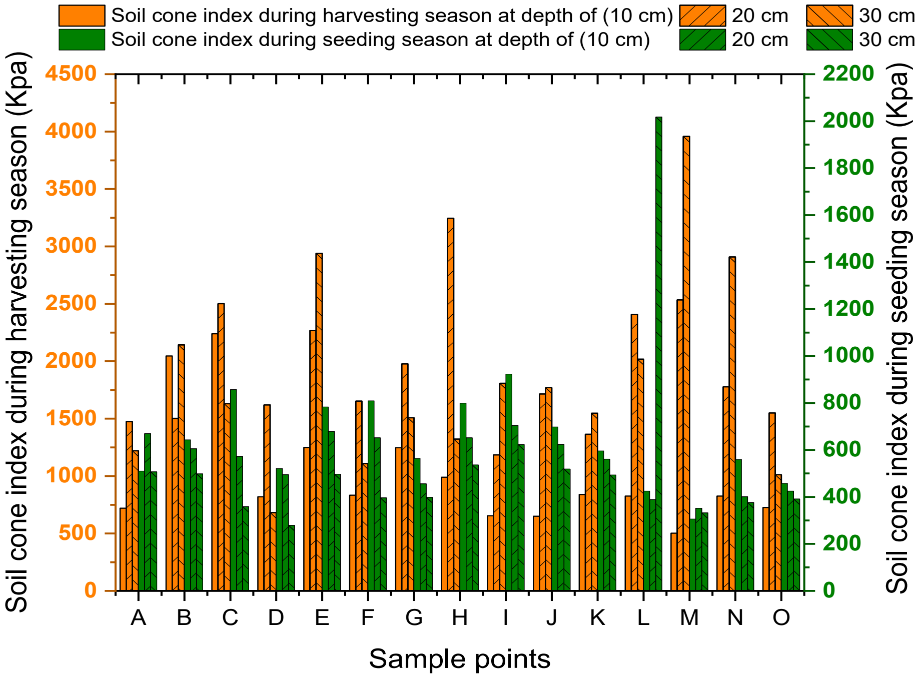

Figure 4.11: Soil CI vs. field sample point for the Bishoftu field test

For the Bishoftu experimental farm field in both experimental seasons, manually measured soil cone index values were higher than hydraulically powered soil cone index values as indicated in Fig.4.12. in the manual soil compaction measurement method, the maximum cone index was at a depth of 30 cm during harvesting season.

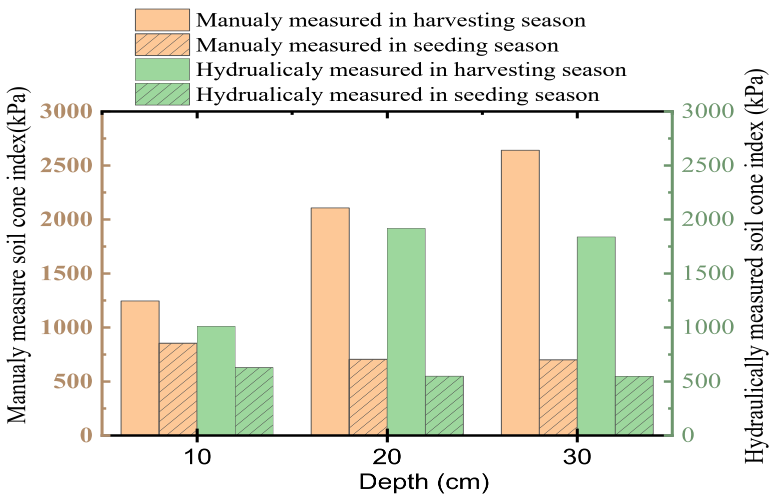

Figure 4.12: Manually and hydraulically measured CI vs. depth for Bishoftu field

4.2.4. Average soil compaction of all farm field

The soil compaction value versus depth plot as indicated in Fig. 4.13 for the three fields (Kulumsa, Melkasa, and Bishoftu) in seeding and harvesting seasons. From the average plot, the highest penetration resistance is recorded at the Kulumsa farm field up to 230 mm depth, and after 230 mm depth the maximum penetration resistance is recorded at the Melkasa farm field. Bishoftu farm site has the lowest penetration resistance. Averagely soil compaction value of the Kulumsa farm field was from 3,511.8 kPa to 3,730.3 kPa and 1,195.5 kPa to 1,227.4 kPa for harvesting and seeding season respectively as indicated in Table 4.2.

For the Melkasa farm field, the average soil compaction value ranges from 3,180.3 kPa to 3,947.3 kPa and 978.3 kPa to 1,383.5 kPa for harvesting and seeding season respectively as indicated in Table 4.2 and Fig. 4.13. Bishoftu farm fields have an average soil compaction value ranging from 1,011.2 kPa to 1,838.3 kPa and 548.2 kPa to 630.1 kPa for harvesting and seeding season respectively as indicated in Table 4.2. In this research work, soil compaction value increases with soil depth except Bishoftu farm field for the seeding season. Furthermore, the data shows a consistent trend of increasing soil compaction with depth during both experimental seasons, aligning with prior research that supports this finding (Chyba J et al., 2014; Hamza et al., 2005; Unger & Kaspar, 1994). As the depth increase the stability nature of the soil is high which results highly dense. But the top or fertile region of the soil is always unstable due to the agricultural activities like primary tillage and secondary tillage operation.

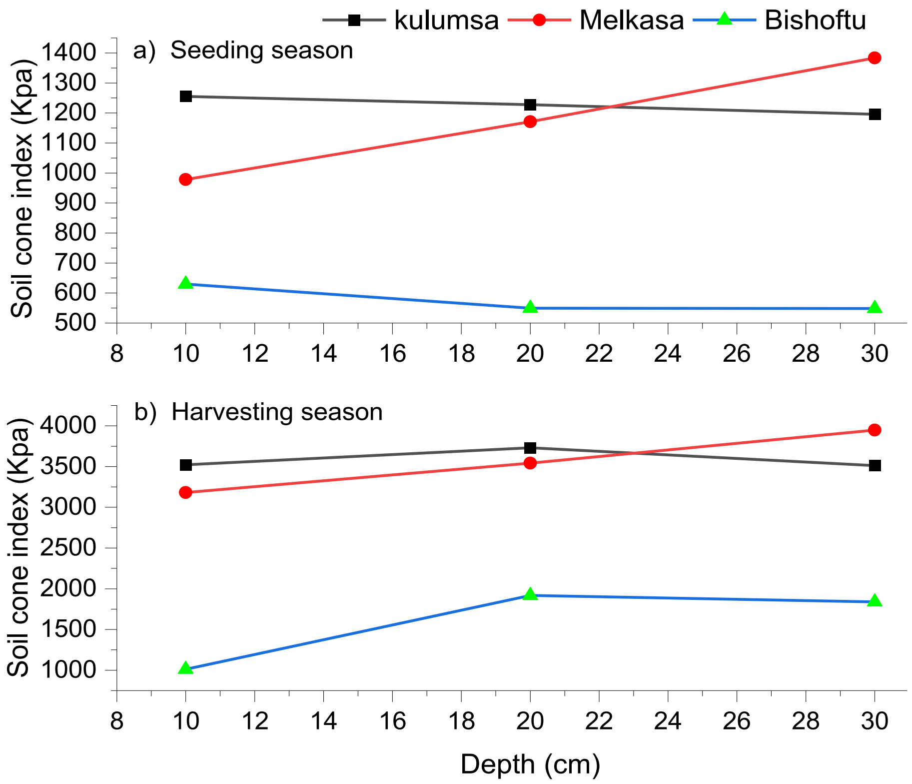

Figure 4.13: Average soil CI vs. depth for three experimental field

4.2.5. Statistical analysis results and discussion for all farm field

Table 4.3: Soil compaction correlation between three experimental field sites

	Kulumsa	Melkasa	Bishoftu
Kulumsa	1		
Melkasa	0.743	1	
Bishoftu	0.734	0.886*	1

*. Correlation is significant at the 0.05 level (2-tailed).
Source: SPSS 26, 2023

When there are significant associations, SPSS indicates one asterisk (*) for a significance level of 0.05 and two asterisks (**) for a level of 0.01. For Melkasa and Bishoftu, the Pearson correlation coefficient is 0.886, which is significant (p.05 for a two-tailed test). According to the findings, Kulumsa and Melkasa have a statistically significant linear association (r=0.743, p 0.05). A statistically significant linear association exists between Bishoftu and Kulumsa (r=0.734, p 0.05), as well as between Melkasa and Bishoftu (r=0.886, p 0.05).

A positive correlation exists between Kulumsa and Melkasa, Bishoftu and Kulumsa, and Melkasa and Bishoftu. Due to their correlation coefficients falling between 0.5 and 0.99, all fields of the association can be inferred to be roughly strongly connected. All soil compaction for the three sites was statistically analyzed using the t-test. The results of the univariate analysis of variance are reported in Table 4.4. Statistical analysis was performed at an error level of 5%.

Table 4.4: The test result of R Squared

Source	Sum of Squares	df	Mean Square	F	Sig.
Kulumsa	0.484	1	0.484	0.047	0.864
Melkasa	13.130	1	13.130	1.275	0.461
Bishoftu	14.945	1	14.945	1.451	0.441
Error	10.301	1	10.301		
Total	1375.000	5			
R Squared =.959 (Adjusted R Squared =.835)					

Source: SPSS 26, 2023

The mean of soil compaction is significantly different for one of the tillage farm site groups ($F_{\text{Kulumsa}} = 0.047, p < 0.05$) from this, the Kulumsa farm field soil has a significant difference when compared to Melkasa and Bishoftu farm field soil compaction. A significantly positive association between soil compaction at sample points between O and B and C and B in the

Kulumsa experimental field is significant at the 0.05 level. There is a significant negative connection between field points between G and C and O is significant at the 0.05 level.

Table 4.5: Soil compaction correlation within Kulumsa experimental field sites

	KA	KB	KC	KD	KE	KF	KG	KH	KI	KJ	KK	KL	KM	KN	KO
KA	1														
KB	.655	1													
KC	.476	.933*	1												
KD	-.875	-.589	-.402	1											
KE	.306	.328	.546	.011	1										
KF	-.804	-.716	-.700	.481	-.756	1									
KG	-.791	-.974**	-.884*	.655	-.415	.840	1								
KH	-.058	-.568	-.512	-.22	-.162	.381	.520	1							
KI	-.506	.249	.509	.516	.337	.036	-.088	-.468	1						
KJ	.668	.585	.355	-.34	.158	-.690	-.689	-.680	-.272	1					
KK	-.413	.347	.451	.523	.110	-.004	-.201	-.826	.850	.149	1				
KL	.577	-.128	-.422	-.53	-.324	-.135	-.036	.290	-.981**	.447	-.744	1			
KM	.849	.582	.597	-.71	.693	-.866	-.709	.100	-.208	.349	-.376	.220	1		
KN	.458	.770	.566	-.29	-.045	-.483	-.752	-.848	.087	.849	.501	.098	.124	1	
KO	.526	.943*	.987**	-.38	.586	-.779	-.918*	-.601	.461	.487	.466	-.352	.614	.643	1

*. Correlation is significant at the 0.05 level (2-tailed); **. Correlation is significant at the 0.01 level (2-tailed), with 'K' in the first letter indicating the Kulumsa farm site; 'A to O" letters next to Kulumsa indicate the sampling point in the field. Source: SPSS 26, 2023

There is a significant positive association between field points O and C is significant at the 0.01 level. There is a significant negative correlation between field points between L and I, G and B significant at the 0.01 level. The overall significant difference happened due to the same farm field there is soil compaction deference due to tire load.

Table 4.6: Soil compaction correlation within Bishoftu experimental field sites

	BA	BB	BC	BD	BE	BF	BG	BH	BI	BJ	BK	BL	BM	BN	BO
BA	1														
BB	.385	1													
BC	.514	.288	1												
BD	.800	.078	.724	1											
BE	.570	.258	.146	.073	1										
BF	.561	-.266	.567	.537	.641	1									
BG	.302	-.529	.336	.311	.556	.944*	1								
BH	.780	-.123	.711	.869	.423	.883*	.729	1							
BI	.421	.219	-.005	-.111	.983**	.545	.507	.266	1						
BJ	.715	.110	.266	.325	.953*	.799	.699	.658	.895*	1					
BK	.284	-.09	.086	-.087	.907*	.737	.768	.388	.923*	.870	1				
BL	.980**	.256	.389	.732	.652	.621	.408	.783	.519	.800	.402	1			
BM	.467	.134	.026	-.032	.987**	.628	.595	.360	.992**	.934*	.944*	.575	1		
BN	.605	.444	.162	.069	.979**	.520	.391	.349	.959**	.903*	.815	.657	.945*	1	
BO	.454	-.51	.369	.481	.530	.957*	.975**	.834	.453	.721	.685	.554	.554	.373	1

** Correlation is significant at the 0.01 level (2-tailed), *. Correlation is significant at the 0.05 level (2-tailed), with 'B' in the first letter indicating the Bishoftu farm site; 'A to O' letters next to Bishoftu indicates the sampling point in the field.

The soil compaction within the Melkasa experimental field sites of sampling points has a significantly positive association at the 0.05 level between G and F, H and F, J and E, J and

I, K and E, K and I, M and J, M and K, N and J, N and M, and O and F. Field points between I and E, L and A, M and E, M and I, N, and E, N and I, and O and G have a high positive correlation at the 0.01 level.

Table 4.7: Soil compaction correlation within Melkasa experimental field sites

	MA	MB	MC	MD	ME	MF	MG	MH	MI	MJ	MK	ML	MM	MN	MO
MA	1														
MB	.444	1													
MC	.523	.912	1												
MD	-.568	-.003	-.362	1											
ME	.915	.725	.775	-.525	1										
MF	-.672	-.764	-.688	.282	-.879	1									
MG	.452	.679	.530	.293	.466	-.292	1								
MH	.827	.672	.853	-.722	.934	-.747	.334	1							
MI	.752	.203	.080	-.209	.666	-.697	.165	.410	1						
MJ	.599	.647	.381	.298	.622	-.635	.798	.337	.666	1					
BK	.773	.890	.842	-.175	.891	-.765	.798	.795	.466	.793	1				
ML	.930	.558	.707	-.727	.964**	-.780	.294	.963**	.625	.424	.767	1			
MM	.176	.706	.872	-.281	.408	-.253	.444	.612	-.402	.030	.565	.381	1		
BN	.447	.709	.685	.077	.491	-.240	.943*	.478	-.031	.596	.800	.372	.692	1	
MO	.468	.903*	.950	-.174	.672	-.522	.735	.731	-.029	.465	.864	.573	.897*	.871	1

**. Correlation is significant at the 0.01 level (2-tailed), *. Correlation is significant at the 0.05 level (2-tailed), with ‘M’ in the first letter indicating the Melkasa farm site; “A to O" letters next to Melkasa indicating sampling point in fields; ’PC’ Personal correlation. Source: SPSS 26, 2023

Within the Bishoftu experimental field sites, there is a high correlation between soil compaction at sample points D and B, L and E, L and H, N and I, and O and I at the 0.01 significant level. There is a strong positive correlation between field points between O and B, N and G, and O and M at the 0.05 significant level.

4.3. Soil Physical Property

Tables 4.8 and 4.9 provide a summary of the laboratory's findings.

Table 4.8: Soil physicochemical properties result in harvesting season

Experimental location	Depth (mm)	Cone index	pH	EC (µS/cm)	Textural			CEC meq/100 g soil)	%TOC	%OM	%TN	% Moisture
					% Sand	% Clay	% Silt					
Bishoftu	10	1011.2	6.17	245	45	27	28	25.5	1.35	2.33	0.08	21.43
	20	1918.1	6.46	251.2	48	25	27	21.3	1.53	2.43	0.12	23.87
	30	1838.3	6.53	257.9	49	25	26	28.6	1.18	2.41	0.09	27.02
Melkasa	10	3180.3	7.28	113.3	37	29	34	18.78	1.21	2.09	0.13	13.97
	20	3542.3	7.42	118.2	37	31	32	22.1	1.43	2.15	0.19	14.35
	30	3947.2	7.12	126.5	36	31	33	28.6	1.18	2.12	0.17	16.04
Kulumsa	10	3522.6	6.04	109.2	25	51	24	25.4	2.78	4.8	0.18	20.04
	20	3730.3	6.8	110.9	27	54	19	31.5	2.83	5.1	0.28	24.13
	30	3511.8	6.25	115.5	23	48	29	34.24	2.53	4.95	0.26	28.92

Abbreviations: - EC=Electrical conductivity, CEC = cation exchange capacity, TOC= Total organic carbon, OM=Organic matter, TN= Total nitrogen
Source: researcher, 2023

Table 4.9: Soil physicochemical properties result in seeding season

Experimental location	Depth (mm)	Cone index	pH	EC (µS/cm)	Textural			CEC (meq/100 g soil)	%TOC	%OM	%TN	% Moisture
					% Sand	% Clay	% Silt					
Bishoftu	10	630.1	6.53	281.9	43	28	29	32.9	1.75	2.52	0.1	46.7
	20	549.3	6.78	293.7	47	23	30	29.7	1.97	2.67	0.17	47.9
	30	548.2	6.92	298.5	45	29	26	31.6	1.52	2.59	0.14	48.3
Melkasa	10	978.3	7.09	139.7	38	27	35	27.59	1.95	2.83	0.16	25.2
	20	1171	7.19	143.2	39	28	33	30.15	2.21	2.91	0.21	27.9
	30	1383.5	7.04	149.8	37	29	34	40.52	1.82	2.8	0.19	30.5
Kulumsa	10	1255.4	6.24	129.9	24	50	26	29.2	3.93	5.3	0.27	30.82
	20	1227.4	6.78	132.6	25	55	20	31.8	3.98	6.09	0.34	36.45
	30	1195.5	6.63	137.1	25	49	26	40.5	3.66	5.79	0.31	41.83

Abbreviations: - EC=Electrical conductivity, CEC = cation exchange capacity, TOC= Total organic carbon, OM=Organic matter, TN= Total nitrogen

4.3.1. Soil texture

The soil texture triangle for soil is drawn in Fig. 4.14 to identify the soil texture class. Based on the soil texture triangle (Estefan, 2013) for Kulumsa farm field was clay with 24% silt, 51% clay, and 25% sand taking the average value for both experimental season.

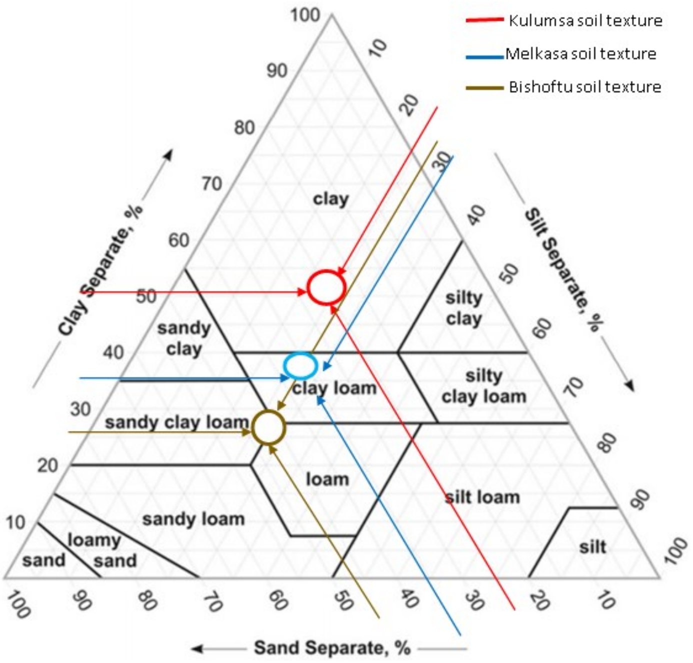

Figure 4.14: Soil texture triangle

For the Melkasa farm field, the soil texture class is clay loam with 33.5% of silt, 29.2% of clay, and 37.3% of sand taking the average value for both experimental season, and the

Bishoftu farm has a soil texture class with a mixture of loam, clay loam, sandy clay loam with 27.6% of silt, 26.2% of clay and 46.2% of sand taking the average value for both experimental season.

4.3.1.1. Sand content

According to Fig. 4.15, all experimental locations had an increase in sand percentage up to a depth of 200 mm, followed by a drop in sand percentage after that point. The highest percentage of sand was recorded for the Bishoftu farm soil whereas the smallest was for the Kulumsa farm soil.

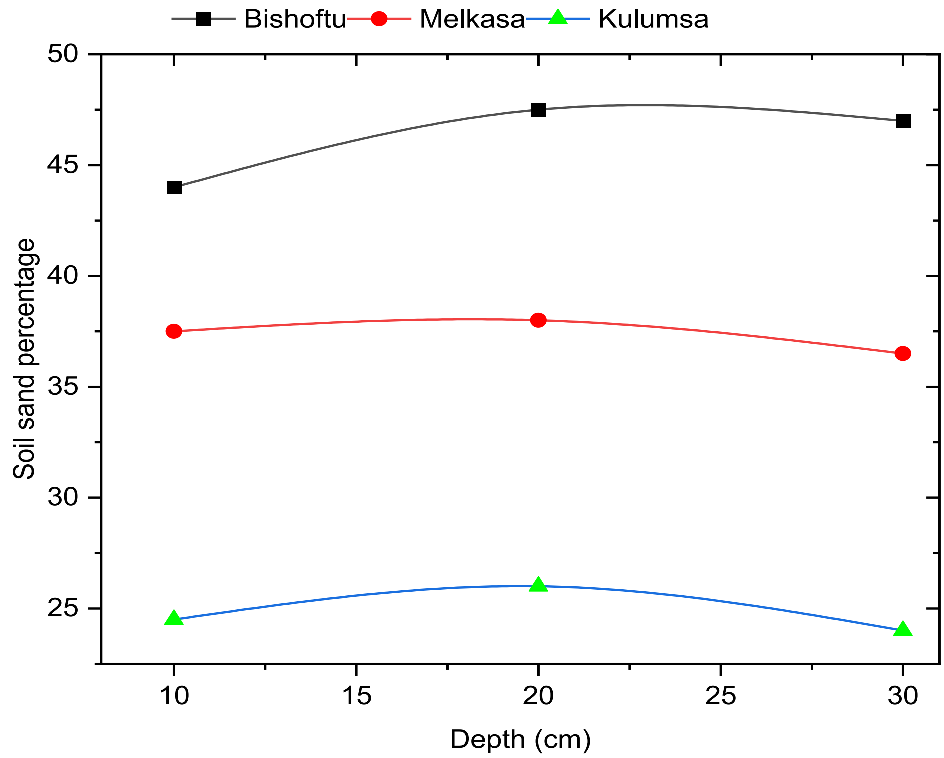

Figure 4.15: Soil sand percent vs. depth for all experimental locations

4.3.1.2. Clay content

Except in Bishoftu farm soil, as shown in Fig. 4.16, the percentage of clay increases as depth increases up to 200 mm. For Kulumsa farm soil, the percentage of clay decreased after 200 mm depth and gradually rose. The Kulumsa farm soil had the largest percentage of clay, while the Bishoftu farm soil had the lowest.

4.3.1.3. Silt content

According to Fig. 4.17, silt percentages reduced for all experimental locations as depth increased up to 200 mm and then began to rise, except for Bishoftu farm soil. The farm soil from Melkasa had the largest amount of silt, whereas the farm soil from Kulumsa had the lowest percentage.

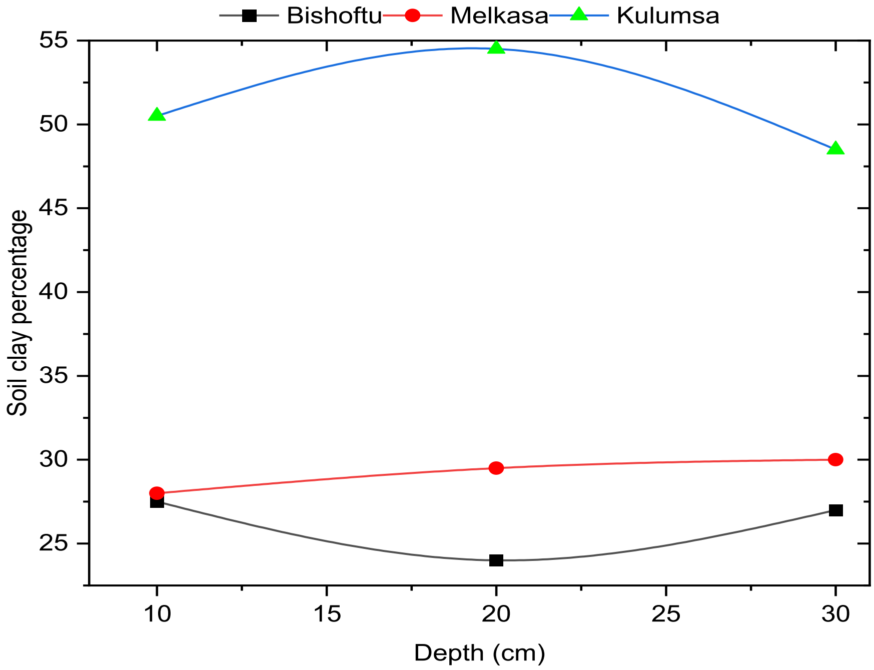

Figure 4.16: Soil clay percent vs. depth for all experimental locations

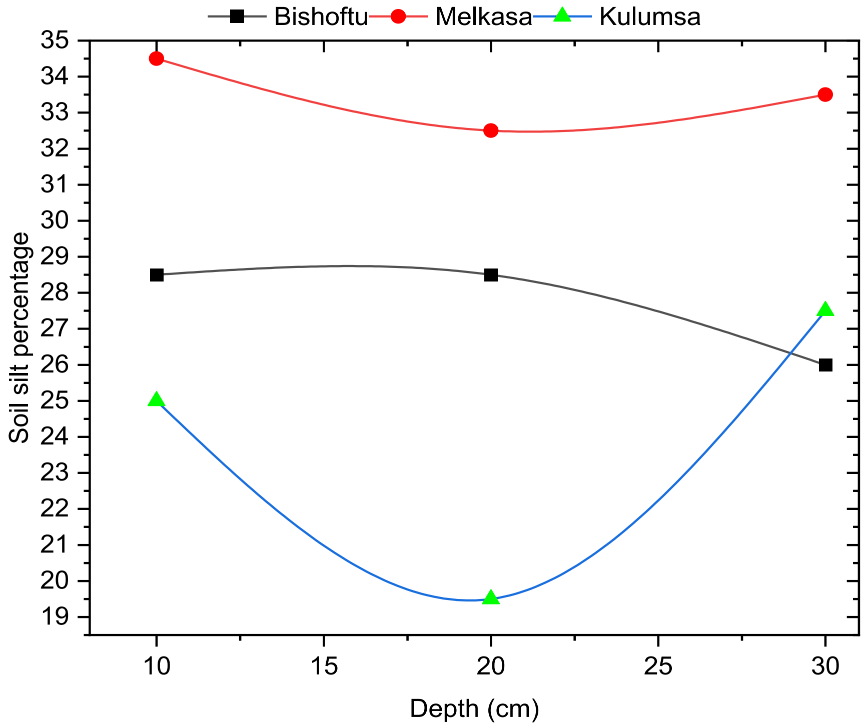

Figure 4.17: Soil silt percent vs. depth for all experimental locations

4.3.2. Moisture content

The moisture content is the percentage ratio of the weight of water to the weight of solids in a particular amount of soil. Equation 3.1 was used to calculate the moisture content of the soil for the three experimental field soils. The results of the calculation are summarized in Table 4.10.

Table 4.10: The soil moisture content of three experimental site field soils

Sample code	% Moisture at 3 different depths in mm				
	Exp. season	100 mm depth	200 mm depth	300 mm depth	Average
Kulumsa	harvesting	20.04	24.13	28.92	24.4
	seeding	30.82	36.45	41.83	36.4
Melkasa	harvesting	13.97	14.35	16.04	14.8
	seeding	25.2	27.9	30.5	27.9
Bishoftu	harvesting	21.43	23.87	27.02	24.1
	seeding	46.7	47.9	48.3	47.6

For the three experimental field soils, the percentage of moisture results indicate for the 3 sites farm fields Kulumsa, Melkasa, and Bishoftu is 24.4%, 14.8%, and 24.1% respectively (average values) for harvesting season as indicated in Fig. 4.18 to 4.20. For the seeding season farm field Kulumsa, Melkasa, and Bishoftu are 36.4%, 27.9%, and 47.6% respectively (average values) as indicated in Fig. 4.18 to 4.20. The moisture contentment of Kulumsa, and Bishoftu is higher than Melkasa. This is due to factors such as gravity, capillary action, and the presence of clay minerals, which can hold onto water more tightly.

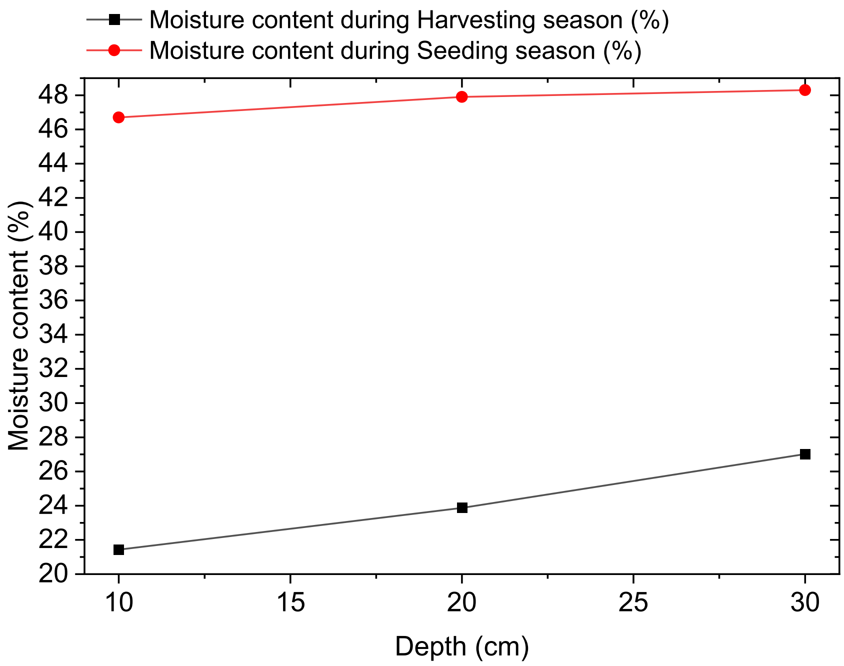

Figure 4.18: Soil moisture content vs. depth for Bishoftu farm

At 300 mm and 100 mm depths, the maximum and minimum percentages of Bishoftu farm soil moisture levels were 27.02% and 21.43% during the harvesting season, and 48.3% and 46.7% during the time of seeding, respectively. The relationship between soil moisture content and depth is represented in Fig. 4.18, which demonstrates that as depth increases, the percentage of soil moisture content increases for both experimental seasons.

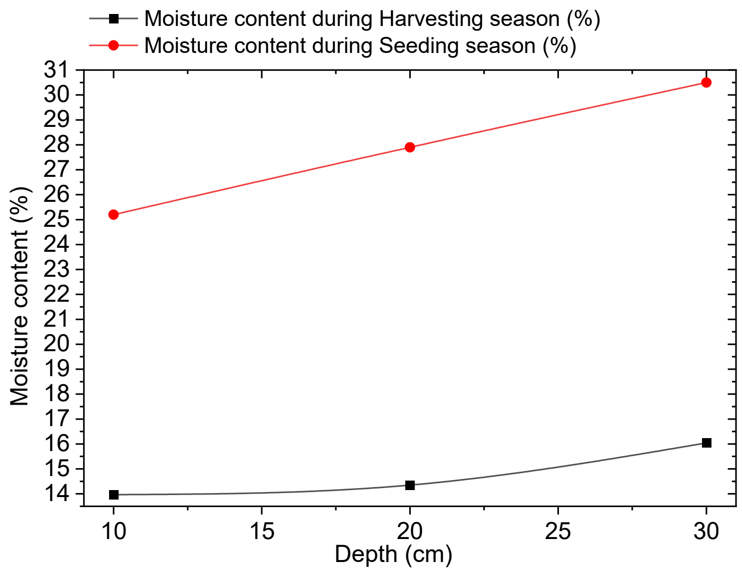

Figure 4.19: Soil moisture content vs. depth for Melkasa farm

As shown in Fig. 4.19 the maximum and minimum percentages of soil moisture values at Melkasa farm were 16.04% and 13.97% during the harvesting season and 30.5% and 25.2% during the seeding season at 300 mm and 100 mm depth, respectively. The relationship between soil moisture content and depth is represented in Fig. 4.19, which demonstrates that as depth increases, so does the percentage of soil moisture content for both experimental seasons.

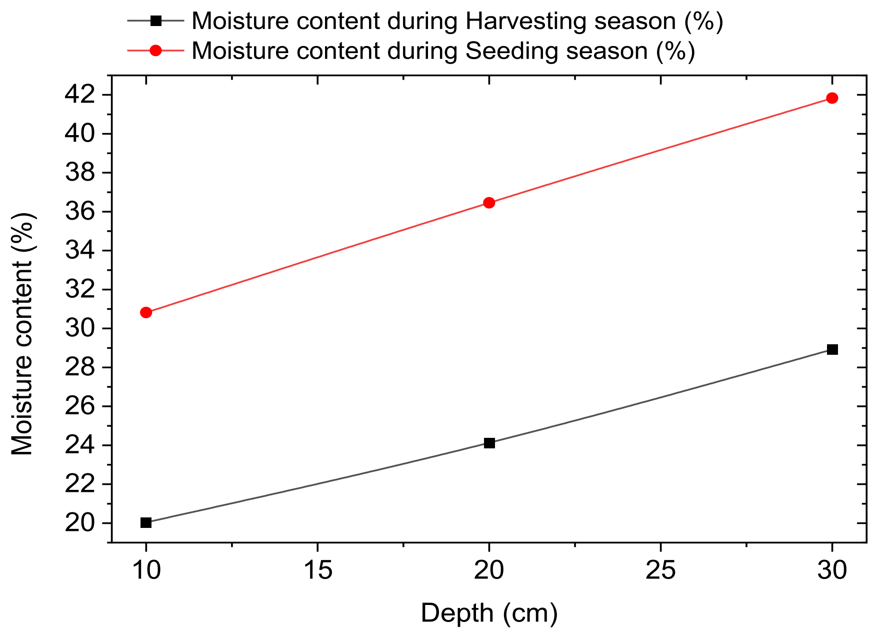

Figure 4.20: Soil moisture content vs. depth for Kulumsa farm

At 300 mm and 100 mm depths, the maximum and minimum percentages of Kulumsa farm soil moisture values were 28.92% and 20.04% during the harvesting season, and 41.83% and 30.82% during the time for seeding, as shown in Fig. 4.20. The relationship between soil moisture content and depth is represented in Fig. 4.20, which demonstrates that as depth increases, so does the percentage of soil moisture content for both experimental seasons. On average Bishoftu farm fields have a high amount of moisture content in both seasons and Melkasa farm field soil has a low moisture content in both seasons. On the other hand, the increase in moisture content with depth is a common phenomenon in many soil profiles. This is due to factors such as gravity, capillary action, and the presence of clay minerals, which can hold onto water more tightly. As you move deeper into the soil profile, moisture tends to accumulate, especially in soils with good water retention properties. Both soil penetration resistance and moisture content increase with depth, corroborating findings from previous studies (Shah et al., 2017; Woldeyohannis et al., 2024).

4.4. Soil Chemical Property

4.4.1. pH value

Soil pH increases as depth increases for the first 200 mm depth, as demonstrated in Fig. 4.21 for both experimental agricultural seasons.

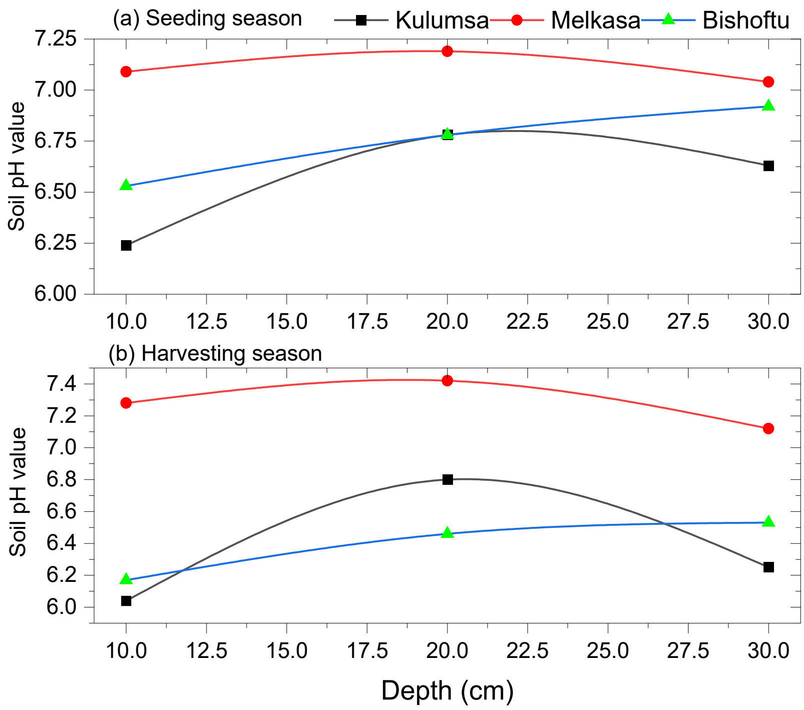

Figure 4.21: Soil pH value vs. depth for all experimental farms

After 200 mm depth, soil pH value starts decreasing in both seasons with depth except Bishoftu experimental farmthis finding supported by previous studies (Seifu et al., 2023; Woldeyohannis, Hiremath, Tola, Wako, & Science, 2022). On average Melkasa farm fields have a high amount of soil pH value in both seasons which is 7.15 this soil pH value indicates the soil is almost neutral. Bishoftu and Kulumsa farm field soil was acidic in both seasons. The availability of nutrients and microbial activity, are two chemical and biological processes that are influenced by soil pH (Fernández & Hoeft, 2009).

4.4.2. Electrical conductivity

Soil electric conductivity increases with depth for all experimental depths as shown in Fig. 4.22. The maximum and minimum percentage of soil electric conductivity values were 257.9 µS/cm and 109.2 µS/cm for the Bishoftu and Kulumsa farm fields respectively during harvesting season and 298.5 µS/cm and 129.9 µS/cm for Bishoftu and Kulumsa farm field during the seeding season at 300 mm and 100 mm depth. On average Bishoftu farm fields have a high amount of soil electric conductivity value in both seasons and Kulumsa farm field soil has a low soil electric conductivity value in both seasons.

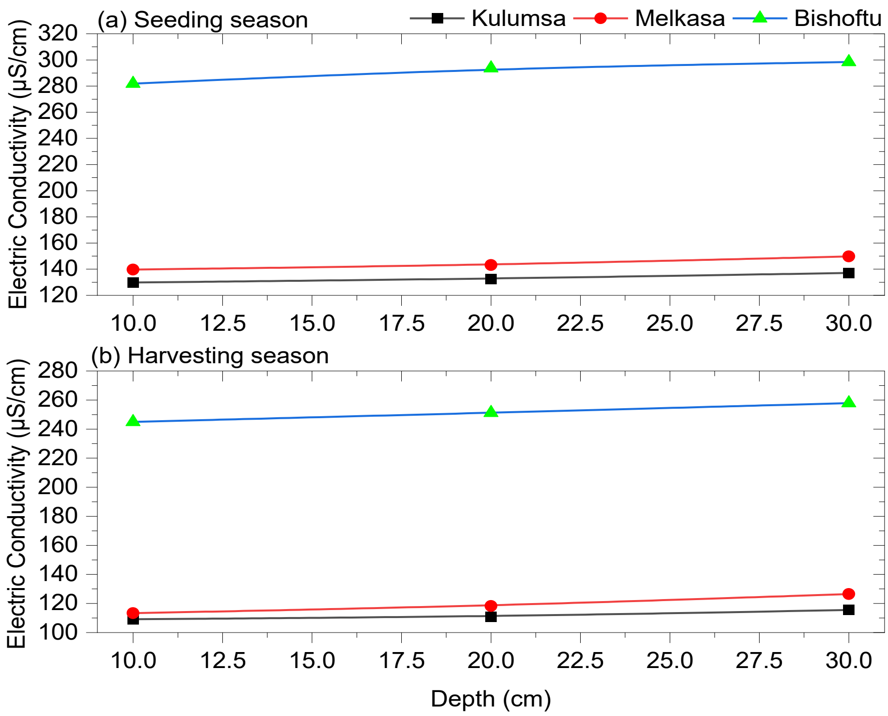

Figure 4.22: Soil electrical conductivity vs. depth

Despite having a greater electrical conductivity (EC) value due to the texture of the soil, clay-rich soils tend to have a higher moisture content (Othaman et al., 2020). Since the tested soil contains all different types of soil, the results were in the moderate range according to previous studies (Seifu et al., 2023; Woldeyohannis, Hiremath, Tola, Wako, & Science, 2022). A few key variables that significantly affect the soil's EC value are temperature, the number of fertilizers used, the type of soil, salinity, moisture content, and irrigation (Othaman et al., 2020). The results were consistent with previous research, and the moisture level aids in the release of ions, allowing EC values to be easily read.

4.4.3. Cation exchange capacity

Kulumsa farm soil has the greatest average CEC value of 33.8 meq/100 g of soil and 30.38 meq/100 g of soil during the seeding and harvesting seasons, respectively. As indicated in Fig. 4.23, the maximum cation exchange capacity of Melkasa and Bishoftu farm soil is 32.75 and 31.4 meq/100 g of soil, respectively, based on average values for all depth samples taken during the seeding season. Soil texture has an impact on EC and moisture content. Sand has a lower electrical conductivity (EC) value and is less effective at storing moisture due to its poor surface contact, whereas silt is wet and has a medium EC value (Friedman, 2005).

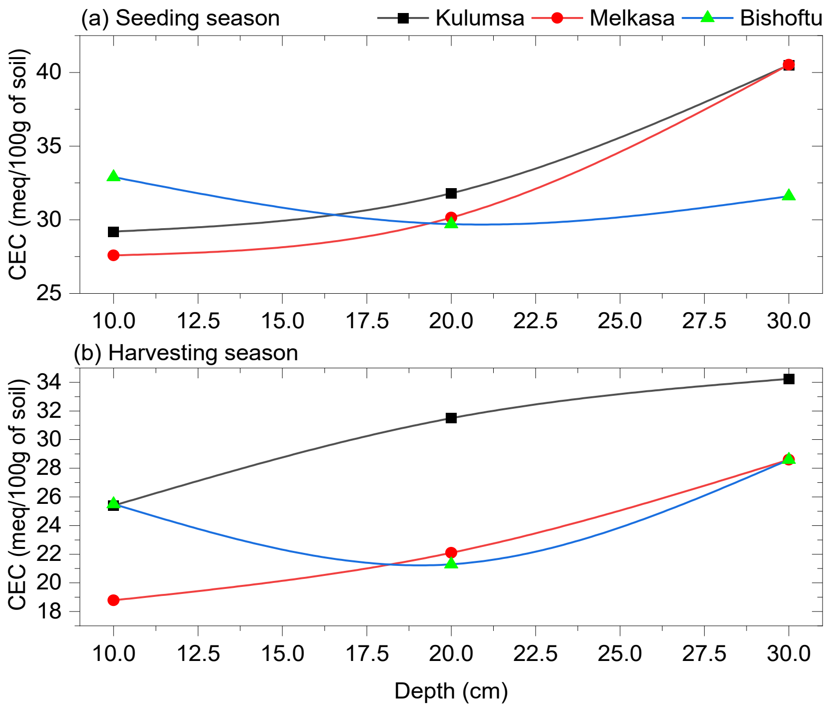

Figure 4.23: Soil CEC vs. depth

4.4.4. Total organic carbon

Total organic carbon with depth has a positive relationship on the top part of soil up to 200 mm depth for both experimental farming seasons. After 200 mm depth, total organic carbon starts decreasing as shown in Fig. 4.24a and 4.24b. On average Kulumsa farm fields have a high amount of soil total organic carbon value in both seasons 2.71% and 3.86% for harvesting and seeding season respectively. These findings are consistent with existing literature, which also indicates that SOC tend to increase with soil compaction and depth in the fertile soil layers, while decreasing in less fertile soil depths. The depression of Carbon mineralization in compacted soils can lead to higher organic matter accumulation.(Bi et al., 2018; De Neve & Hofman, 2000).

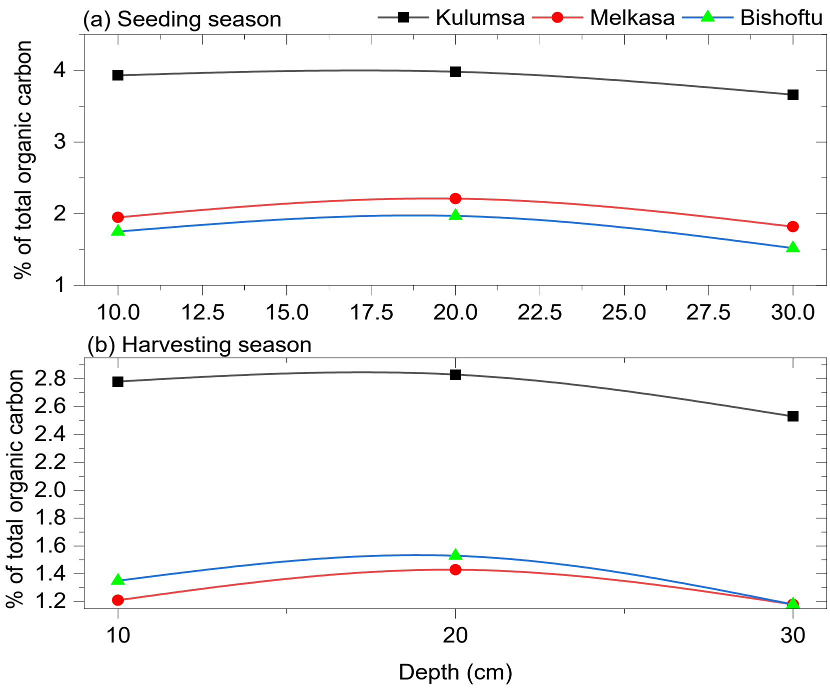

Figure 4.24: Total organic carbon percent vs depth

4.4.5. Organic matter

In both of the experimental farming seasons, this study demonstrated a favorable association between soil organic matter and depth on the top part of the soil up to a depth of 200 mm. (Tiessen et al., 1994) also showed the same result in their research work. Soil organic matter with depth has a positive relationship on the top part of soil up to 200 mm depth for both experimental farming seasons. After 200 mm depth, soil organic matter starts decreasing as shown in Fig. 4.25a and 4.25b. On average Kulumsa farm fields have a high amount of soil organic matter value in both seasons 2.71% and 5.7% for harvesting and seeding seasons respectively and Bishoftu farm fields have a minimum value of soil organic matter in the seeding season of 2.59% whereas Melkasa has a minimum value of soil organic matter 2.12% for harvesting seasons. In most soils, organic matter content decreases with increasing depth from the surface but in this finding, for the farm field Melkasa and Bishoftu during the seeding season, there were uniform from top to 30 cm depth this is due to the fact seeding seasons are rain seasons which makes the uniform mixture of soil due to ploughing effect in the rainy season. These findings are consistent with existing literature, based on the fertile nature of soil layers depths (Bi et al., 2018).

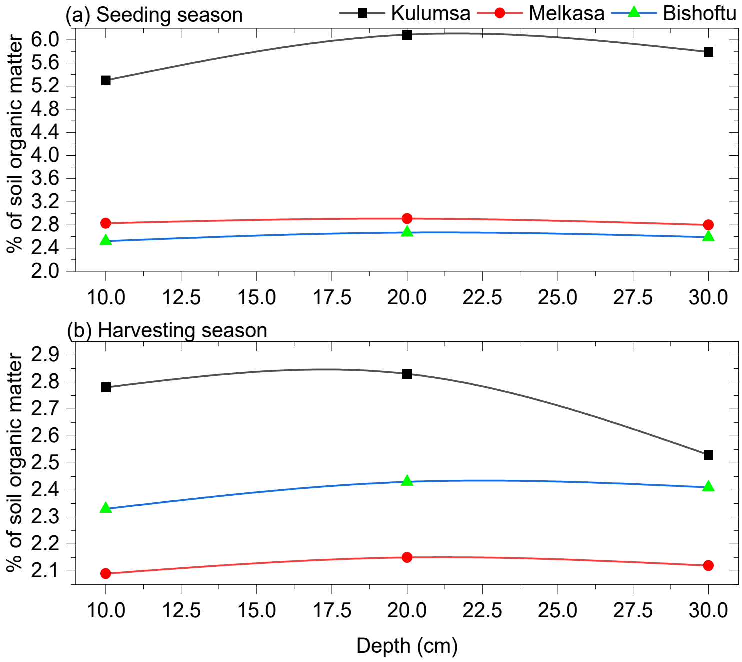

Figure 4.25: Soil organic matter percent vs. depth

4.4.6. Total nitrogen

The finding of this study showed that soil total nitrogen with depth has a positive relationship on the top part of soil up to 200 mm depth for both experimental farming seasons. After 20cm depth soil total nitrogen start decreasing as shown in Fig. 4.26a and 4.26b.

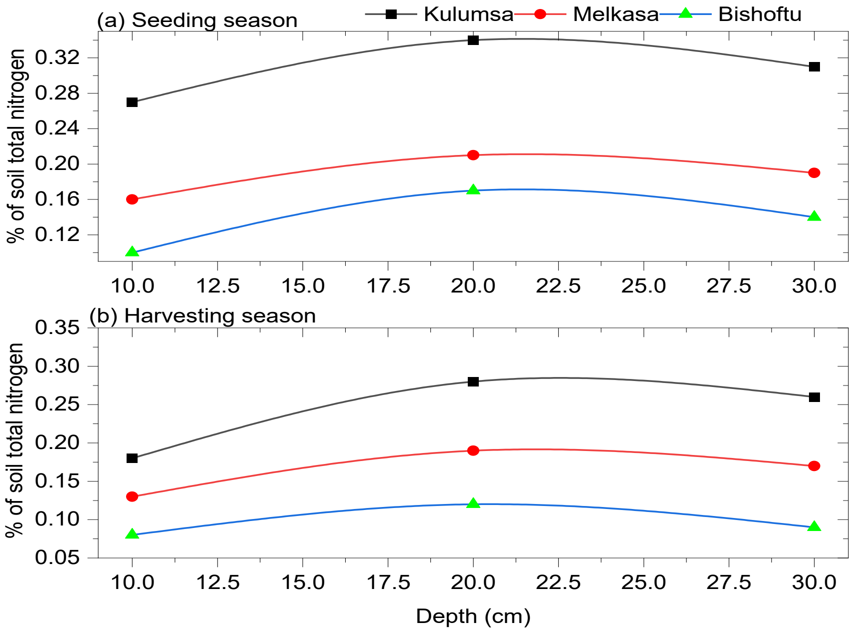

Figure 4.26: Total nitrogen percent of soil vs. depth

On average Kulumsa farm fields have a high amount of soil total nitrogen value in both seasons 0.24% and 0.31% for harvesting and seeding seasons respectively and Bishoftu farm fields have a minimum value of soil total nitrogen in both seasons 0.097% and 0.0137% for harvesting and seeding season respectively. These findings are consistent with existing literature, which also indicates that STN tend to increase with soil compaction and depth in the fertile soil layers, while decreasing in less fertile soil depths (Bi et al., 2018). According to (Mazzoncini et al., 2011), soil total nitrogen (STN) is a key driver and indicator of soil fertility and quality in an agricultural environment. It also has a close relationship with soil productivity. According to Fig 4.26, the current investigation demonstrated a linear connection between STN in the top (300 mm) soils and depth during both the seeding and harvesting seasons.

4.5. Statistical Analysis

4.5.1. Descriptive statistics of variables

The independent and dependent variables were used to derive descriptive statistics such as minimum, maximum, range, averages, standard deviations, variance, skewness, and kurtosis.

Table 4.11: Descriptive Statistics for soil physicochemical and compaction

Variables	Min	Max.	Range	Mean	SD	Variance	Skewness	Kurtosis
CI	548	3730.3	3182.1	1524.07	1071.51	1148125	1.144	0.227
Moisture	13.9	48.30	34.33	29.1872	11.071	122.571	0.520	-0.696
Sand	23	49.00	26.00	36.1111	9.13229	83.399	-0.176	-1.442
Clay	23	55.00	32.00	35.5000	11.663	136.029	0.734	-1.379
Silt	19	35.00	16.00	28.3889	4.65440	21.663	-0.440	-0.361
pH	6.04	7.42	1.38	6.7372	0.40845	0.167	-0.092	-1.023
EC	109.2	298.50	189.30	175.2328	71.89	5168.331	0.796	-1.248
CEC	18.8	40.52	21.74	29.4433	50.77	33.274	0.211	0.286
STOC	1.2	3.98	2.80	2.1561	0.94	0.874	0.925	-0.302
SOM	2.1	6.09	4.00	3.4378	1.43	2.039	0.816	-1.130
STN	.08	.34	.26	0.188	0.076	0.006	0.502	-0.632

To examine and describe the data that has been gathered, descriptive analysis is performed (Kothari, 2004). As demonstrated in Table 4.11, all items have a near-to-normal distribution when skewness and kurtosis values are between -2 and 2 (George & Mallery, 2010). The plotted residuals are contrasted with the normal distribution's diagonal, which is typically a straight line (Templeton, 2011). Soil physiochemical measurements and data on soil compaction employed in this investigation had a normal distribution.

4.5.2. Correlations analysis

The results of the personal correlation are shown in Table 4.12 and are interpreted using the rules outlined by (Field, 2005). According to Field, a relationship is weak if it is measured between 0.1 and 0.29, moderate between 0.30 and 0.49, and strong above 0.50. The positive and negative signs indicate the direction of a relationship. Each of the variables that make up the independent variable moisture content, soil texture, pH, cation exchange capacity, electric conductivity, total organic carbon, organic matter, and soil total nitrogen shows a high degree of connection. According to Table 4.12, the correlation coefficient in this study between season and soil CI value is r = 0.71 and is within the range of r = 0.50 to 1.0, indicating a strong association. When we evaluate the degree of significance, the season and soil CI have a significant association at the p = 0.01 level (2-tailed). The soil CI value and experimental field location have a high positive association of r = 0.519, which is within the range of r = 0.50 to 1.0. There is a significant relationship between experimental field location and soil CI at $p = 0.05$ level (2-tailed). The correlation between depth and soil CI value is r =0.093 which is a positively weak relationship. There is no significant relationship between depth and soil CI value.

(Lewis-Beck & Mitchell II, 1993) claim that the presence of a correlation of 0.8 or above suggests a multicollinearity issue. Since there is a problem with multicollinearity in parameters like experimental field location and soil sand percentage, between soil organic carbon and soil total nitrogen content, and between sand percentage and clay percentage, it can be inferred from the results of the aforementioned correlation matrix that the highest correlation is 0.98. However, for other parameters, there are no findings with correlations above 0.8, indicating that the multicollinearity issue between the model's variables was not present.

Table 4.12: Correlations of soil physicochemical parameters and compaction

	Season	Field	Depth	CI	Moisture	Sand	Clay	Silt	pH	EC	CEC	STOC	SOM	STN
Season	1													
Field	-	1												
Depth	-	-	1											
CI	-.71**	.519*	.093	1										
Moisture	.753**	-.209	.218	-.430	1									
Sand	-.025	-.98**	.023	-.511*	.122	1								
Clay	-.015	.900**	-.006	.593**	.006	-.93**	1							
Silt	.086	-.331	-.030	-.485*	-.253	.364	-.68**	1						
pH	.158	-.111	.195	-.393	-.178	.209	-.377	.534*	1					
EC	.206	-.87**	.065	-.446	.589*	.804**	-.61**	-.045	-.21	1				
CEC	.574*	.280	.542*	-.121	.615**	-.321	.312	-.151	-.11	-.01	1			
STOC	.414	.780**	-.081	.196	.302	-.8**	.858**	-.58*	-.35	-.43	.440	1		
SOM	.205	.838**	.039	.424	.221	-.86**	.946**	-.7**	-.43	.48*	.456	.952**	1	.
STN	.291	.860**	.219	.280	.150	-.84**	.833**	-.432	.003	-.7**	.481*	.873**	.872**	1

**. Correlation is significant at the 0.01 level (2-tailed).
*. Correlation is significant at the 0.05 level (2-tailed).
Source: SPSS 26

4.5.3. Regression analysis

The value of adjusted R square is 85.43% of soil physiochemical properties were explained by the soil CI as indicated in Table 4.13. The soil CI is affected by other than soil physiochemical properties by 14.57%. The R square value obtained for the regression was 0.9314. this shows that the variables of the soil CI account for 93.14% variation in soil physiochemical properties. The variation associated with the soil physiochemical properties, therefore, has a greater effect on soil compaction since the value of R square is greater than 50 %. The 93.14% also implies that there might be other factors that bring about 6.84% in the soil compaction. These other factors are left for future researchers.

Table 4.13: Regression Analysis output

S	R-sq	R-sq (adj.)	R-sq (pred.)
408.970	93.14%	85.43%	68.75%

Source: SPSS 26

According to the findings in Table 4.14, the coefficient value for soil moisture content is 201.4. This suggests that soil compaction increased 201.4 times with a 1% increase in soil moisture content. In the case of sand percentage, a 1% increase in sand percentage resulted in a 462 times increase in soil compaction. The coefficient value for other soil physiochemical parameters is indicated in Table 4.14 in a coefficient column.

Table 4.14: Coefficients of soil physicochemical properties and compaction

Term	Coef.	SE Coef.	T-Value	P-Value	VIF
Constant	19689	5988	3.29	0.011	
Moisture	201.4	75.7	2.66	0.029	71.41
Sand	462	155	2.98	0.018	203.66
Clay	279.9	82.5	3.39	0.009	94.04
pH	-4898	1339	-3.66	0.006	30.41
EC	-58.2	19.8	-2.94	0.019	205.56
CEC	-103.7	38.3	-2.71	0.027	4.96
STOC	-2488	500	-4.98	0.001	22.20
SOM	-947	744	-1.27	0.239	114.61
STN	22325	6855	3.26	0.012	27.99

Source: SPSS 26

4.5.4. Analysis of variance

We can determine whether the total model is statistically significant and effective in forecasting the soil compaction variable by using the ANOVA. The F ratio greater than one indicates whether the outcome of the regression model may have been the product of chance. It also indicates that systematic variation is bigger than unsystematic variation. In this research, the maximum and minimum values of the F ratio are for the soil total organic carbon and soil organic matter (24.76 at 0.001) and (1.62 at 0.239) respectively as indicated in Table 4.15. According to the regression model, the mean value of the soil's physiochemical characteristics provides a considerably better prediction of the soil compaction value. The F-value column in Table 4.15 contains the value of the F ratio for additional soil physiochemical characteristics.

Table 4.15: ANOVA tests

Source	DF	Adj SS	Adj MS	F-Value	P-Value
Regression	9	18180066	2020007	12.08	0.001
Moisture	1	1183460	1183460	7.08	0.029
Sand	1	1485277	1485277	8.88	0.018
Clay	1	1926250	1926250	11.52	0.009
pH	1	2237522	2237522	13.38	0.006
EC	1	1445631	1445631	8.64	0.019
CEC	1	1225572	1225572	7.33	0.027
STOC	1	4141083	4141083	24.76	0.001
SOM	1	271002	271002	1.62	0.239
STN	1	1774104	1774104	10.61	0.012
Error	8	1338052	167256		
Total	17	19518118			

Source: SPSS 26

4.5.5. Interval plots analysis

The effect of plots of depth, season, and soil physicochemical properties on soil compaction are described in this section from Fig 4.27 to 4.29). The interval plot indicated in Fig. 4.27 the soil compaction range through three experimental fields. In this interval plot, the Bishoftu and Melkaa experimental fields overlapped, but not with the Kulumsa experimental field interval. Therefore, the mean of the Kulumsa experimental field is significantly different from the means of the Bishoftu and Melkaa experimental fields.

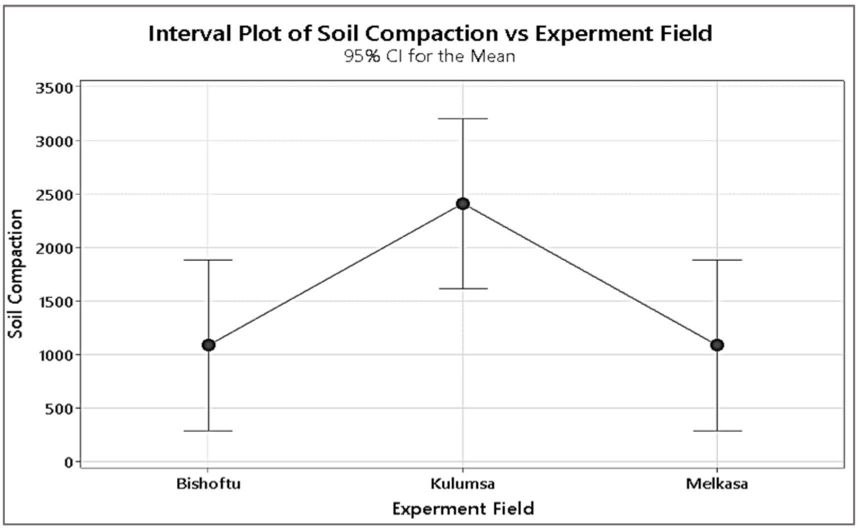

Figure 4.27: Interval plots of soil compaction vs. experimental field

The interval plot indicated in Fig. 4.28 the soil compaction range through three depths. In this interval plot, all depth intervals overlap with each other. Therefore, the mean of the depth is not significantly different. The maximum means value of soil compaction was at the depth of 200 mm.

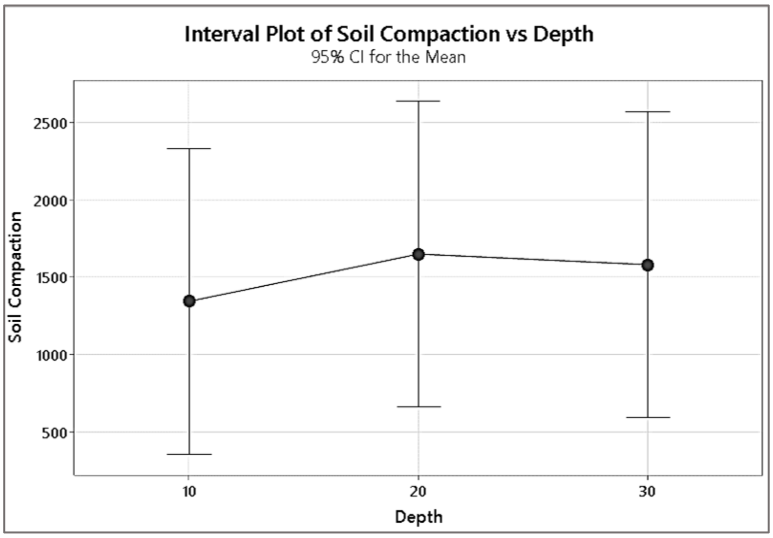

Figure 4.28: Interval plots of soil compaction vs. depth

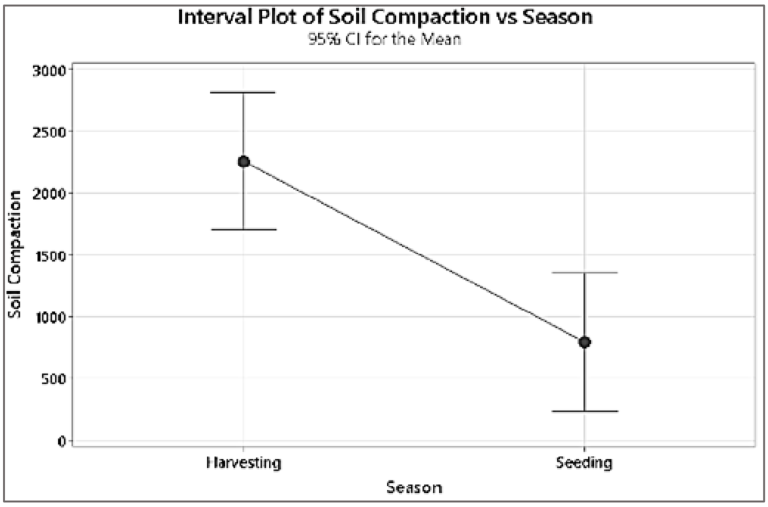

Figure 4.29: Interval plots of soil compaction vs. season

The interval plot indicated in Fig. 4.29 the soil compaction of two experimental seasons. The mean of the two seasons could be significantly different from each other. Also, Fig. 4.29 indicates the maximum soil compaction value was recorded during harvesting season.

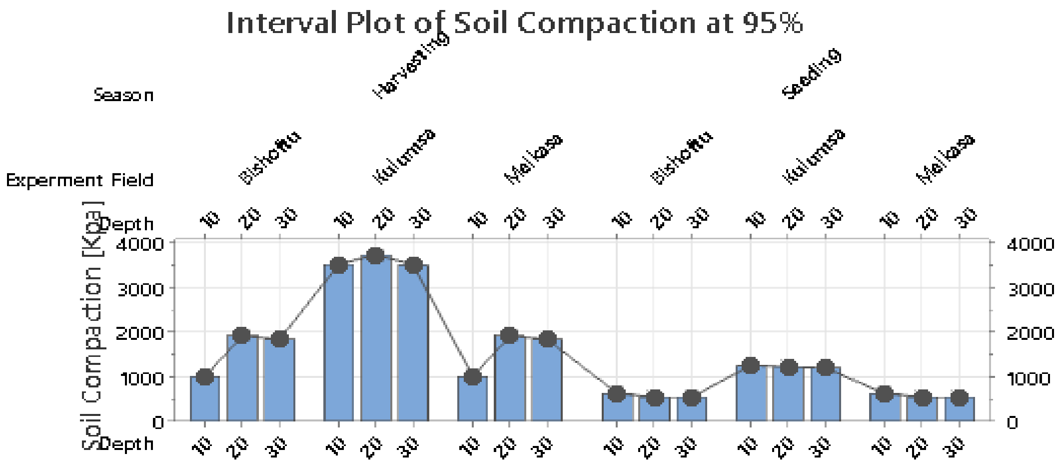

Figure 4.30: Effect of depth, season, and experimental field on compaction

The interval plot in Fig. 4.30 described the effect of depth, season, and experimental field on soil compaction. During harvesting season maximum value of soil compaction was recorded. Kulumsa field experiments have high compaction value in both farm seasons.

4.5.6. Interaction plot analysis

The interaction plots in Fig 4.31 showed interactions between depth, season, and experimental field on soil compaction. On the horizontal axis, one factor's levels are shown, and various colored lines and symbols are used to represent the other factor. If two lines are parallel to one another, there is no interaction between the two factors; if they are not, there is interaction between the two elements.

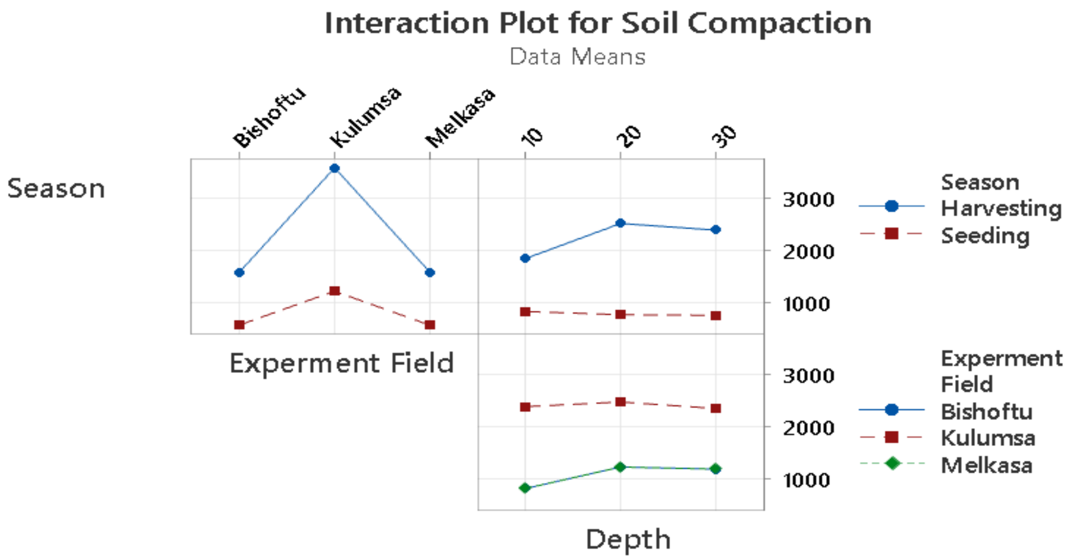

Figure 4.31: Interaction plots for soil compaction

The levels of the factor are depth, season, and experimental field as shown by the horizontal axis, of Fig. 4.32, and their respective impact on soil compaction are shown by other colored lines and symbols.

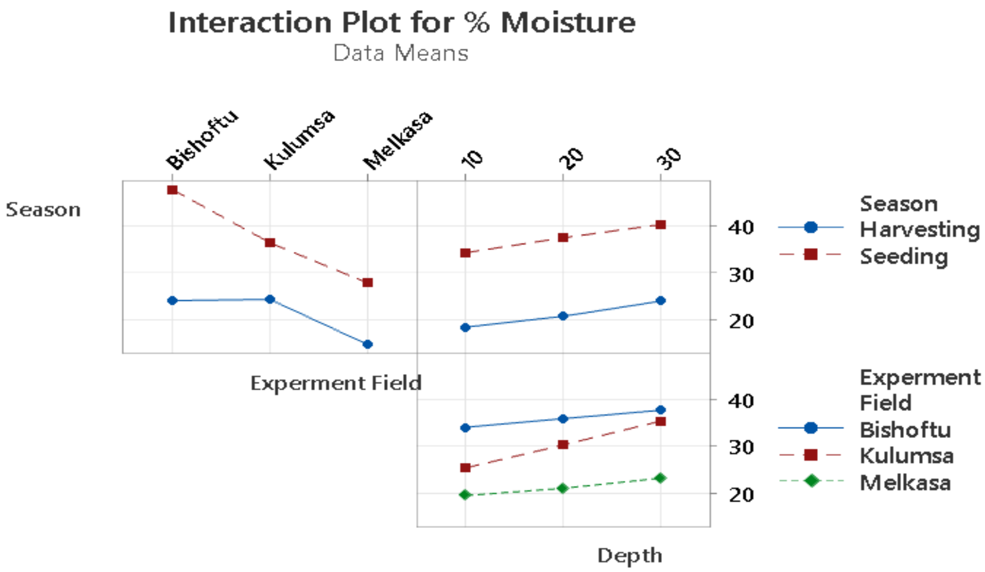

Figure 4.32: Interaction plots for soil moisture content

Based on the plot season to field and depth no interaction with soil moisture content. However, the experimental fields related to depth lines are not parallel so, there is an interaction between the two factors. The interaction plots of soil physiochemical properties to soil compaction are listed under Appendix B.

4.5.7. Main effect plots

The response characteristic's relationship to each component is displayed in the main effects graphs. The extent of the major effect on soil compaction increases with the degree to which the line deviates from the X-axis. The main effects of depth, season, and experimental field on soil compaction are not horizontal when we look at Fig. 4.33. Season and experimental fields have higher differences in the vertical positions of the plotted points. But depth has smaller differences in the vertical positions of the plotted points hence, the size of the major effect on soil compaction is less.

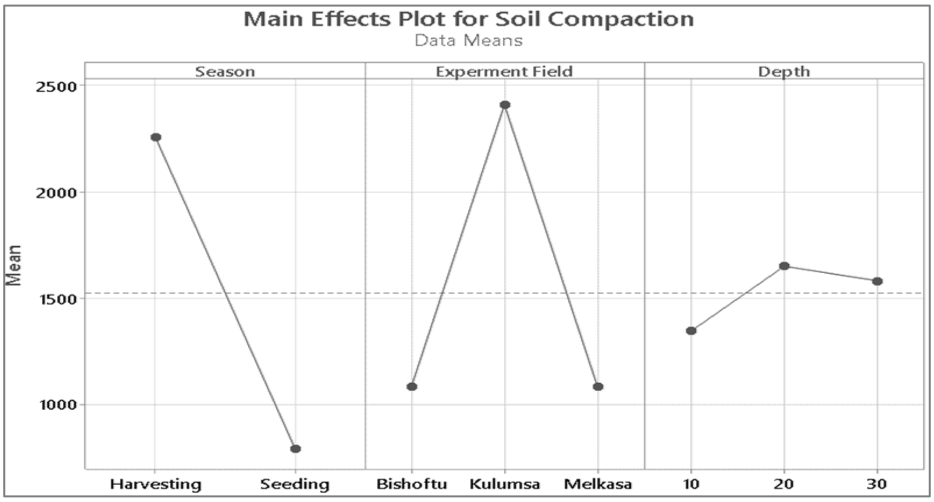

Figure 4.33: The main effect of soil compaction

Fig. 4.34 depicts depth, season, and the experimental field's main effect on soil moisture content. Season and experimental fields have a larger difference in the vertical plot points resulting in, a larger main effect on soil moisture content. But depth has still a smaller main effect on soil moisture content.

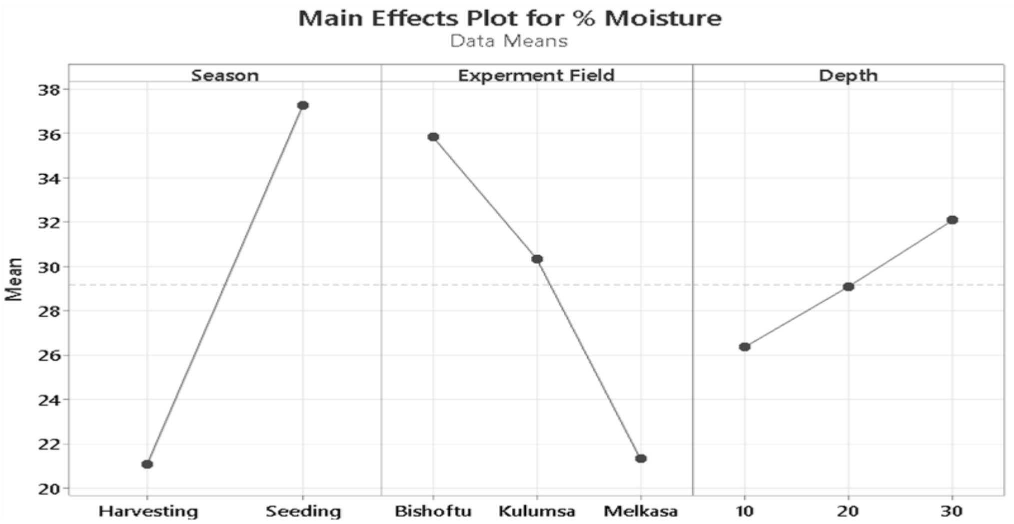

Figure 4.34: The main effect of soil moisture content

4.6. Tractor Field Performance

A traditional tillage system with a mounted mouldboard plough with three bottoms was utilized in this study to collect data from a four-wheel drive Chery tractor (Model RM750). A laboratory was used to determine the soil texture class. The soil CI value was determined using a digital compaction meter built into a tractor. The program was developed in Visual Basics 6.0 to calculate the tractive performance parameters based on the tractor parameters, soil type, depth of operation, implement geometry, and implement the type. The specifications of the tractor are shown in Table 4.16.

Visual Basic is an object-oriented programming language that focuses on the user's interaction with the program. Class modules, modules, and forms are the three main building blocks of visual basics. An object's methods, properties, and other details are described in each class module. The modules include a list of actions that must be taken. The visible portion of visual basics is represented by the forms. The visual basics programming form window used in this simulation consists of an object window and a code window.

Table 4.16: Technical information Chery RM750 tractor

Parameters	Size
Fuel	Diesel
Front tires size	6.5-20 in
Rear tires size	14.9-30 in
Weight	2669 kg
Length	3.98 m
Width	1.65 m
Wheelbase	2.18 m
Ground clearance	0.42 m
Rear tread size	1.5291m
Front tread size	1.3995 m
Engine size	4900 cc
Number of cylinders	4 cylinders
Horsepower	55.9 kW
Power RPM	2200 rpm
Engine torque	320.0 Nm
Engine torque RPM	1600 rpm
Bore stroke	(108 x 135) mm
PTO claimed power	66.4 hp or 49.5 kW
Rear PTO RPM	540 rpm

Source: Tractor specification manual

The object window is the place where the overall input and output parameters are added to the software as indicated in Fig.4.36 and Fig. 4.37. The code widow is the command window where the codes are written shown in Fig.4.38. The object window is the screen consisting of a label to write the name of parameters with their units, a text box to insert the input value for the parameters and to display the result value of the parameters, a combo box to choose the model of tractor, drive type, fuel type, experimental farm location, soil texture class, and tillage implement type, the picture box to insert the picture. The flow chart of the developed software for the prediction of the drawbar performance of the tractor implement is shown in Fig. 4.35.

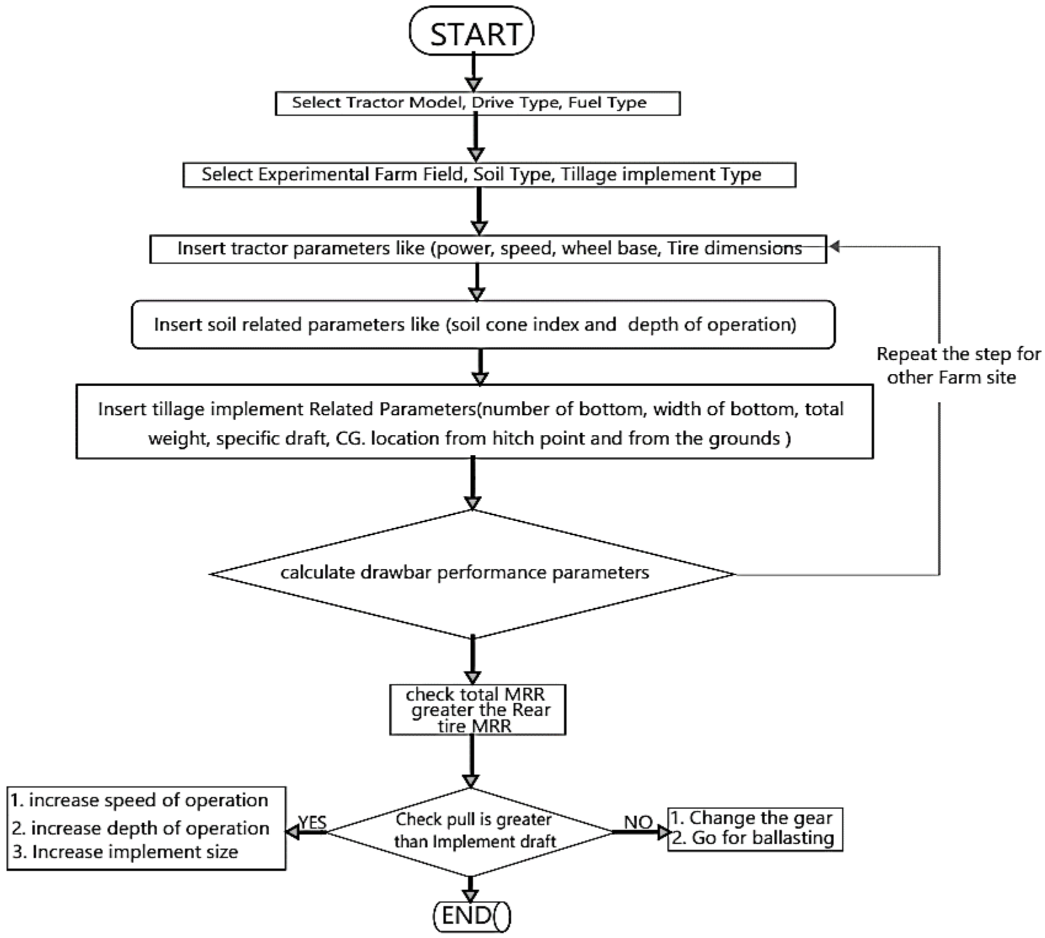

Figure 4.35: Performance flowchart of tractor implement combination

The input parameters for predicting the performance of tractors and implements in the farm field are shown in Fig.4.36. The performance of tractors and implements is shown in Fig. 4.37 of the performance result output display screen. Motion resistance ratio, growth traction ratio, and net traction ratio were calculated in the program based on the (Tiwari, 2006) Equation.

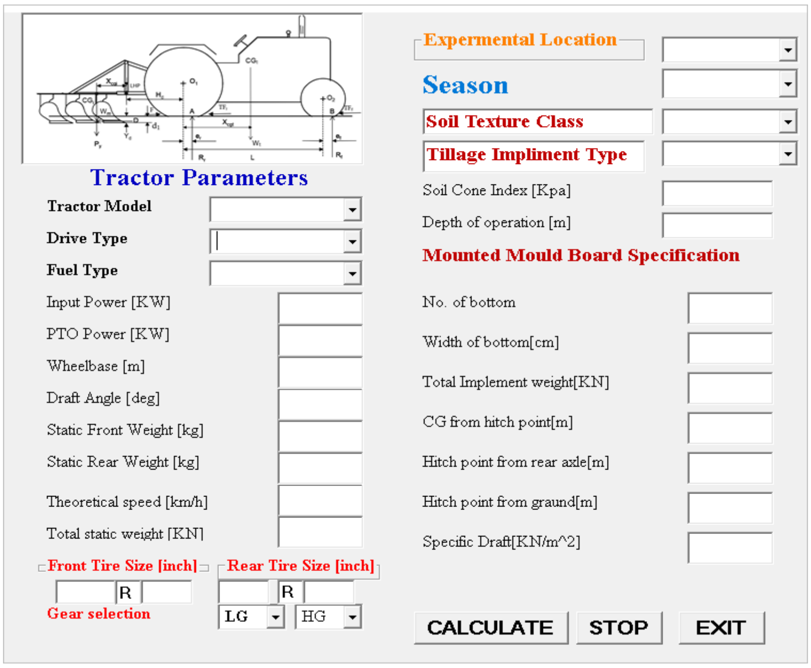

Figure 4.36: Tractors and implements specification input database

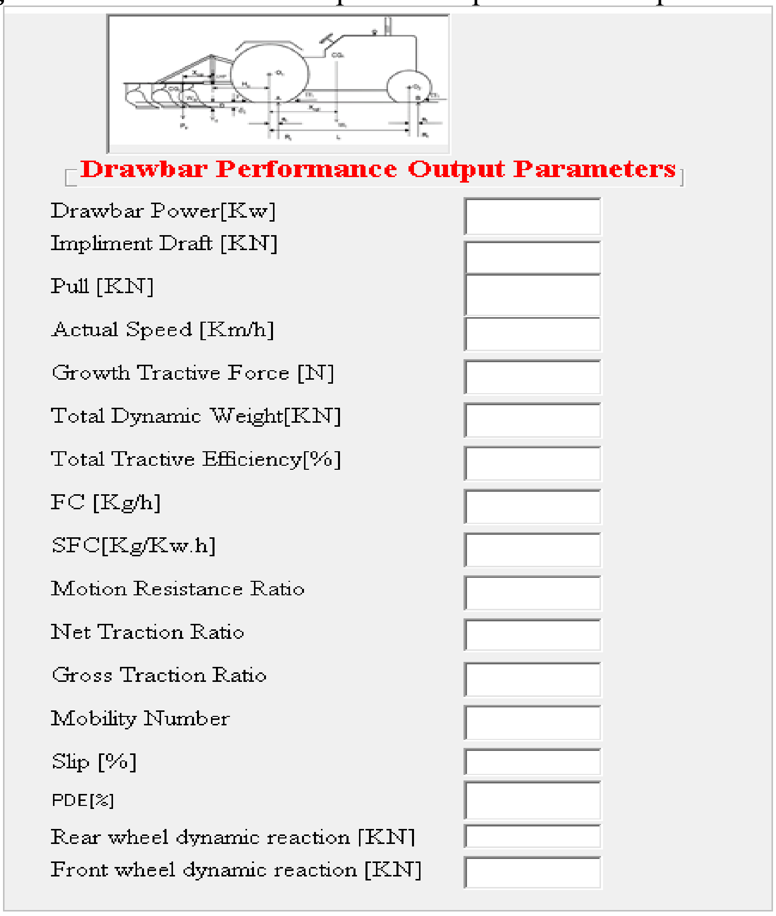

Figure 4.37: Performance results output display screen

```
cmd1                                        Click
Private Sub cmd1_Click()
txtas = Val(4.5)
txtss = Val(0.125)
txtid = Val(txtdoo * txtwob * txtnb * txtsd)
txtdp = Val(txtip * 0.6)
txtpull = Val(txtdp / txtas)
txtmn = Val(txtsci * 0.0110537)
txtfc = Val(0.223 * 49.5 * 0.33)
txtsfc = Val((6.3124 - 5.8995) * 0.91 * 49.5 * 0.033)
txtgtr = Val(0.88 * (1 - (2.718 ^ -(0.1 * txtmn))) * (1 - (2.718 ^ -(9.5 * txtss))) + 0.032)
txtmrr = Val((0.9 / txtmn) + 0.032 + ((0.5 * txtss) / (txtmn ^ 0.5)))
txtntr = (txtgtr - txtmrr)
txttte = Val(((1 - (txtntr / txtgtr)) * (1 - txtss)) * 100)
txtpde = Val((txtdp / txtip) * 100)
txtgtf = Val(txtgtr * txttsw)
txtrwdr = Val(((26.2 * 1.91) + (4.992 * 3.35) - (txtpull * 0.4)) / 2.18)
txtfwdr = Val((26.2 + 2.992 + 2) - txtrwdr)
txttdw = Val(txtrwdr + txtfwdr)
End Sub
```

Figure 4.38: Program code window

The result of this study covers the visual basics simulation output by varying the depth of operation and soil CI as indicated in Table 4.17 for three experimental farm fields (Bishoftu, Kulumsa, and Melkasa). The soil texture class is determined in the soil laboratory and the implement is a mounted mould board plow.

Table 4.17: Changeable input parameters

Depth	Season	Soil CI (kPa)		
		Kulumsa	Melkasa	Bishoftu
10	Harvesting	3522.6	3180.3	1011.2
	Seeding	1255.4	978.3	630.1
20	Harvesting	3730.3	3542.3	1918.1
	Seeding	1227.4	1171.0	549.3
30	Harvesting	3511.8	3947.3	1838.3
	Seeding	1195.5	1383.5	548.2

Drawbar power, implement a draught, pull, tractive force, fuel consumption, slip, power delivery efficiency, dynamic weight, and wheel dynamic reactions were calculated from the simulation output by adjusting depth and soil CI value. For a depth of 30 cm, the visual fundamentals simulation for the Kulumsa field's harvesting and seeding seasons is shown in Fig. 4.39; the findings for further depths and agricultural fields are shown in Appendix F.

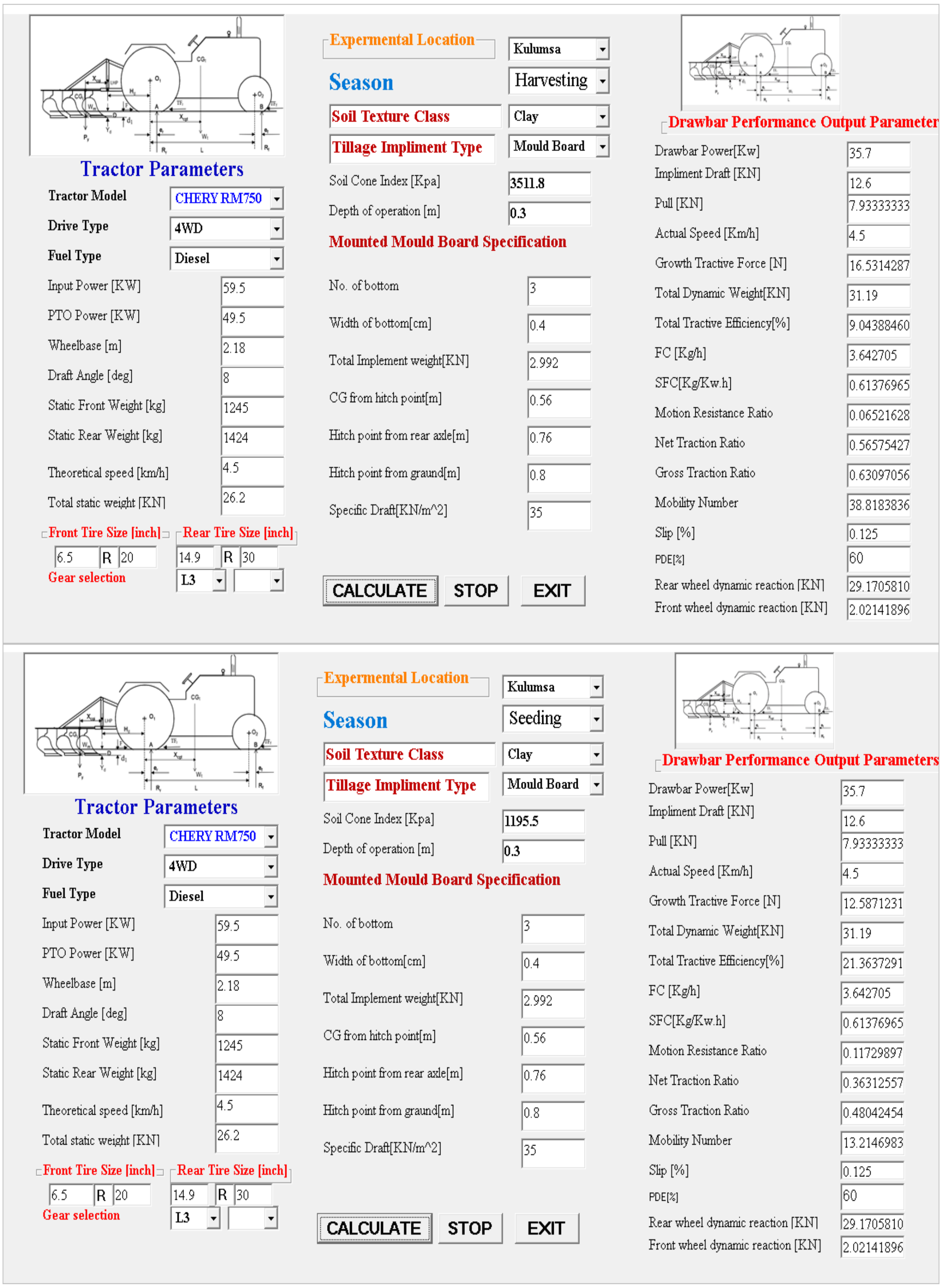

Figure 4.39: Input and output display window

The maximum output performance parameters found at 30cm depth are: - drawbar power of 35.7 kW, pull 7.9 kN, fuel consumption of 3.64 kg/h, slip12.5%, power delivery efficiency of 60%, and dynamic weight of 31.19 kN. From the above parameters, the relation of; soil CI, tractive force, and implement a draft to a depth of operation was plotted in Fig.4.40.

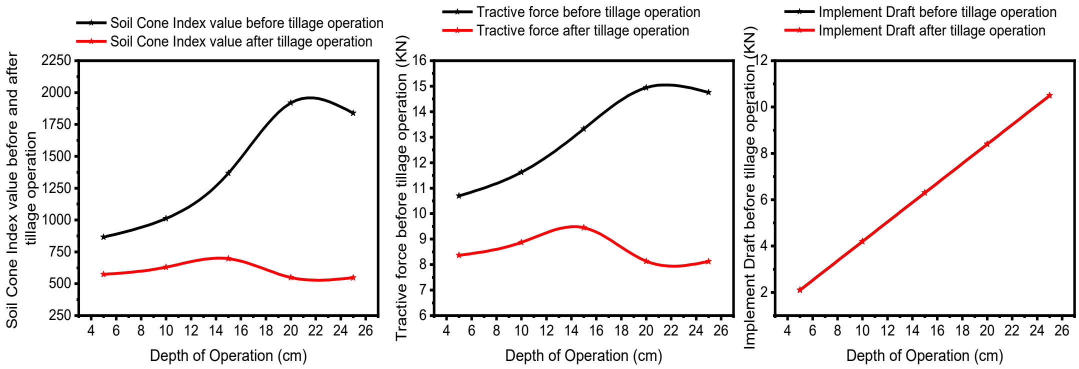

Figure 4.40: Soil CI, implement draft and tractive force vs. depth relation

According to Fig. 4.40, for the experimental field, the soil cone indices generally tended to rise with soil depth up to 200 mm and then start to fall after 200 mm for the harvesting season. For the seeding season, soil cone indices often increased with soil depth up to 15 cm and then began to decline after that depth. The soil compaction value of the two seasons is shown in Fig.4.40 the compaction value harvesting season is higher than the compaction value for the seeding season. The relation between tractive force and depth was the same as the relation between soil CI and depth. The tillage of the implement draft continuously increases as the depth increases. For estimating the field performance of tractor implement combinations, visual basic software has been established.

4.7. Summary

Chapter four discussed the simulation of a hydraulically powered soil compaction measurement system integrated into traction. The hydraulic system like a pump and pressure relief valve, a solenoid operated directional control valve, a double-acting cylinder for creating linear movement, and inserting cone penetrometer into the soil was discussed. The result of the hydraulic cylinder simulation for the cylinder extension and retraction, pressure variation, soil compaction resistance, the flow rate through the pump to the hydraulic cylinder, hydraulic power, and torque was addressed. The theoretical considerations and results of soil compaction in different fields and statistical analysis of the individual fields were discussed. The laboratory procedure and results associated with soil physical and chemical properties in the present study were discussed. Statistical analysis both descriptive and inferential analysis of soil compaction and soil physical and chemical properties was included in the discussion. Tractor and implement mathematical modeling concerning soil tire interaction, tire parameters, tire deformation, and mechanics of pneumatic traction wheel using visual basics computer programming software were covered in the analysis.

CHAPTER 5

5. CONCLUSIONS AND SCOPE FOR FUTURE WORK

5.1. Conclusions

- Soil compaction is one of the negative factors associated with the top layer of the soil by heavy agricultural machinery in the agricultural field that limits plowing tool movement, plant growth, and crop yield. In this research work, an attempt has been made to hydraulically operated soil compaction measurement system modeling and simulation on MATLAB Simulink 2018 to asses parameters like vertical force as variable mass and the soil as stiffness and damping property as preliminary before field experiment.
- Then the field test were conducted to measure soil compaction at three different farm field locations and data were collected.
- At the same farm fields soil samples were taken and physical and chemical property laboratory tests were tested.
- Finally, the soil's physical and chemical properties effect on soil compaction was investigated as well and the impact of soil compaction on tractor drawbar performance was studied using visual basics computer programming.

- The result of the study covers the relationship between soil penetration resistance of three farm fields with different geographical locations and different soil properties with physical properties of soil like; moisture content, soil texture, soil pH, EC, soil organic content, and CEC at different depths.

- The highest soil compaction for Kulumsa experimental field value from the fifteen-sample point during harvesting and the seeding season was 5,900 kPa and 2,076 kPa at 200 mm. Whereas the minimum soil compaction value during harvesting and the seeding season was 1,600 kPa and 612 kPa at 300 mm.

- For Melkasa experimental field the highest and lowest soil compaction values were 6,159 kPa and 327 kPa at a depth of 300 mm r for the harvesting season and the highest and lowest soil compaction values of 3,052 kPa and 563 kPa at a depth of 300 mm and 100 mm respectively for the seeding season.

- For the Bishoftu experimental field from fifteen sample points, the result indicates the highest soil compaction during harvesting and the seeding season was 3,958 kPa and 2,018 kPa at a depth of 300 mm respectively. Whereas the minimum soil compaction values from the fifteen-sample point during harvesting and seeding season were 502 kPa and 279 kPa at depths of 100 mm and 300 mm respectively.

- On average, the highest penetration resistance is recorded at the Kulumsa farm field up to 200 mm depth, and after 200 mm depth, the maximum penetration resistance is recorded at the Melkasa farm field. Bishoftu farm site has the lowest penetration resistance. The result of the study indicates the highest to lowest penetration resistance farm soil respectively are Kulumsa, Melkasa, and Bishoftu.

- Based on the average of all sample points the soil compaction value of the Kulumsa farm field ranges from 3,511.8 kPa to 3,730.3 kPa and 1,195.5 kPa to 1,227.4 kPa for harvesting and seeding season respectively. For the Melkasa farm field, the average soil compaction value ranges from 3,180.3 kPa to 3,947.3 kPa and 978.3 kPa to 1,383.5 kPa for harvesting and seeding season respectively. Bishoftu farm fields have an average soil compaction value ranging from 1,011.2 kPa to 1,838.3 kPa and 548.2 kPa to 630.1 kPa for harvesting and seeding season respectively. From all experimental farm sites, CI value had a general tendency to increase with soil depth except Bishoftu farm field for the seeding season.

- The laboratory result shows that Kulumsa farmland soil is clay. For Melkasa farmland soil CL and Bishoftu farmland soil have a soil texture mixture of loam, CL, and sandy clay loam. The average result of soil texture shows that Bishoftu farm soil has a high percentage of sand 46.2% and Kulumsa farm soil has less amount of sand percentage 24.8%. From this result the higher the soil penetration resistance the lower the sand percentage.

- The cation exchange capacity of laboratory results indicates average, Kulumsa farm soil has the highest value of CEC of 33.8 meq/100 g of soil and 30.38 meq/100 g of soil respectively for seeding and harvesting season. The maximum cation exchange capacity of Melkasa and Bishoftu farm soil is 32.75 and 31.4 meq/100 g of soil respectively taking average values for all depth samples in the seeding season.

- For the three experimental field soils, the percentage of moisture content laboratory results indicate farm fields Kulumsa, Melkasa, and Bishoftu were 24.4%, 14.8%, and 24.1% respectively for harvesting season and for the seeding season were 36.4%, 27.9%, and 47.6% respectively. As depth increases percent of soil moisture content also increases for both experimental seasons.

- Soil pH value increases when depth increases for the first 200 mm depth for both experimental farming seasons. After 200 mm depth, soil pH value starts decreasing in both seasons with depth except Bishoftu experimental farm. On average Melkasa farm fields have a high amount of soil pH value in both seasons which is 7.15 this soil pH value indicates the soil is almost neutral. Bishoftu and Kulumsa farm field soil was acidic in both seasons.

- The maximum and minimum percentage of soil electric conductivity values were 257.9 µS/cm and 109.2 µS/cm for the Bishoftu and Kulumsa farm fields respectively during harvesting season. For seeding season 298.5 µS/cm and 129.9 µS/cm for the Bishoftu and Kulumsa farm fields at 30 cm and 10 cm depth. On average Bishoftu farm fields have a high amount of soil electric conductivity value in both seasons and Kulumsa farm field soil has a low soil electric conductivity value in both seasons.

- Total organic carbon with depth has a positive relationship on the top part of soil up to 200 mm depth for both experimental farming seasons. After 200 mm depth, total organic carbon starts decreasing. On average Kulumsa farm fields have a high amount of soil total organic carbon value in both seasons 2.71% and 3.86% for harvesting and seeding season respectively.

- This study showed that soil organic matter with depth has a positive relationship on the top part of soil up to 200 mm depth for both experimental farming seasons. After 200 mm depth, soil organic matter starts decreasing. On average Kulumsa farm fields have a high amount of soil total nitrogen value in both seasons 2.71% and 5.7% for harvesting and seeding seasons respectively and Bishoftu farm fields have a minimum value of soil organic matter in the seeding season of 2.59% whereas Melkasa has a minimum value of soil organic matter 2.12% for harvesting seasons.

- This study showed that soil total nitrogen with depth has a positive relationship on the top part of soil up to 200 mm depth for both experimental farming seasons. After 200 mm depth soil total nitrogen starts decreasing. On average Kulumsa farm fields have a high amount of soil total nitrogen value in both seasons 0.24% and 0.31% for harvesting and seeding seasons respectively and Bishoftu farm fields have a minimum value of soil total nitrogen in both seasons 0.097% and 0.0137% for harvesting and seeding season respectively.

- Total organic carbon, organic matter, and total nitrogen have a linear increment relationship with depth and soil compaction on top part of soil depth. After 200 mm depth soil penetration resistance continues increasing but the percentage of total organic carbon, organic matter, and total nitrogen starts decreasing.

5.2. Scope for Future Work

This research was limited to testing soil physiochemical properties such as soil texture, moisture content, electrical conductivity, cation exchange capacity, total organic carbon, organic matter, total nitrogen, soil pH, and soil penetration resistance within the study area. Based on this the researcher recommends the following tips for future research.

- During the field experiment the depth taken for soil compaction and soil physiochemical study was limited to 10, 20, and 30 cm. It is better if the ranges are minimized and if it is more than 30 cm in depth.
- The research findings apply only to the clay, clay loam, loam, and sandy clay loam due to limited research areas so, to speak on the impact of soil texture on the soil compaction further research will be required on all types of soil texture class.
- The study considered the effects of depth, season, different farm locations, and some soil physical and chemical properties as the main factors affecting soil compaction as a result of using heavy farm machinery and equipment. It is necessary to address other factors like the number of passes, rain, irrigation nature, etc.
- The tractor instrumental integration system where not measure soil compaction at stony farmland to save the cone penetrometer from breakage. We recommend the researchers add further modifications to the control system to measure soil compaction at all farm field nature.
- We recommend that future researchers address tractor implement combination field performance since, this research work does not perform field tests only, computer modeling and simulations for predicting tractor performance were performed.

REFERENCES

Aase J, Bjorneberg D, & Sojka RJTotA. (2001). Zone–subsoiling relationships to bulk density and cone index on a furrow–irrigated soil. *44*(3), 577.

Agricultural ASo, & Engineers B. (2006). Soil cone penetrometer: ASAE standard S313. 3. In: ASABE St. Joseph.

Al-Hamed S, Grisso R, Zoz F, Von Bargen KJC, & Agriculture Ei. (1994). Tractor performance spreadsheet for radial tires. *10*(1), 45-62.

Alexander MJSS. (1978). Introduction to soil microbiology. *125*(5), 331.

Ambruster K, & Kutzbach H. (1989). Development of a single wheel tester for measurement on driven angled wheel. Proceedings of 5th European conference of the ISTVS, Wageningen, The Netherlands,

Andrews SS, Karlen DL, & Cambardella CAJSSSoAJ. (2004). The soil management assessment framework: A quantitative soil quality evaluation method. *68*(6), 1945-1962.

Arvidsson J, & Ristic SJJoT. (1996). Soil stress and compaction effects for four tractor tyres. *33*(5), 223-232.

ASABE SJSJ, MI, USA: American Society of Agricultural, & Engineers B. (2011). ASAE S313. 3: Soil Cone Penetrometer.

ASAE. (2013). ASAE_EP542 Procedures for Using and Reporting Data Obtained with the Soil Cone Penetrometer. *American Society of Agricultural and Biological Engineers*. https://doi.org/https://doi.org/10.13031/2013.35790

Ashmore C, Burt EC, & Turner JLJTotA. (1987). An empirical equation for predicting tractive performance of log-skidder tires. *30*(5), 1231-1236.

Bekker, M. G. (1956). *Theory of land locomotion: the mechanics of vehicle mobility*. Ann Arbor, MI: University of Michigan press.

Bekker MG. (1966). Off - Road Locomotion on the moon and earth. *Journal of Terramechanics*, *3*(3), 83 to 91.

Bekker MG. (1967). Evolution of approach to off-road locomotion. *Journal of Terramechanics*, *4*(1), 49 to 58.

Bekker, M. (1969). G., 1960: Off-the-road locomotion. *Ann Arbor, MI: University of Michigan Press*.

Bekker MJST. (1985). Parametric Analyses of Pneumatic Tires Update—Samples of Engineering Problems and Solutions in Off-Road Locomotion. 970-983.

Benevenute PAN, Morais EGd, Souza AA, Vasques ICF, Cardoso DP, Sales FR, Severiano EC, Homem BGC, Casagrande DR, & Silva BM. (2020). Penetration resistance: An effective indicator for monitoring soil compaction in pastures. *Ecological Indicators*, *117*. https://doi.org/10.1016/j.ecolind.2020.106647

Bertonha RS, Furlani CEA, Silva VFA, & Wright DL. (2015). Tractor performance and corn crop development as a function of furrow opener and working depth. *AJCS*, *9*(9), 812-818. https://doi.org/https://search.informit.org/doi/10.3316/informit.528435195298283

Bhattacherjee A. (2012). Social science research: Principles, methods, and practices.

Bi X, Li B, Nan B, Fan Y, Fu Q, & Zhang XJJoAL. (2018). Characteristics of soil organic carbon and total nitrogen under various grassland types along a transect in a mountain-basin system in Xinjiang, China. *10*, 612-627.

Boon NE, Yahya A, Kheiralla AF, Wee BS, & Gew SK. (2005). A Tractor-mounted, Automated Soil Penetrometer–shearometer Unit for Mapping Soil Mechanical Properties. *Biosystems Engineering*, *90*(4), 381-396.

Bottinelli N, Jouquet P, Capowiez Y, Podwojewski P, Grimaldi M, Peng XJS, & Research T. (2015). Why is the influence of soil macrofauna on soil structure only considered by soil ecologists? , *146*, 118-124.

Brixius WJASoAE. (1987). Traction prediction equations for bias ply tires.

Bronick CJ, & Lal R. (2005). Soil structure and management: a review. *Geoderma*, *124*(1), 3-22. https://doi.org/https://doi.org/10.1016/j.geoderma.2004.03.005

Burce ME, Kataoka T, & Okamoto H. (2013). Seeding Depth Regulation Controlled by Independent Furrow Openers for Zero Tillage Systems *EAEF*, *6*(1), 1-6.

Burt A, & Goudie RBJH. (1979). Diagnosis of primary thyroid carcinoma by immunohistological demonstration of thyroglobulin. *3*(4), 279-286.

Burt EC, Bailey AC, & Taylor JHJTotA. (1980). Effect of dynamic load distribution on the tractive performance of tires operated in tandem. *23*(6), 1395-1400.

Busscher WJ. (1990). Adjustment of flat-tipped penetrometer resistance data to a Common water content. *Transactions of the ASAE*, *33*(2).

Carter. LM. (1968). portable-recording-penetrometer-measures-soil-strength-profiles. *Journal of Terramechanics*, *5*(4), 65-70.

Chapman HJMosaPC, & properties m. (1965). Cation-exchange capacity. *9*, 891-901.

Cho Y, HoonLee D, Park W, & Lee KS. (2015). Development of a Real-Time Measurement System for Horizontal Soil Strength. *Journal of Biosystems Engineering*, *40*(3), 165-177.

Chyba J, Kroulík M, Krištof K, Misiewicz P, & Chaney KJAR. (2014). Influence of soil compaction by farm machinery and livestock on water infiltration rate on grassland. *12*(1), 59-64.

Chyba J, Kroulík M, Krištof K, Misiewicz PA, & Chaney K. (2014). Influence of soil compaction by farm machinery and livestock on water infiltration rate on grassland. *Agronomy Research*, *12*(1), 59–64.

Clark RL, & Dahua ZJTotA. (1995). A theoretical ballast and traction model for a wide span tractor. *38*(6), 1613-1620.

Corwin DL, Lesch SMJC, & agriculture ei. (2005). Apparent soil electrical conductivity measurements in agriculture. *46*(1-3), 11-43.

De Neve S, & Hofman G. (2000). Influence of soil compaction on carbon and nitrogen mineralization of soil organic matter and crop residues. *Biology and Fertility of Soils*, *30*(5), 544-549. https://doi.org/10.1007/s003740050034

Défossez P, Richard G, Boizard H, & O'Sullivan MF. (2003). Modeling change in soil compaction due to agricultural traffic as function of soil water content. *Geoderma*, *116*(1-2), 89-105.

Delgado A, & Gómez JA. (2016). The soil. Physical, chemical and biological properties. In *Principles of agronomy for sustainable agriculture* (pp. 15-26). Springer.

Dembner S. (1988). *Agricultural engineering in development : guidelines for establishment of village workshops*. : Food and Agriculture Organization of the United Nations.

Dinkins C, & Jones CJMSUEMPnMA. (2013). Interpretation of soil test results for agriculture.

Duiker SWJAf. (2002). Diagnosing soil compaction using a penetrometer (soil compaction tester). *63*(4).

Dwyer L, Hayhoe H, & Culley JJCjops. (1990). Prediction of soil temperature from air temperature for estimating corn emergence. *70*(3), 619-628.

Dwyer M, & Heigho DJJoAER. (1984). The tractive performance of some large tractor drive wheel tyres compared with dual wheels. *29*(1), 43-50.

Elfeel, Warrag, & Musnad. (2009). Effect of seed origin and soil type on germination and growth of heglig tree (balanites aegyptiaca (del.) L.var. Aegyptiaca). *Journal of Science and Technology 10*(3).

ENAMS. (2010). development of agricultural_mechanization in ethiopia and the role of national policies. *FACASI Project, Activity*.

Estefan G. (2013). Methods of soil, plant, and water analysis: a manual for the West Asia and North Africa region. In: International Center for Agricultural Research in the Dry Areas (ICARDA).

Evans L. (1991). *Traffic safety and the driver*. Science Serving Society.

FAO. (1990). *Agricultural engineering in development : guidelines for mechanization systems and machinery rehabilitation programmes*. : Food and Agriculture Organization of the United Nations.

Fernández FG, & Hoeft RGJIah. (2009). Managing soil pH and crop nutrients. *24*, 91-112.

Field APJPm. (2005). Is the meta-analysis of correlation coefficients accurate when population correlations vary? , *10*(4), 444.

Frantisek Varga, Mojzis M, & Abraham R. (2013). Soil resistance and its Impact on Tillage Depth. *Acta Technologica Agriculturae*, *1*(1), p. 26–30.

Freitag DR. (1966). *A Dimensional Analysis of the Performance of Pneumatic Tires on Clay*.

Freitag RD. (1996). *The scope of conflict, political culture, and public welfare policy in the states*. The University of Texas at Austin.

Ganiyu SA, Olurin OT, Oladunjoye MA, & Badmus BS. (2020). Investigation of soil moisture content over a cultivated farmland in Abeokuta Nigeria using electrical resistivity methods and soil analysis. *Journal of King Saud University - Science*, *32*(1), 811-821. https://doi.org/10.1016/j.jksus.2019.02.016

Gee-Clough DJJoaer. (1980). Selection of tyre sizes for agricultural vehicles. *25*(3), 261-278.

George D, & Mallery PJG, Boston, MA: Pearson Education, Inc. (2010). SPSS for Windows step by step. A simple study guide and reference (10. Baskı). *10*.

GILL WR. (1968). Soil Dynamics In Tillage and Traction. *Agricultural Research Service United States Department of Agriculture*.

Gizachew L, & Smit GN. (2008). Relationships between plant and soil nutrient status and position in the landscape on Pellic Vertisols of Ethiopia. *South African Journal of Plant and Soil*, *22*(2). https://doi.org/10.1080/02571862.2008.10639905

Grisso RD, Alley MM, Holshouser DL, & Thomason WE. (2005). Precision farming tools. soil electrical conductivity.

Grisso RD, Kocher MF, & Vaughan DHJAEiA. (2004). Predicting tractor fuel consumption. *20*(5), 553.

Gu Y, & Kushwaha RJJot. (1994). Dynamic load distribution and tractive performance of a model tractor. *31*(1), 21-39.

Guimaraes Junnyor WDS, Diserens E, De Maria IC, Araujo-Junior CF, Farhate CVV, & de Souza ZM. (2019). Prediction of soil stresses and compaction due to agricultural machines in sugarcane cultivation systems with and without crop rotation. *Sci Total Environ*, *681*, 424-434. https://doi.org/10.1016/j.scitotenv.2019.05.009

Haile FvSAM, Alemehayu T, Almirew T, & Geleta Y. (2011). Status and Potential of Spate Irrigation in Ethiopia. *JrnlID*. https://doi.org/10.1007/s11269-011-9780-7

Hakansson I. (2005). *Machinery-induced compaction of arable soils: incidence, consequences, counter-measures*. SLU, Department of Soil Sciences, Division of Soil Management.

Håkansson I, Lipiec JJS, & Research T. (2000). A review of the usefulness of relative bulk density values in studies of soil structure and compaction. *53*(2), 71-85.

Ham J-Pvd. (2008). Dodota Spate Irrigation System Ethiopia A case study of Spate Irrigation Management and Livelihood options.

Hamza M, Anderson WKJS, & research t. (2005). Soil compaction in cropping systems: A review of the nature, causes and possible solutions. *82*(2), 121-145.

Hatley D, Wiltshire J, Basford B, Royale S, Buckley D, & Johnson PJRr. (2005). Soil compaction and potato crops. *260*.

Hayes JC, & Ligon JT. Traction Prediction Using Soil Physical Properties. *ASAE*, *No. 77-1054*(St. Joseph, MI.).

Hendrick JG. (1969). Recording Soil Penetrometer. *J. agric. Engng Res.(1969) 14 (2) 183-186*.

Herrick JE, & Jones TL. (2002). A dynamic cone penetrometer for measuring soil penetration resistance. *Soil Science Society of America Journal*, *66*(4), 1320-1324. https://doi.org/ https://doi.org/10.2136/sssaj2002.1320

Hu W, Jia X, Zhu X, Su A, Du Y, & Huang B. (2020). Influence of moisture content on intelligent soil compaction. *Automation in Construction*, *113*. https://doi.org/10.1016/j.autcon.2020.103141

IBC IoBC. (2012). Ethiopia third country report on the state of plant genetic resources for food and agriculture. *Report*.

IMWIC. (2014). Farm mechanization and conservation Agriculture for sustainable intensification (FACASI) project *FACASI*.

Ishaq M, Hassan A, Saeed M, Ibrahim M, Lal RJS, & Research T. (2001). Subsoil compaction effects on crops in Punjab, Pakistan: I. Soil physical properties and crop yield. *59*(1-2), 57-65.

Janosi Z, & Hanamoto B. (1961). *An analysis of the drawbar pull vs slip relationship for track laying vehicles*.

Jat ML, Bijay S, Stirling CM, Jat HS, Tetarwal JP, Jat RK, Singh R, Lopez-Ridaura S, & Shirsath PB. (2018). Chapter Four - Soil Processes and Wheat Cropping Under Emerging Climate Change Scenarios in South Asia. In DL Sparks (Ed.), *Advances in Agronomy* (Vol. 148, pp. 111-171). Academic Press. https://doi.org/https://doi.org/10.1016/bs.agron.2017.11.006

Kannan P, Saravanan A, Krishnakumar S, Natarajan SJRJoA, & Sciences B. (2005). Biological properties of soil as influenced by different organic manures. *1*(2), 181-183.

Kebede AA, Olani DD, Edesa TG, & Damtew YT. (2016). Heavy Metal Content and Physico Chemical Properties of Soil around Solid Waste Disposal Sites. *Am. J. Sci. Ind. Res.*, *7*(5), 129-136. https://doi.org/10.5251/ajsir.2016.7.5.129.136

Kees G. (2005). Hand-Held Electronic Cone Penetrometers. *USDA, MT*.

Keller T, Arvidsson J, Schjønning P, Lamandé M, Stettler M, & Weisskopf PJSS. (2012). In situ subsoil stress-strain behavior in relation to soil precompression stress. *177*(8), 490-497.

Khaledian Y, Brevik EC, Pereira P, Cerdà A, Fattah MA, & Tazikeh HJC. (2017). Modeling soil cation exchange capacity in multiple countries. *158*, 194-200.

Kifle M, Dimtsu G, & Gebretsadikan T. (2018). Evaluation of the effect of mouldboard plow and tied-ridger on wheat productivity in Atsibi and Ganta Afeshum districts, Ethiopia. *Advances in Agricultural Science*, *6*(3), 17-24.

Kim H, Anderson S, Motavalli P, & Gantzer CJG. (2010). Compaction effects on soil macropore geometry and related parameters for an arable field. *160*(2), 244-251.

Kim W-S, Kim Y-J, Baek S-Y, Baek S-M, Kim Y-S, Choi Y, Kim Y-K, & Choi I-SJJoT. (2020). Traction performance evaluation of a 78-kW-class agricultural tractor using cone index map in a Korean paddy field. *91*, 285-296.

Koolen AJ, & Kuipers H. (2012). *Agricultural soil mechanics* (Vol. 13). Springer Science & Business Media.

Kucharik CJ, Brye KR, Norman JM, Foley JA, Gower ST, & Bundy LGJE. (2001). Measurements and modeling of carbon and nitrogen cycling in agroecosystems of southern Wisconsin: potential for SOC sequestration during the next 50 years. *4*, 237-258.

Kulkarni S, Bajwa S, & Huitink GJTotA. (2010). Investigation of the effects of soil compaction in cotton. *53*(3), 667-674.

Kumar R. (2015). *Traction Potential of Radial-Ply Tyres Used in Agricultural Tractors* IIT Kharagpur].

Kumar V, Kumar P, Sahni RK, & Thomas E. (2019). Design of tractor mounted hydraulically operated soil compaction measurement system. *Central Institute of Agricultural Engineering, Bhopal*, *VIII*(XXVIII).

Lee R, Kim H, Fischer J, Thess A, & Smalley RJN. (1997). Conductivity enhancement in single-walled carbon nanotube bundles doped with K and Br. *388*(6639), 255-257.

Leviticus L, & Reyes JJMc. (1983). Traction on concrete. II. Tractive efficiency [Farm machinery].

Lewis-Beck MS, & Mitchell II GEJES. (1993). French electoral theory: the National Front test. *12*(2), 112-127.

Li H, Van den Bulcke J, Wang X, Gebremikael MT, Hagan J, De Neve S, & Sleutel S. (2020). Soil texture strongly controls exogenous organic matter mineralization indirectly via moisture upon progressive drying — Evidence from incubation experiments. *Soil Biology and Biochemistry*, *151*. https://doi.org/10.1016/j.soilbio.2020.108051

Lindenmuth BJTpt. (2006). An overview of tire technology. *1*, 13136.

Lipiec J, Hajnos M, & Świeboda RJG. (2012). Estimating effects of compaction on pore size distribution of soil aggregates by mercury porosimeter. *179*, 20-27.

Lipiec J, & Hatano RJG. (2003). Quantification of compaction effects on soil physical properties and crop growth. *116*(1-2), 107-136.

Liu H, Colombi T, Jack O, Keller T, & Weih M. (2021). Effects of soil compaction on grain yield of wheat depend on weather conditions. *Science of the Total Environment*, *807*(Pt 1), 150763. https://doi.org/10.1016/j.scitotenv.2021.150763

Maclaurin BJJot. (2007). Comparing the NRMM (VCI), MMP and VLCI traction models. *44*(1), 43-51.

Macmillan RHJAEICJ. (2003). The mechanics of tractor-implement performance.

Maikhuri RK, Rao KSJIJoE, & Sciences E. (2012). Soil quality and soil health: A review. *38*(1), 19-37.

Mallarino A, Sawyer J, & Barnhart S. (2013). A general guide for crop nutrient and limestone recommendations in Iowa.

Manson AJR, & Bulletin T. (2018). Soil organic matter. 20017-20018.

Marczyk GR, DeMatteo D, & Festinger D. (2010). *Essentials of research design and methodology* (Vol. 2). John Wiley & Sons.

Margolin ERaM. (1991). An economical hand-held recording penetrometer. *oil & Tillage Research, I9 (1991) 67-75*(Elsevier Science Publishers B.V., Amsterdam).

Marshall TJ, Holmes JW, & Rose CW. (1996). *Soil physics*. Cambridge university press.

Mazzoncini M, Sapkota TB, Barberi P, Antichi D, Risaliti RJS, & research t. (2011). Long-term effect of tillage, nitrogen fertilization and cover crops on soil organic carbon and total nitrogen content. *114*(2), 165-174.

McLaughlin NB, Campbell AJ, & Owen GT. (2019). Performance of hoe and triple disc furrow openers on no-till grain drills in a fine sandy loam soil. *Soil and Tillage Research*, *195*.

McLean E, Hartwig R, Eckert D, & Triplett GJAJ. (1983). Basic Cation Saturation Ratios as a Basis for Fertilizing and Liming Agronomic Crops. II. Field Studies 1. *75*(4), 635-639.

Michopoulos P, Baloutsos G, & Economou AJSF. (2008). Nitrogen cycling in a mature mountainous beech forest. *42*(1), 5.

Mihretie FA, Tsunekawa A, Haregeweyn N, Adgo E, Tsubo M, Ebabu K, Masunaga T, Kebede B, Meshesha DT, Tsuji W, Bayable M, & Berihun ML. (2021). Tillage and crop management impacts on soil loss and crop yields in northwestern Ethiopia. *International Soil and Water Conservation Research*. https://doi.org/10.1016/j.iswcr.2021.04.006

Miles C, DeVetter L, Ghimire S, & Hayes DGJH. (2017). Suitability of biodegradable plastic mulches for organic and sustainable agricultural production systems. *52*(1), 10-15.

Mudarisov S, Gainullin I, Gabitov I, Hasanov E, & Farhutdinov I. (2020). Soil compaction management Reduce soil compactionusing a chain-track tractor. *Journal of Terramechanics*, *89*, 1-12. https://doi.org/10.1016/j.jterra.2020.02.002

Nackley LL, & Kim SHJGB. (2015). A salt on the bioenergy and biological invasions debate: salinity tolerance of the invasive biomass feedstock a rundo donax. *7*(4), 752-762.

Nelson D, & Sommers LJAj. (1973). Determination of total nitrogen in plant material 1. *65*(1), 109-112.

Othaman NC, Isa MM, Ismail R, Ahmad M, & Hui C. (2020). Factors that affect soil electrical conductivity (EC) based system for smart farming application. AIP Conference Proceedings,

Pagani A. (2011). *Soil pH and lime management for corn and soybean*. Iowa State University.

Pandey I, Sharma S, Tiwari S, & Bharati VJIJoWS. (2001). Effect of tillage and weed management on grain yield and nutrients removal by wheat (Triticum aestivum) and weeds. *33*(3and4), 107-111.

Patil PB, Prof.V.A.Kamble, & S.V.Chavan P. (2018). Effect of Soil Forces On Ridger Plough under Different Working Conditions During Earthing up Operation of Sugar Cane. *IRJET*, *5*(5), 4081-4084.

Phogat VK, Tomar VS, & Dahiya R. (2015). Soil Physical Properties.

Plackett CJJoAER. (1984). The ground pressure of some agricultural tyres at low load and with zero sinkage. *29*(2), 159-166.

Raper RJJoT. (2005). Agricultural traffic impacts on soil. *42*(3-4), 259-280.

Reichert JM, Suzuki LEAS, Reinert DJ, Horn R, Håkansson IJS, & Research T. (2009). Reference bulk density and critical degree-of-compactness for no-till crop production in subtropical highly weathered soils. *102*(2), 242-254.

Rhoades J, Manteghi N, Shouse P, & Alves WJSSSoAJ. (1989). Soil electrical conductivity and soil salinity: New formulations and calibrations. *53*(2), 433-439.

Rhoades JJMosaPc, & properties m. (1983). Cation exchange capacity. *9*, 149-157.

Roeber JB, Pitla SK, Kocher MF, Luck JD, Hoy RMJC, & Agriculture Ei. (2016). Tractor hydraulic power data acquisition system. *127*, 1-14.

Roşca R, Cârlescu P, Ţenu IJS, & Research T. (2014). A semi-empirical traction prediction model for an agricultural tyre, based on the super ellipse shape of the contact surface. *141*, 10-18.

Rowland D, & Peel JJIome. (1975). Soft ground performance prediction and assessment for wheeled and tracked vehicles. *205*, 81.

Rummer R, & Ashmore CJASoAEnfn-. (1985). Factors affecting the rolling resistance of rubber-tired skidders.

Schoenholtz SH, Van Miegroet H, Burger JJFe, & management. (2000). A review of chemical and physical properties as indicators of forest soil quality: challenges and opportunities. *138*(1-3), 335-356.

Seifu Y, Hiremath SS, Tola S, & Wako AJAJoAR. (2023). Depth and soil physiochemical properties effects on soil compaction in agricultural field. *19*(2), 170-177.

Serem P, Kipkorir E, Ng'etich WJJoA, & Research C. (2016). Effects of sprinkler irrigation on physical properties of soil and on the yields of green gram. *4*(3), 35-42.

Shah AN, Tanveer M, Shahzad B, Yang G, Fahad S, Ali S, Bukhari MA, Tung SA, Hafeez A, Souliyanonh BJES, & Research P. (2017). Soil compaction effects on soil health and cropproductivity: an overview. *24*, 10056-10067.

Sharma A, Weindorf DC, Man T, Aldabaa AAA, & Chakraborty SJG. (2014). Characterizing soils via portable X-ray fluorescence spectrometer: 3. Soil reaction (pH). *232*, 141-147.

Sharma D, & Mukesh S. (2019). *Farm machinery design: Principles and problems*. Jain brothers.

Shmulevich I, Ronai D, & Wolf DJJoT. (1996). A new field single wheel tester. *33*(3), 133-141.

Singh VK, Kumar D, Kashyap P, Singh PK, Kumar A, & Singh SKJJoH. (2020). Modelling of soil permeability using different data driven algorithms based on physical properties of soil. *580*, 124223.

Sivarajan S, Maharlooei M, Bajwa S, Nowatzki JJS, & Research T. (2018). Impact of soil compaction due to wheel traffic on corn and soybean growth, development and yield. *175*, 234-243.

Soane G, Godwin R, Marks M, Spoor GJSU, & Management. (1987). Crop and soil response to subsoil loosening, deep incorporation of phosphorus and potassium fertilizer and subsequent soil management on a range of soil types.: Part 2: Soil structural conditions. *3*(3), 123-130.

Spurway CHJSBMAES. (1941). Soil reaction (pH) preferences of plants. *306*.

Standard AJSCPA, St. Joseph, MI, USA. (2000). ASAE S313. 3.

Standards A. (2004). S313. 3: Soil cone penetrometer. In: ASAE St. Joseph, MI.

Sumner ME, & Miller WP. (1996). Cation exchange capacity and exchange coefficients. *5*, 1201-1229.

Swanson GD, & Patin TR. (1973). Penetration resistance maesurements in thin layer of fine grained soil.

Tekin Y, & Okursoy R. (2007). Development of a Hydraulic-driven Soil Penetrometer for Measuring Soil Compaction in Field Conditions. *Journal of Applied Sciences 7 (6): 918-921, 2007*.

Templeton GFJCotafis. (2011). A two-step approach for transforming continuous variables to normal: implications and recommendations for IS research. *28*(1), 4.

Tiessen H, Cuevas E, & Chacon PJN. (1994). The role of soil organic matter in sustaining soil fertility. *371*(6500), 783-785.

Tiwari V, Pandey K, & Pranav PJJoT. (2010). A review on traction prediction equations. *47*(3), 191-199.

Tiwari VK. (2006). *Traction potential of bias-ply tyres used in agricultural tractors* IIT, Kharagpur].

Tonui WK. (2015). *Assessment of soil compaction levels by farm machinery in cultivated sandy loam soils* University of Eldoret].

Topakci M, Ilker U, Murad C, Kursat CH, & Davut K. (2010). Design of a Horizontal Penetrometer for Measuring On-the-Go Soil Resistance. *Sensors*, *10*(10), 9337-9348.

Turnage G. (1972). *Performance of soils under tire loads-application of test results to tire selection for off-road vehicles*.

Turnage GW. (1972). *Performance of soils under tire loads. Report 8. Application of test results to tire selection for off-road vehicles*.

Unger PW, & Kaspar TCJAj. (1994). Soil compaction and root growth: a review. *86*(5), 759-766.

Ungureanu N, Croitoru Ş, Biriş S, Voicu G, Vlăduţ V, Selvi KÇ, Boruz S, Marin E, & Matache M. (2015). agricultural soil compaction under the action of agricultural machinery. *Conference Paper Simpozij Aktualni Zadaci Mehanizacije Poljoprivrede*

Upadhyaya S, Mehlschau J, Wulfsohn D, & Glancey JJTotA. (1986). Development of a unique, mobile, single wheel traction testing machine. *29*(5), 1243-1246.

Upadhyaya S, Sime M, Raghuwanshi N, & Adler BJJot. (1997). Semi-empirical traction prediction equations based on relevant soil parameters. *34*(3), 141-154.

Upadhyaya SJTotA. (1988). Effect of tread design on bias ply tire tractive characteristics. *31*(5), 1338-1344.

van Verseveld CJW, & Gebert J. (2020). Effect of compaction and soil moisture on the effective permeability of sands for use in methane oxidation systems. *Waste Manag*, *107*, 44-53. https://doi.org/10.1016/j.wasman.2020.03.038

Vaz CMP, Manieri JM, de Maria IC, & Tuller M. (2011). Modeling and correction of soil penetration resistance for varying soil water content. *Geoderma*, *166*(1), 92-101.

Vitousek PM, & Farrington HJB. (1997). Nutrient limitation and soil development: experimental test of a biogeochemical theory. *37*, 63-75.

Voorhees ML, & Walker PN. (1977). Tractionability As a Function of Soil Moisture. *Transactions of the ASAE*(5), 806-809.

Wells LG, & Treesuwan O. (1978). The Response of Various Soil Strength Indices to Changing Water Content and Bulk Density. *ASAE paper*, *No. 77-1055*(St. Joseph, M).

Wismer R, & Luth HJJoT. (1973). Off-road traction prediction for wheeled vehicles. *10*(2), 49-61.

Woldeyohannis YS, Hiremath SS, Tola S, Wako AJA, & Science ES. (2022). Investigation of Soil Physiochemical Properties Effects on Soil Compaction for a Long Year Tilled Farmland. *2022*.

Woldeyohannis YS, Hiremath SS, Tola S, Wako AJEJoS, & Development S. (2022). Modelling and Simulation of Hydraulic System to Measure Soil Compaction for Agricultural Field. *9*(1), 19-28.

Woldeyohannis YS, S SH, Tola S, & Wako A. (2024). Influence of soil physical and chemical characteristics on soil compaction in farm field. *Heliyon*, *10*(3), e25140. https://doi.org/10.1016/j.heliyon.2024.e25140

Wong JY. (2001). Theory of Ground Vehicles *book*, *3rd edition*.

Zombori JJJoT. (1967). Drawbar pull tests of various traction devices on sandy soils. *4*(1), 9-17.

Zoz FM, & Grisso RD. (2003a). Traction and tractor performance. *ASAE St. Joseph*, *27*.

Zoz FM, & Grisso RD. (2003b). *Traction and tractor performance* (Vol. 27). American Society of Agricultural Engineers St. Joseph, MI.

APPENDIX

APPENDIX A: INTERVAL PLOTS

Effect of plots of depth, season, and soil physiochemical on soil compaction are described under this appendix. Centers determine whether any confidence intervals overlap. If the intervals for two means do not overlap, the population means may be statistically significant.

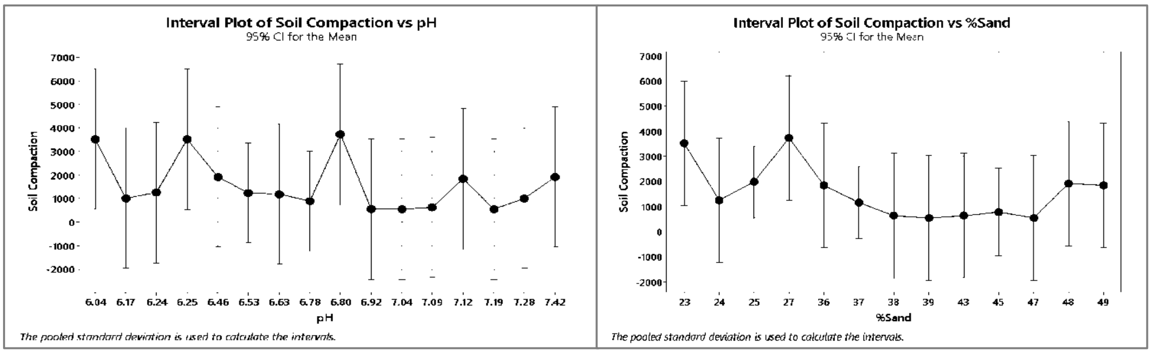

Figure A1: Interval plots of soil compaction vs. soil pH value and soil sand %

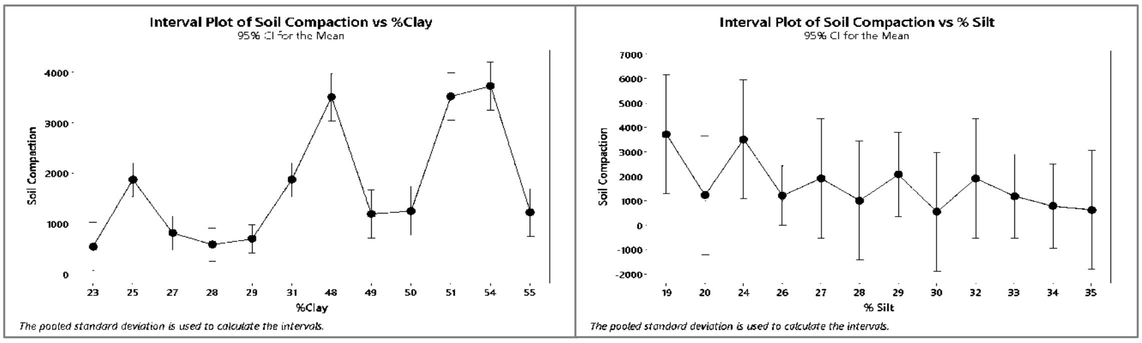

Figure A2: Interval plots of soil compaction vs. soil clay % and soil silt %

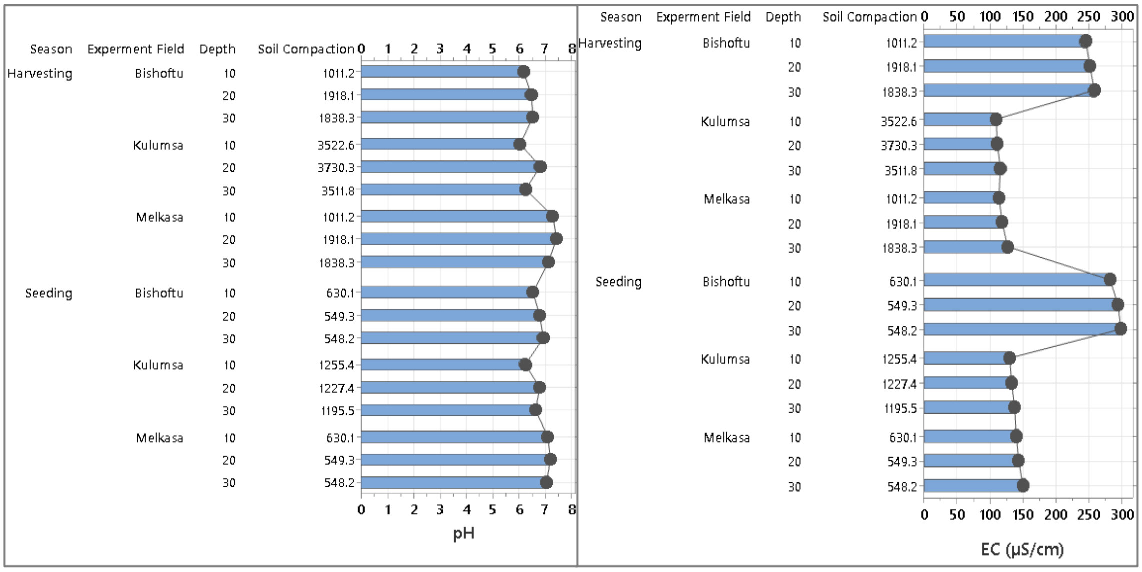

Figure A3: Effect plots of depth, season, soil EC and soil pH on soil compaction

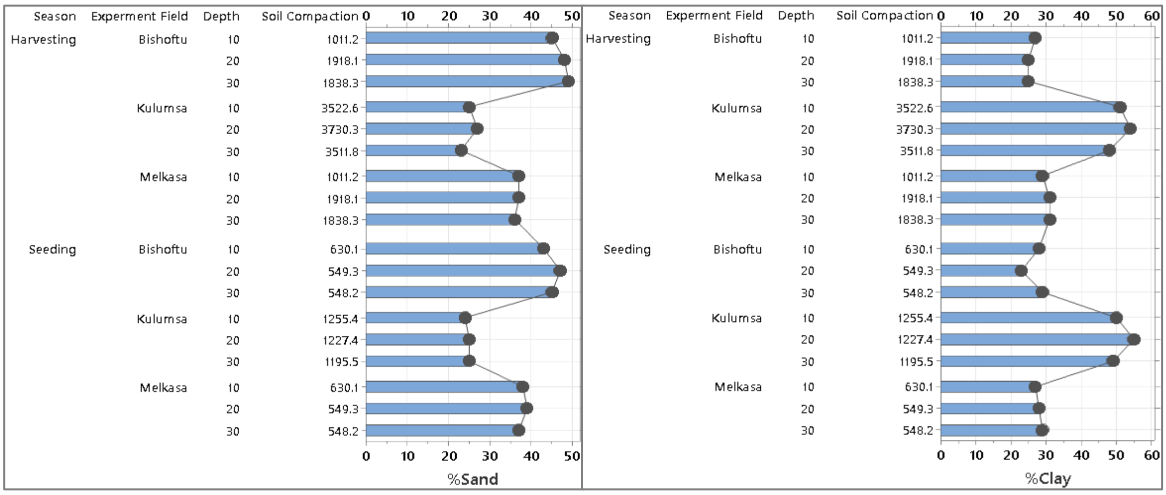

Figure A4: Effect of depth, season, sand % and clay % on soil compaction

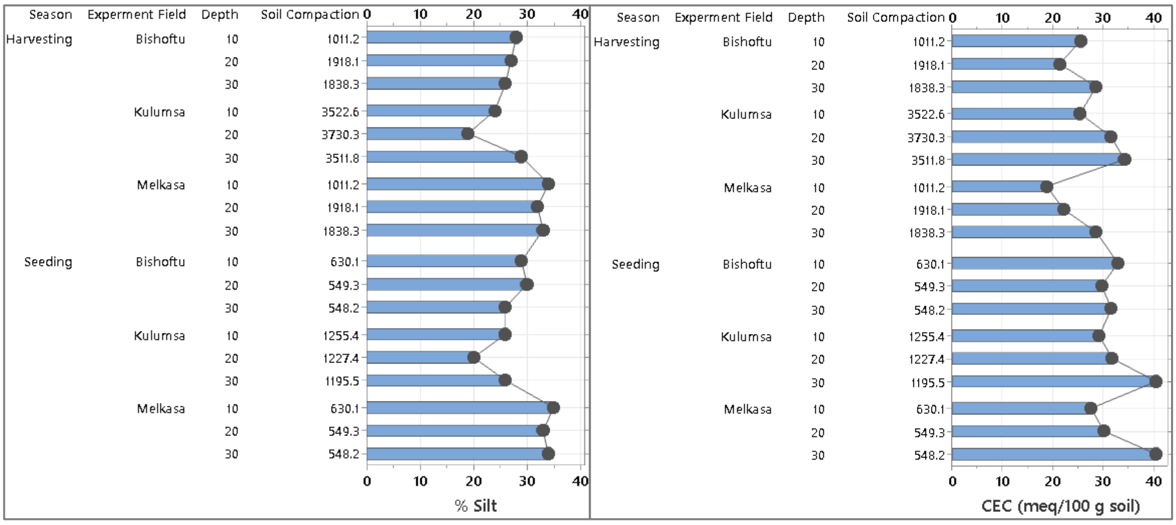

Figure A5: Effect of depth, season, silt % and CEC on soil compaction

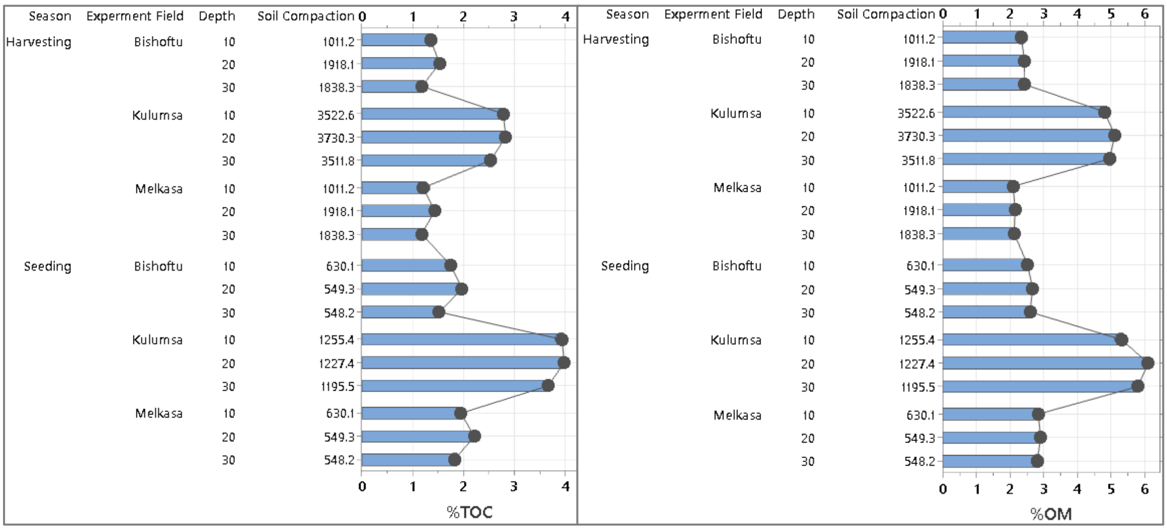

Figure A6: Effect of depth, season, TOC, and OM on soil compaction

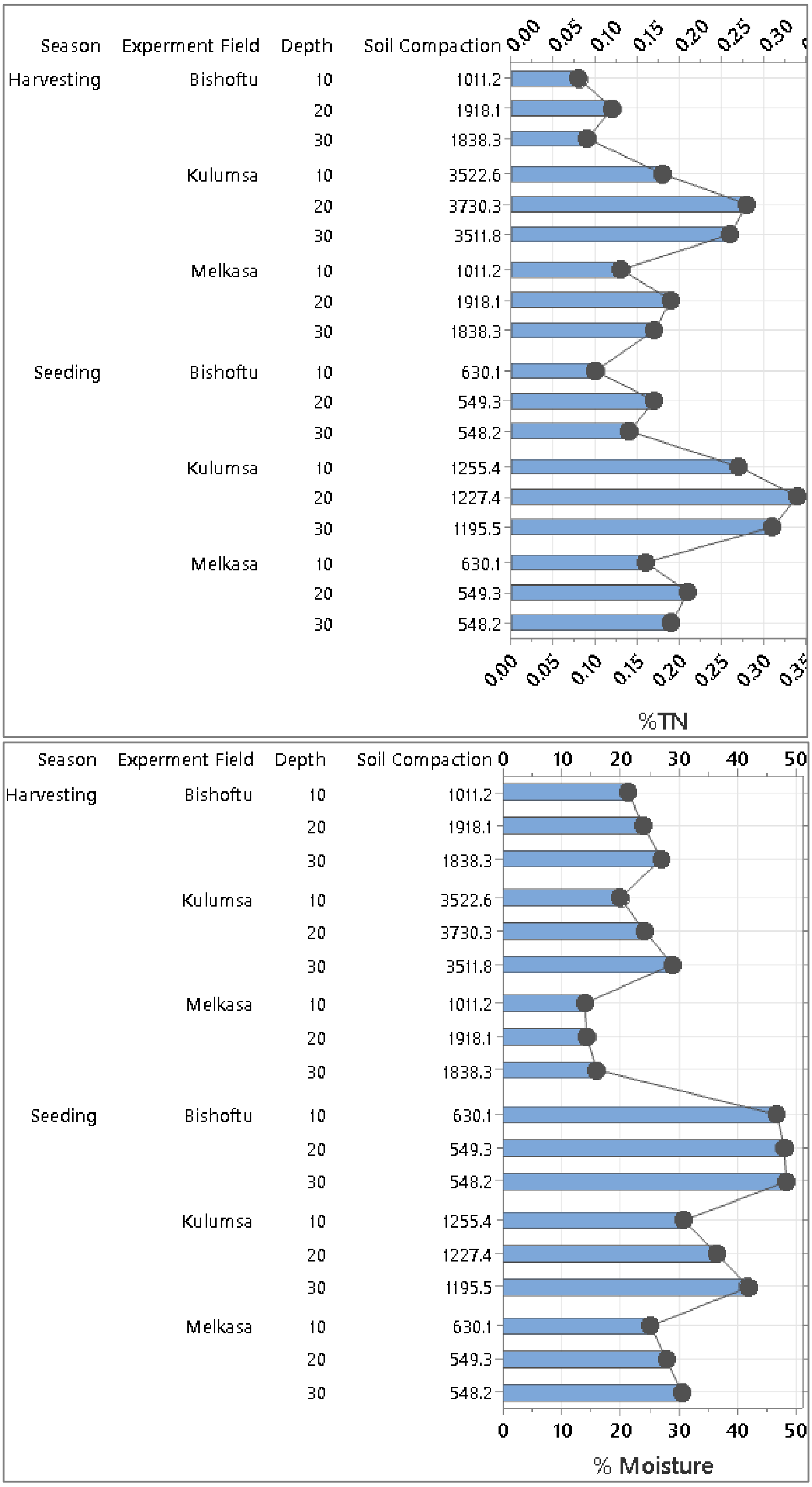

Figure A7: Effect of depth, season, TN and moisture on soil compaction

APPENDIX B: INTERACTION PLOT

The interaction plots show interactions between factors. Minitab creates an interaction plot by plotting for two or more factors the characteristic average for each combination of factor levels. The levels of one factor are indicated on the horizontal axis, whereas the levels of the other factor are indicated by different colored lines and symbols. If the lines are parallel to each other, then there is no interaction between the two factors and if the lines are not parallel to each other, then there is an interaction between the two factors.

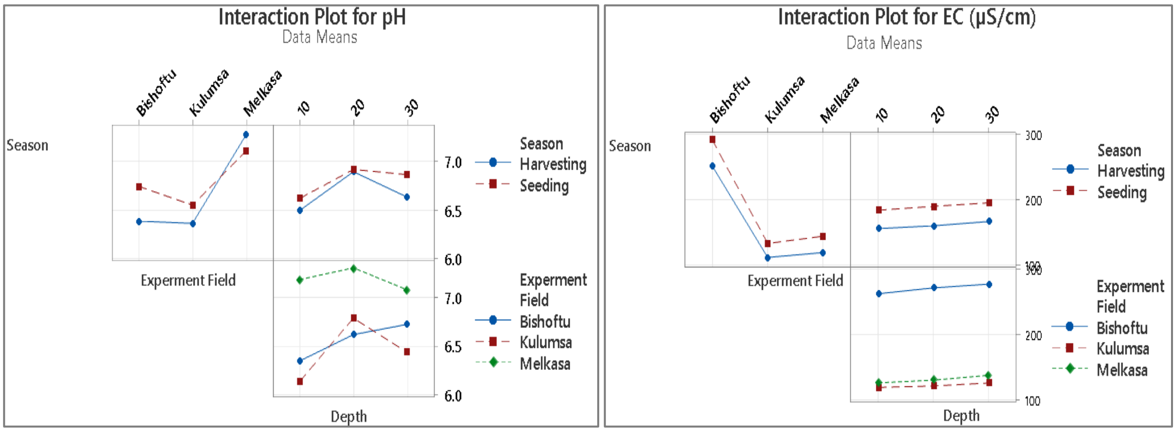

Figure B1: Interaction plots for soil Ph and soil EC

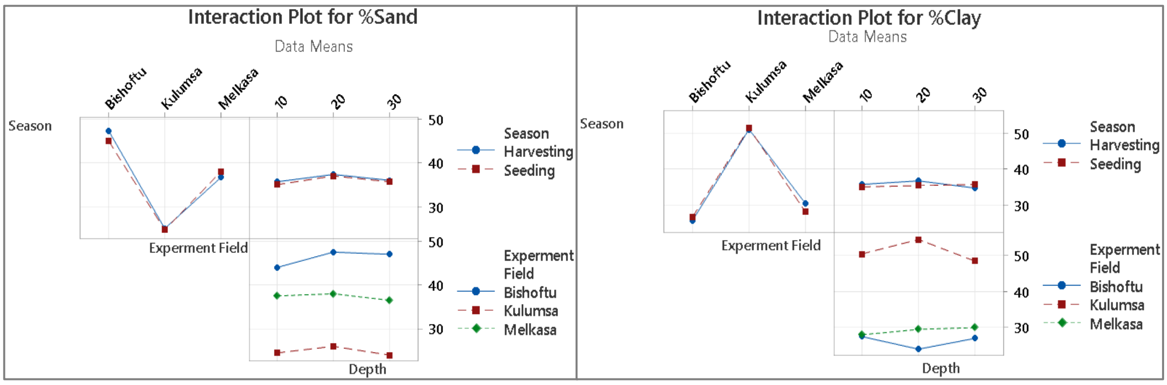

Figure B2: Interaction plots for soil sand % and soil clay %

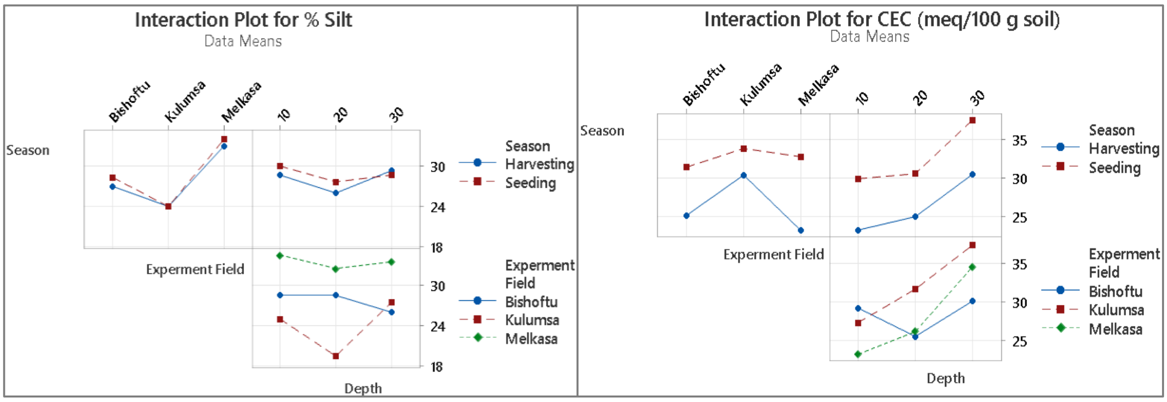

Figure B3: Interaction plots for soil silt % and soil CEC

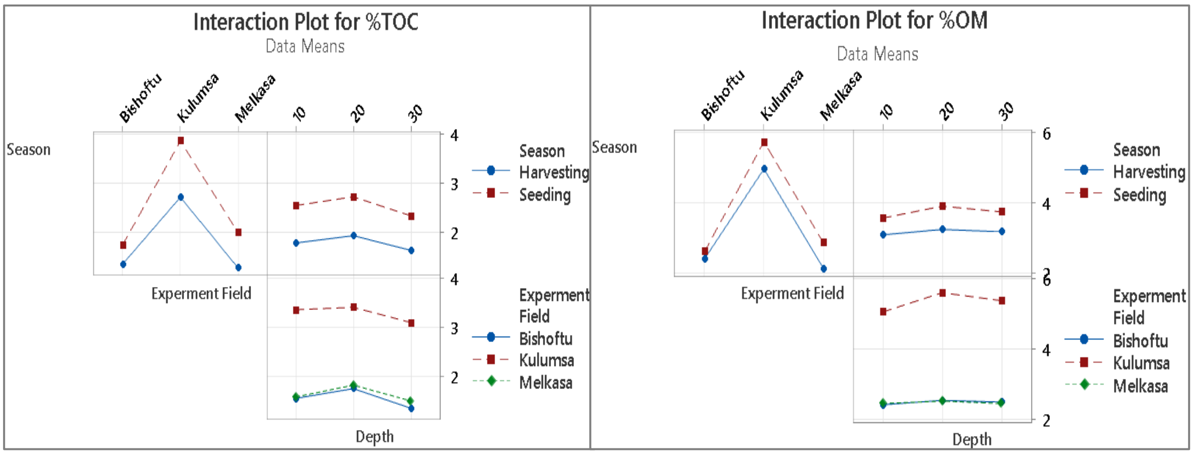

Figure B4: Interaction plots for soil TOC and soil OM

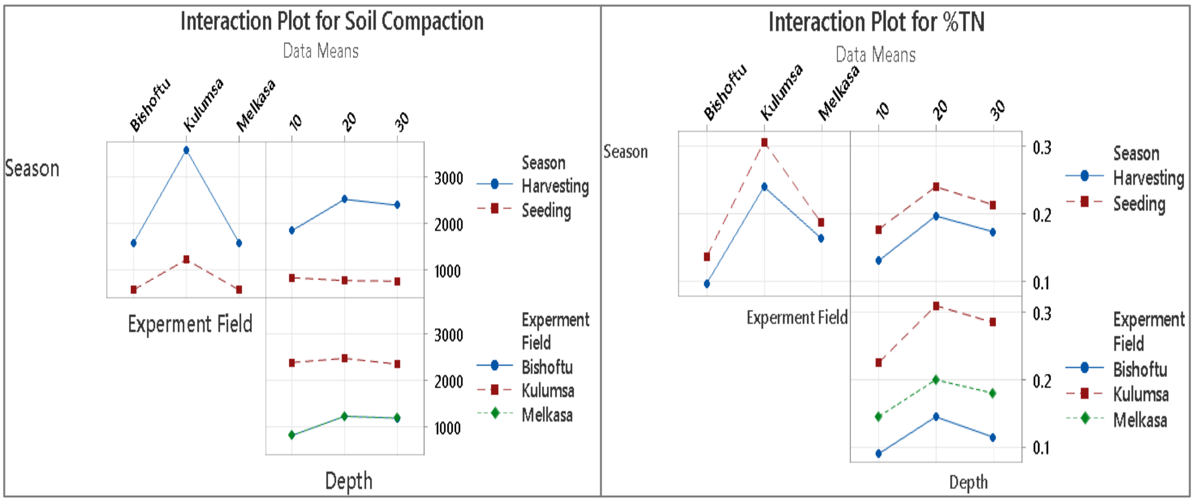

Figure B5: Interaction plots for soil compaction and soil TN

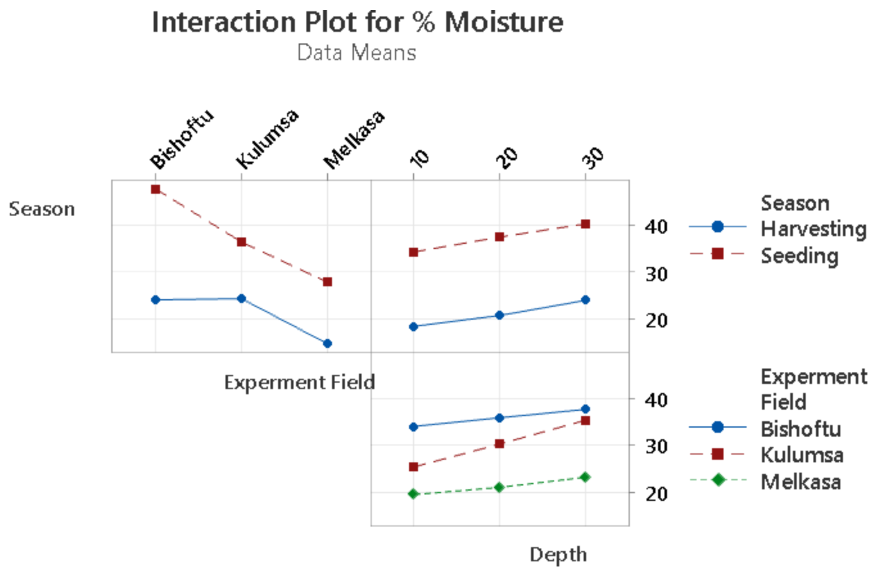

Figure B6: Interaction plots for soil moisture content

APPENDIX C: MAIN EFFECT PLOTS

Main effects plots show how each factor affects the response characteristic Minitab creates the main effects plot by plotting the characteristic average for each factor level. Look at the line to determine whether a main effect for a factor exists. When the line is horizontal, then there is no main effect and When the line is not horizontal, then there is a main effect. Different levels of the factor affect the characteristic differently. The larger the difference in the vertical position of the plotted points (the more the line is not parallel to the X-axis), the larger the magnitude of the main effect.

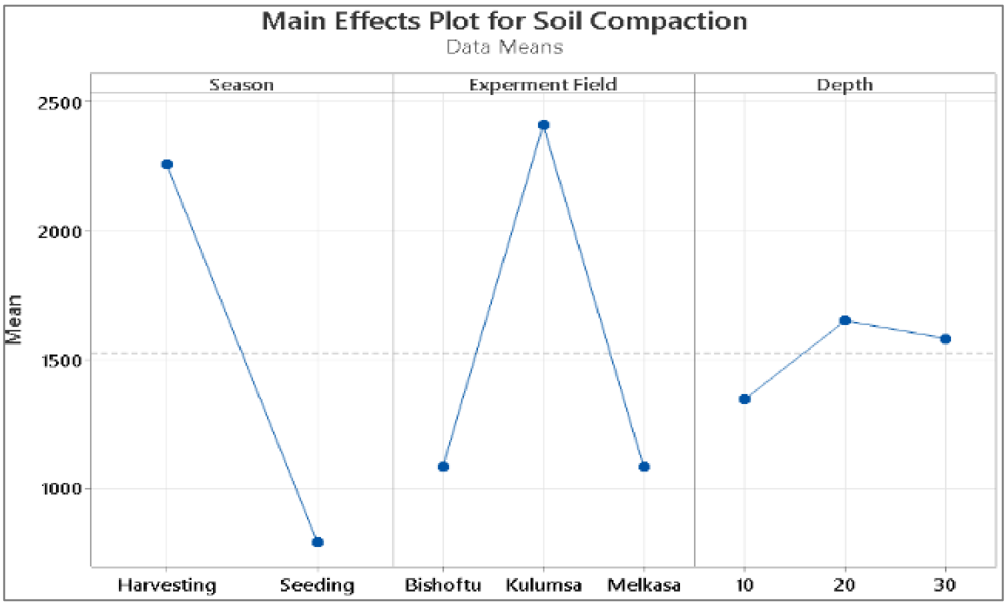

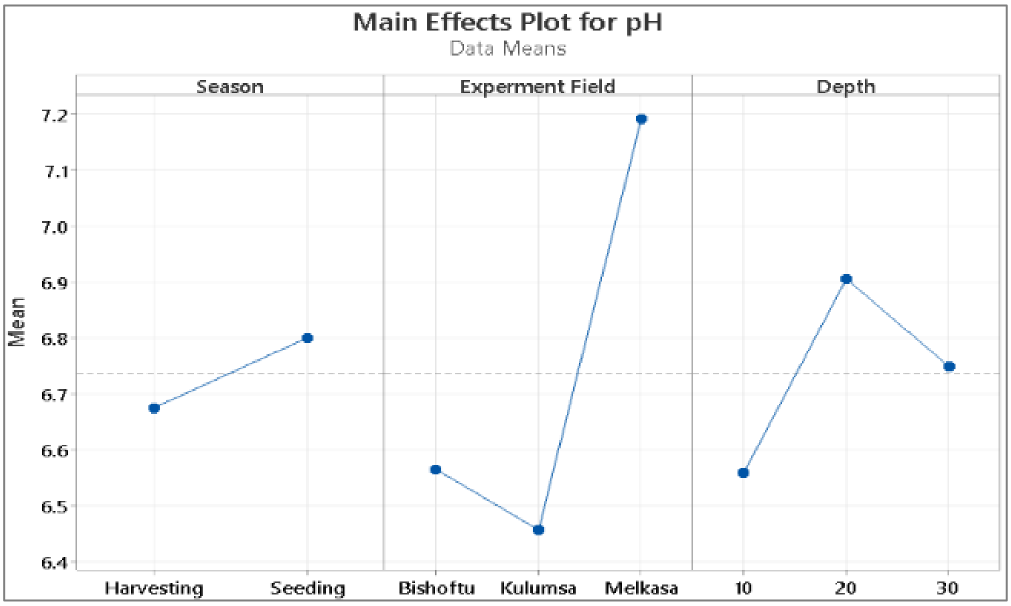

Figure C1: Main effect of soil compaction and soil pH

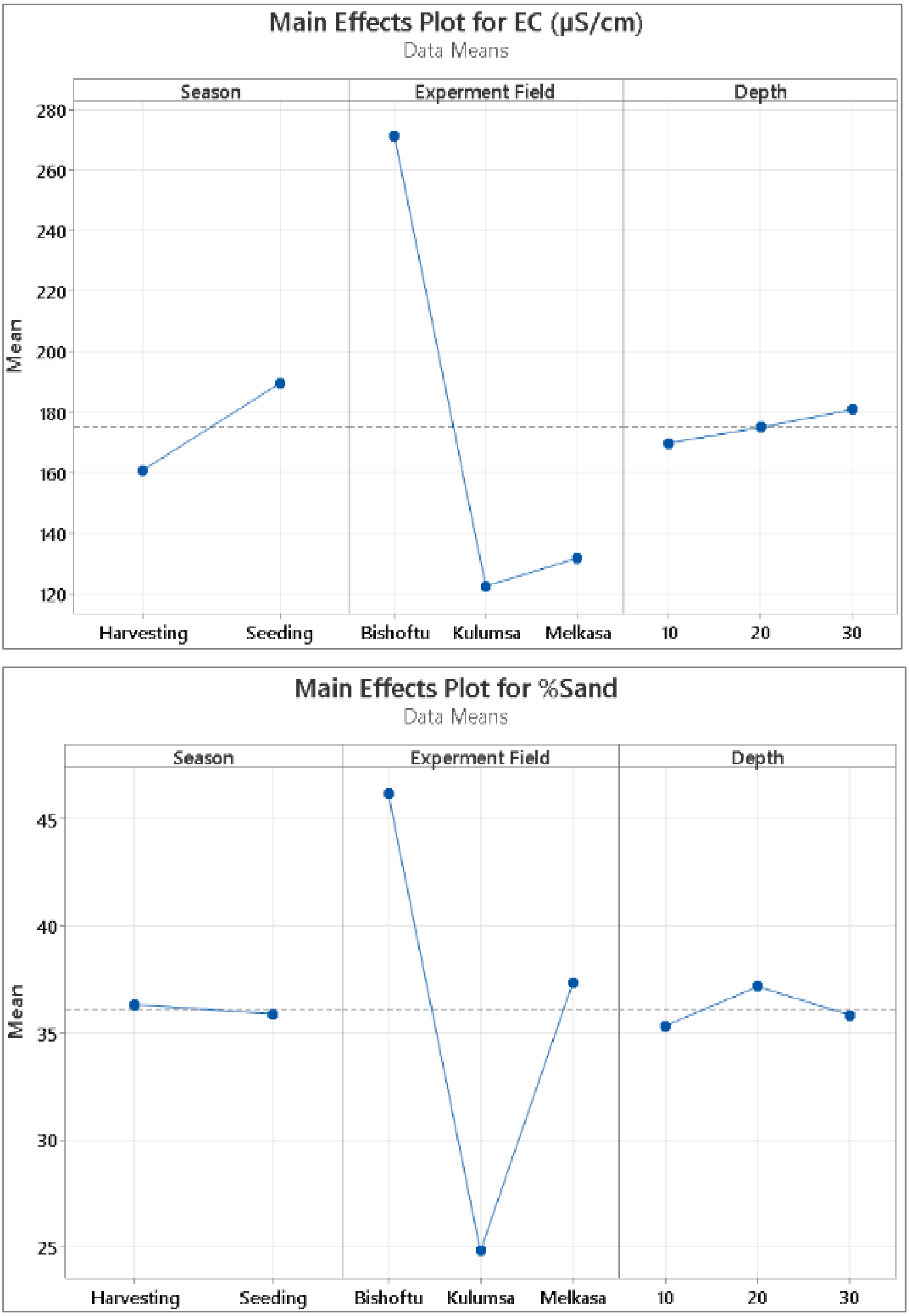

Figure C2: Main effect of soil EC and soil sand %

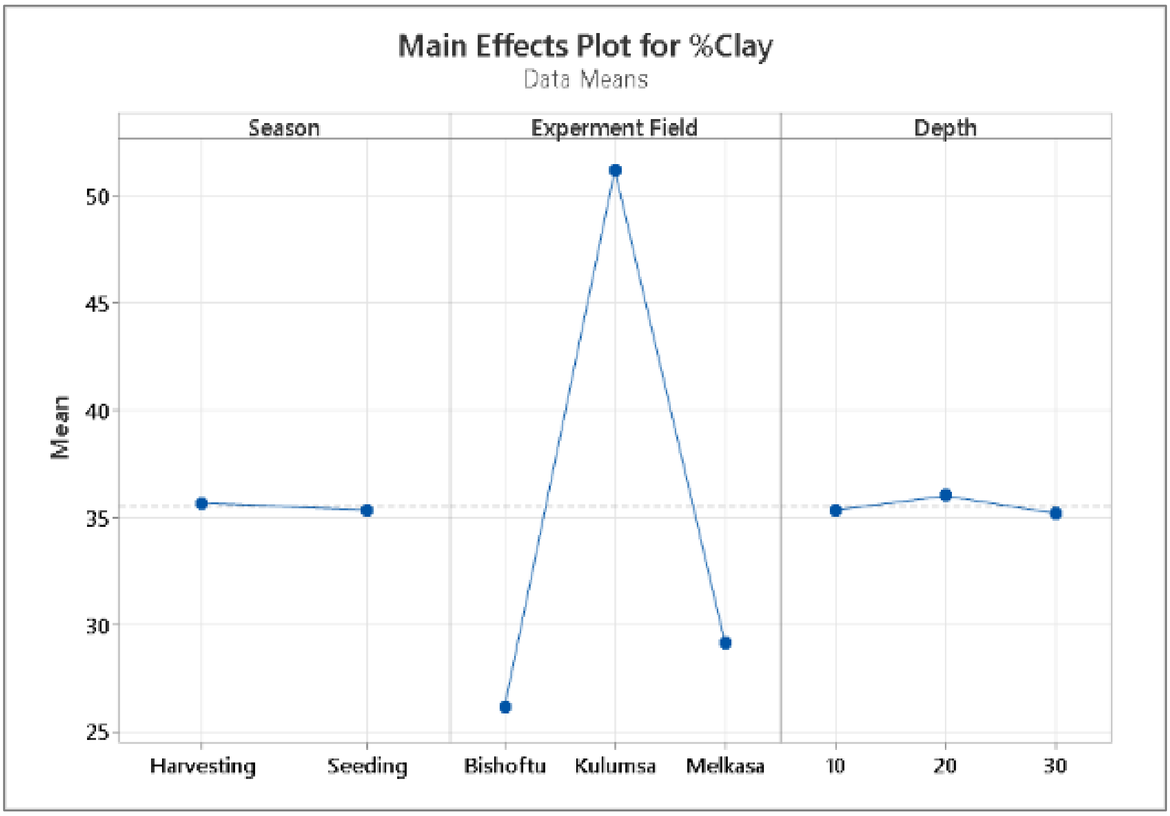

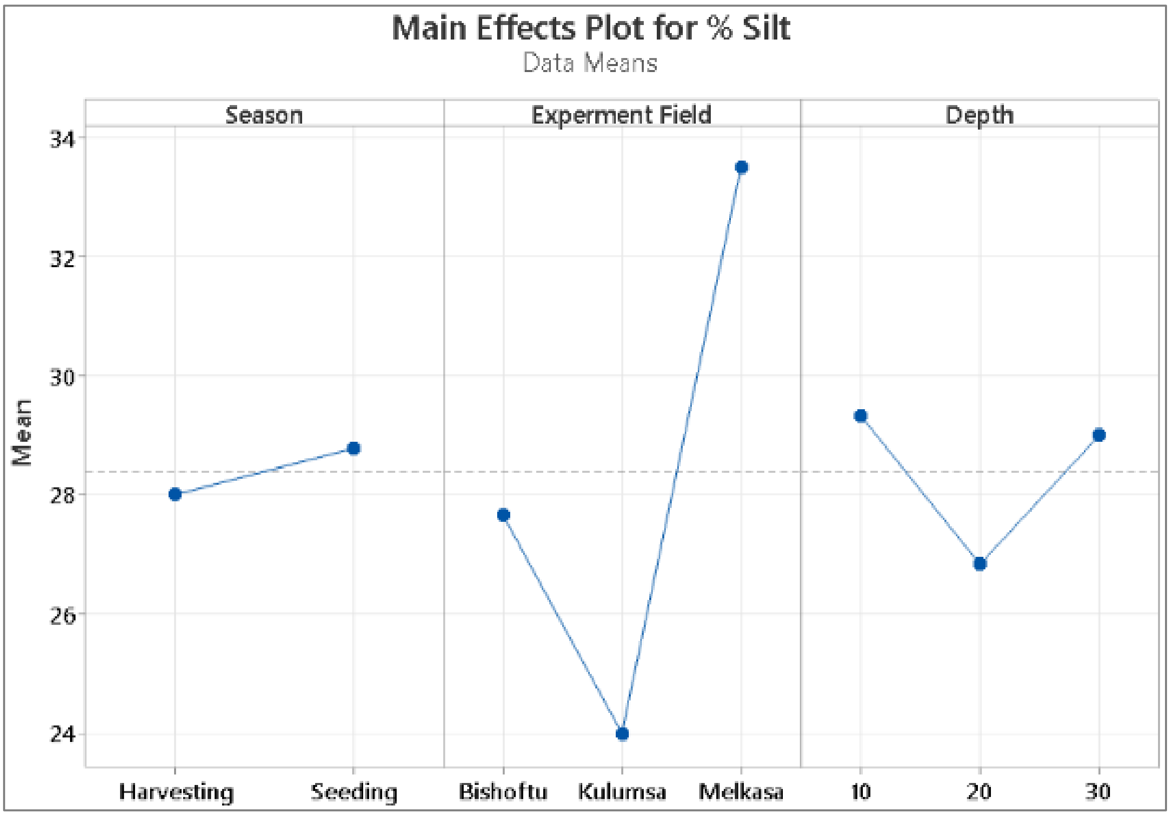

Figure C3: Main effect of soil clay % and soil silt %

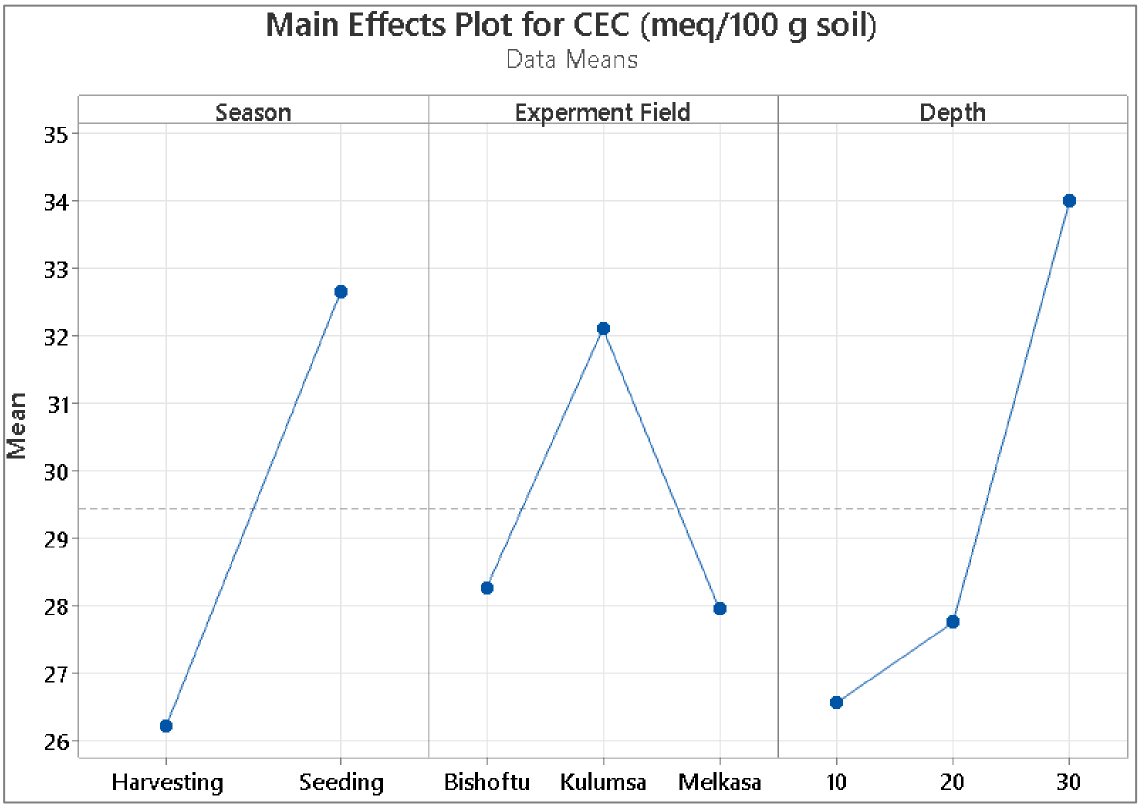

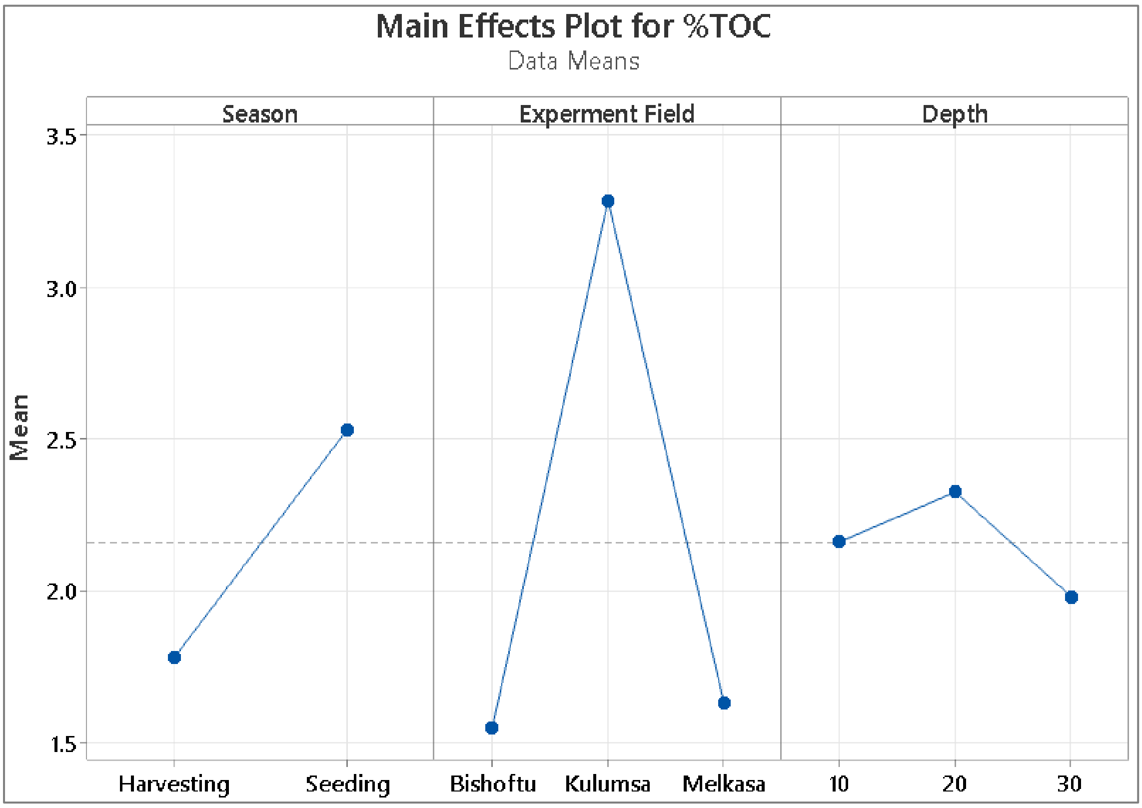

Figure C4: Main effect of soil CEC and soil TOC

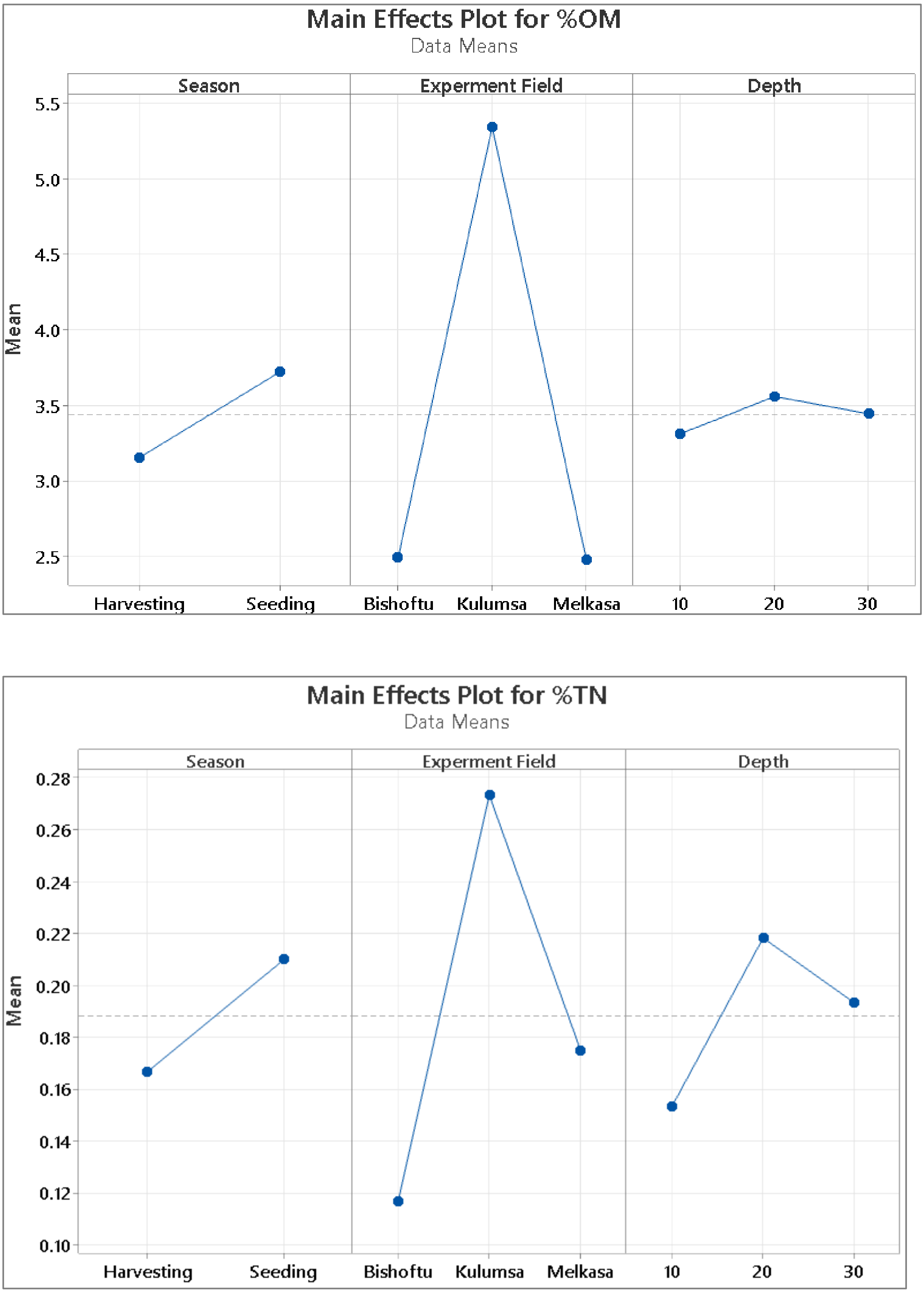

Figure C5: Main effect of soil OM and soil TN

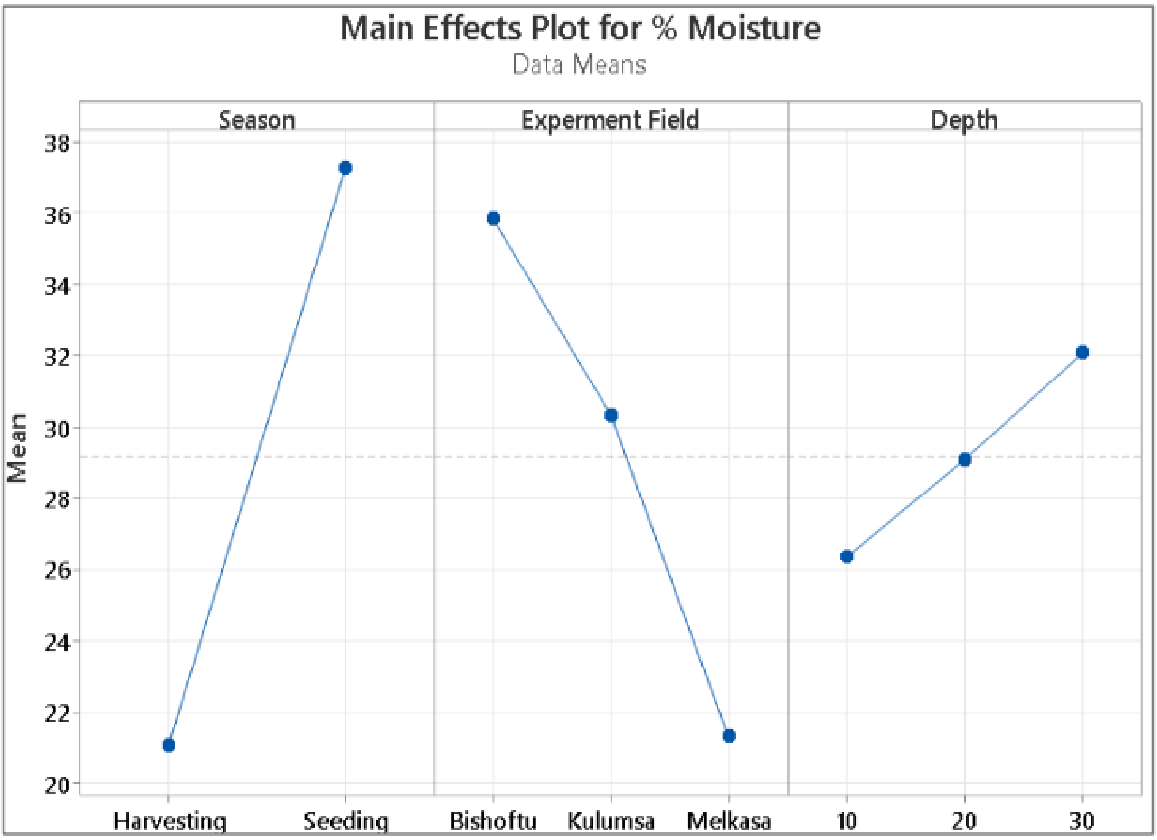

Figure C6: Main effect of soil moisture content

APPENDIX D: CONTOUR PLOTS

Use a contour plot to see how a response variable relates to two predictor variables. A contour plot provides a two-dimensional view in which all points that have the same response are connected to produce contour lines of constant responses.

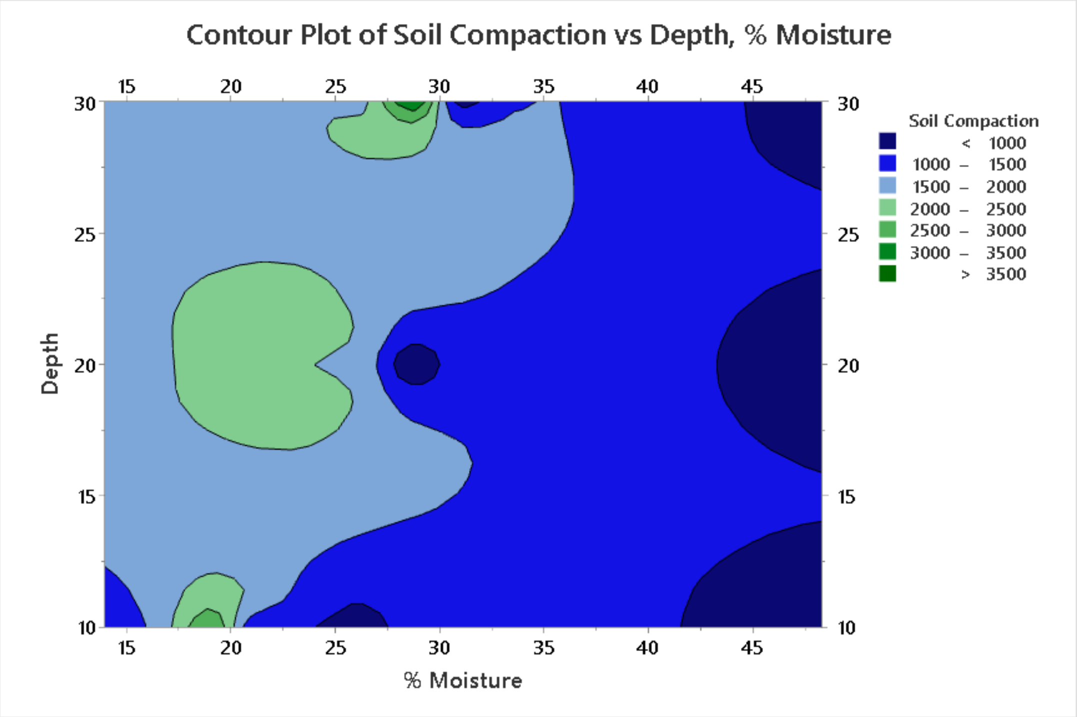

Figure D1: Contour plot for effect of depth and moisture on soil compaction

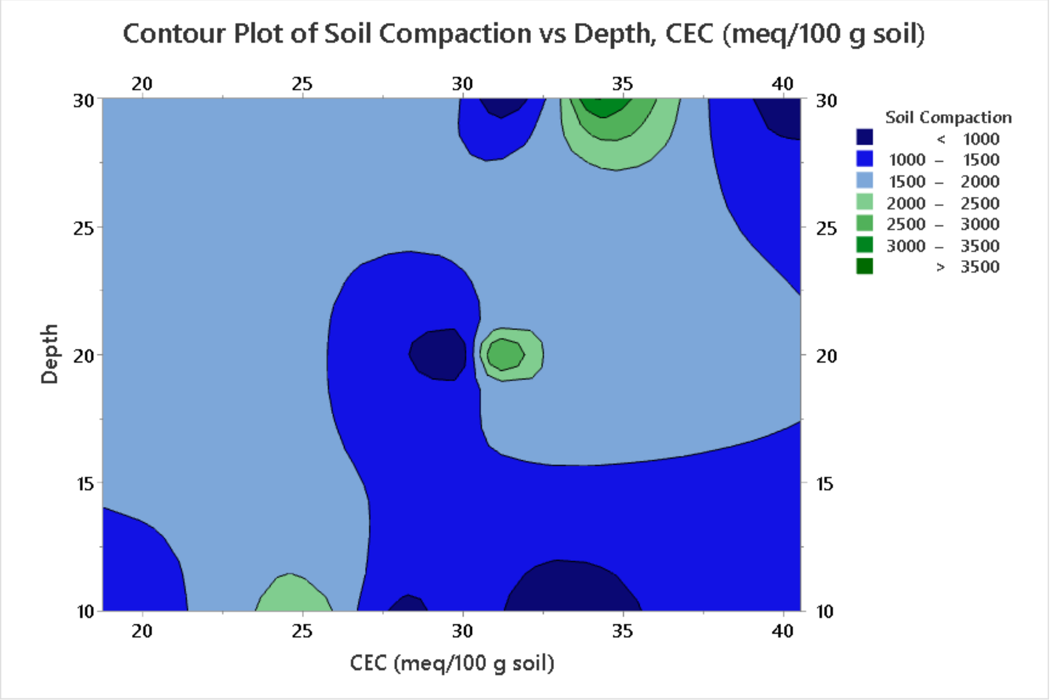

Figure D2: Contour plot for effect of depth and CEC on soil compaction

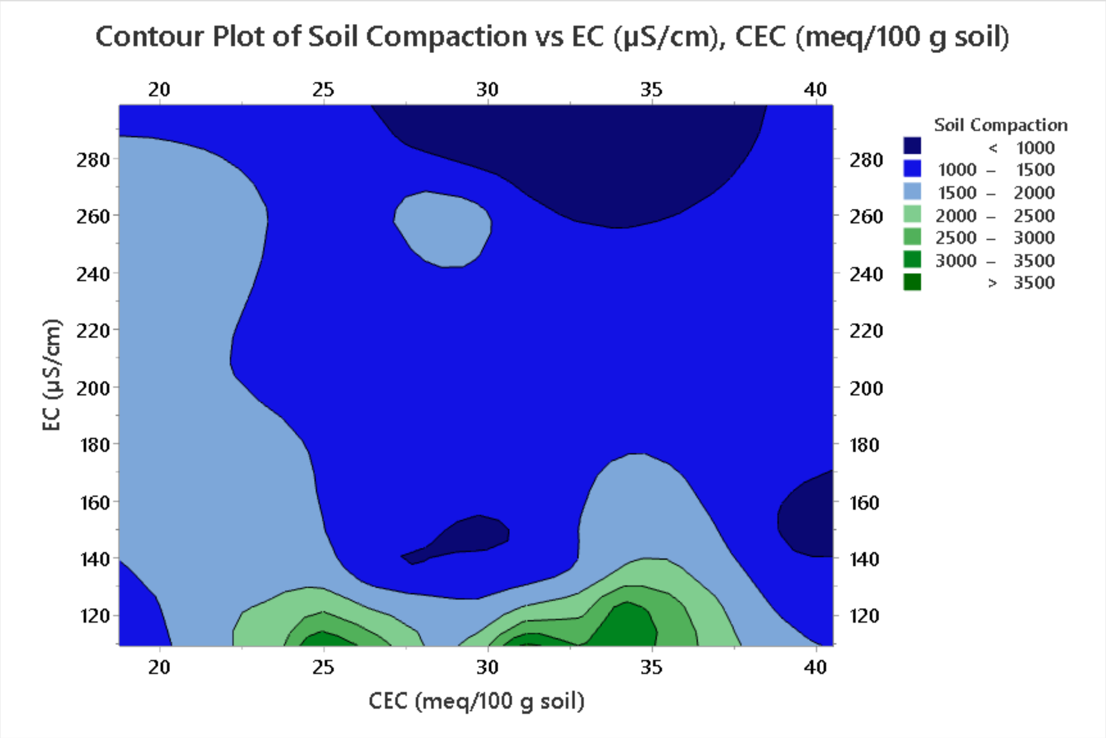

Figure D3: Contour plot for effect of EC and CEC on soil compaction

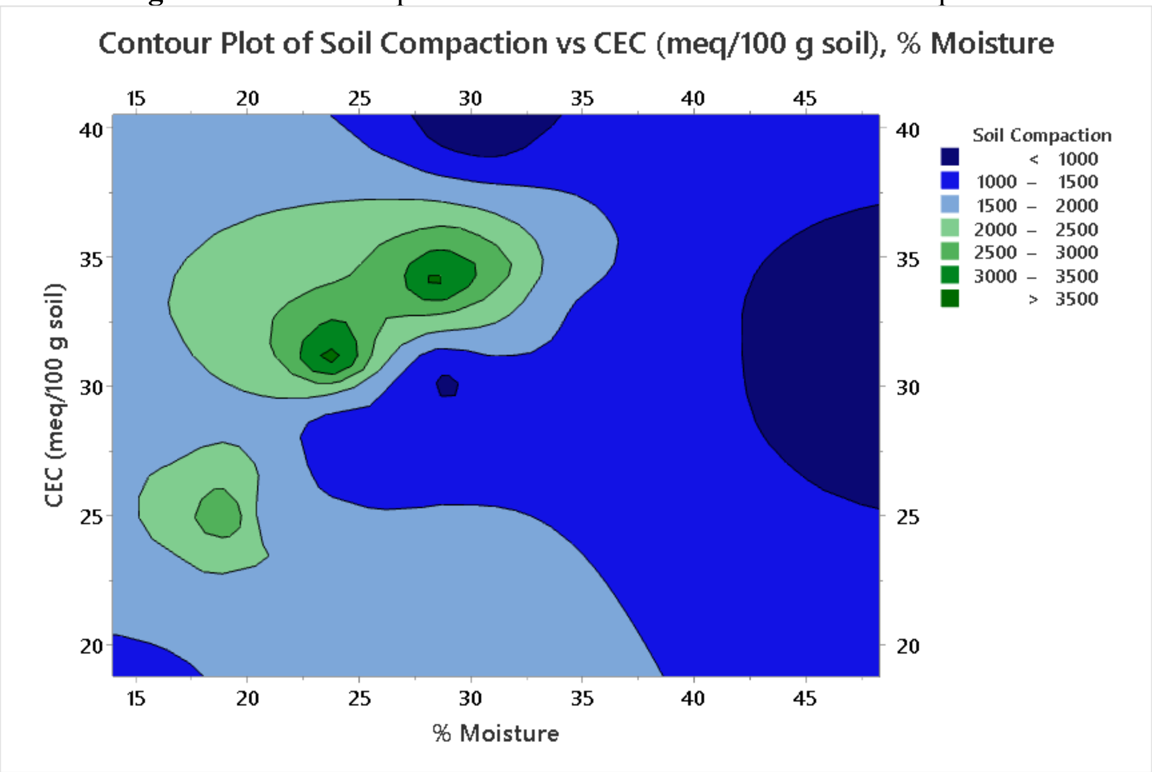

Figure D4: Contour plot for effect of moisture and CEC on soil compaction